

ФЕДЕРАЛЬНОЕ АГЕНТСТВО ПО ОБРАЗОВАНИЮ  
Государственное образовательное учреждение высшего профессионального образования  
**«НАЦИОНАЛЬНЫЙ ИССЛЕДОВАТЕЛЬСКИЙ  
ТОМСКИЙ ПОЛИТЕХНИЧЕСКИЙ УНИВЕРСИТЕТ»**

---

УТВЕРЖДАЮ  
Проректор-директор ИПР

\_\_\_\_\_ А.К. Мазуров  
« \_\_ » \_\_\_\_\_ 2011 г.

**LABORATORY TESTING OF SOILS**  
Part III. Dynamical properties of soils

Методические указания к выполнению лабораторных работ  
по курсу «Грунтоведение»  
для студентов обучающихся по направлению 130100  
«Геология и разведка полезных ископаемых».

*Составитель* **Крамаренко В.В.**

Издательство  
Томского политехнического университета  
2010

УДК 624.131.37(076.5)

ББК 26.3я73

Л-125

**Крамаренко В.В.**

Laboratory testing of soils. Part III. Dynamical properties of soils: Методические указания к выполнению лабораторных работ по курсу «Грунтоведение» для студентов, обучающихся по направлению 130100 «Геология и разведка полезных ископаемых». / сост. В.В. Крамаренко; Национальный исследовательский Томский политехнический университет. – Томск: Изд-во Томского политехнического университета, 2011. – 76 с.

УДК 624.131.37(076.5)

ББК 26.3я73

Методические указания рассмотрены и рекомендованы  
к изданию методическим семинаром кафедры  
гидрогеологии, инженерной геологии и гидрогеоэкологии ИГНД  
«26» января 2009

Зав. кафедрой ГИГЭ

Доктор геолого-минералогических наук

\_\_\_\_\_ *С.Л. Шварцев*

Председатель учебно-методической  
комиссии

\_\_\_\_\_ *Н. Г. Наливайко*

*Рецензент*

канд. геол.-минер. наук доцент ТПУ Т.Я. Емельянова

© Составление. ГОУ ВПО «Национальный  
исследовательский Томский политехнический  
университет», 2011

© Крамаренко В.В. 2011

© Оформление. Издательство Томского  
политехнического университета, 2011

## 6. DYNAMIC PROPERTIES OF SOILS

### 6.1. Dynamic deformation characteristics of soil

Dynamic analyses to evaluate the response of the earth structures to dynamic stress applications are finding increased applications in civil engineering practice (figure 6.1). The first published investigation of the dynamic loading of soils concerned the effect of bomb explosions on the Panama Canal, but dynamic loading of soils can originate from several other sources such as earthquakes, construction operations, traffic and wheel loads, machine vibrations, wind loading or the wave action of water. These types of loads are different from other loads due to their repeated, or “cyclic”, nature. Dynamic deformation characteristics test and behavior of soil subjected to cyclic loading are described in this paper.

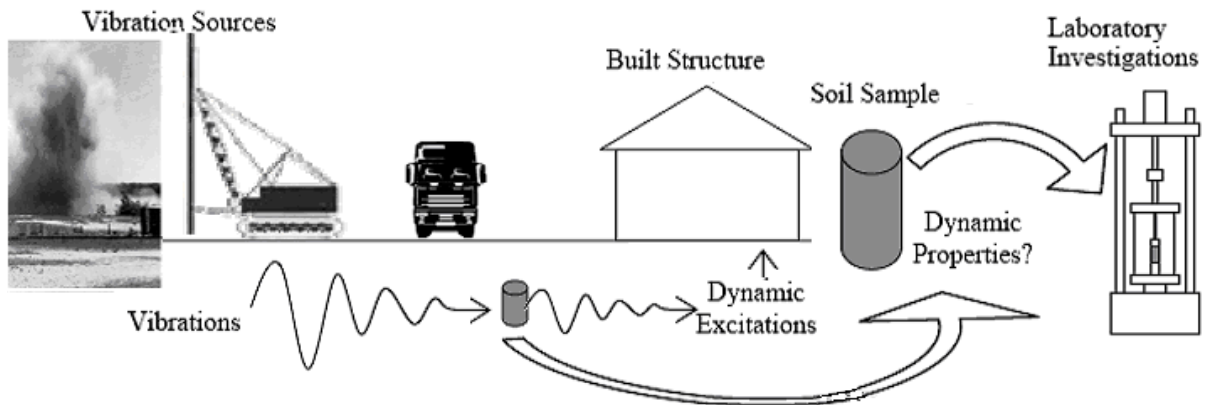


Figure 6.1. Vibrations in the Soil [9]

In order to evaluate the response of foundations subjected to vibrations and the manner of vibrations and its transmission through the ground, the dynamic characteristics of soils must be determined. Design of geotechnical engineering problems that involve dynamic loading of soils and soil–structure interaction systems requires the determination some important dynamic parameters: the *shear modulus  $G$* , *elastic modulus  $E$* , *constrained modulus  $M$* , *Poisson’s ratio  $\mu$*  and *the damping ratio  $D$*  of the soils.

Currently, most of the soil parameters relevant to dynamic analyses are frequently performed with the help of special dynamic procedures in the field and laboratory. There are several type waves-particle motion in soil, among them *compressive and shear*. Compressive waves-particle motion is parallel to the wave direction (figure 6.2); shear waves-particle motion is perpendicular to the wave direction.

**Shear wave velocity ( $V_s$ )** is the most commonly used measured parameter used in shallow soil for soil characterization. It is used to calculate the following parameters in the elastic range of soil behavior. The importance

in its utility is that the particle of motion travels perpendicular to the direction of wave propagation being able to measure the shear properties of the soil skeleton and not the fluids that cannot take shear.

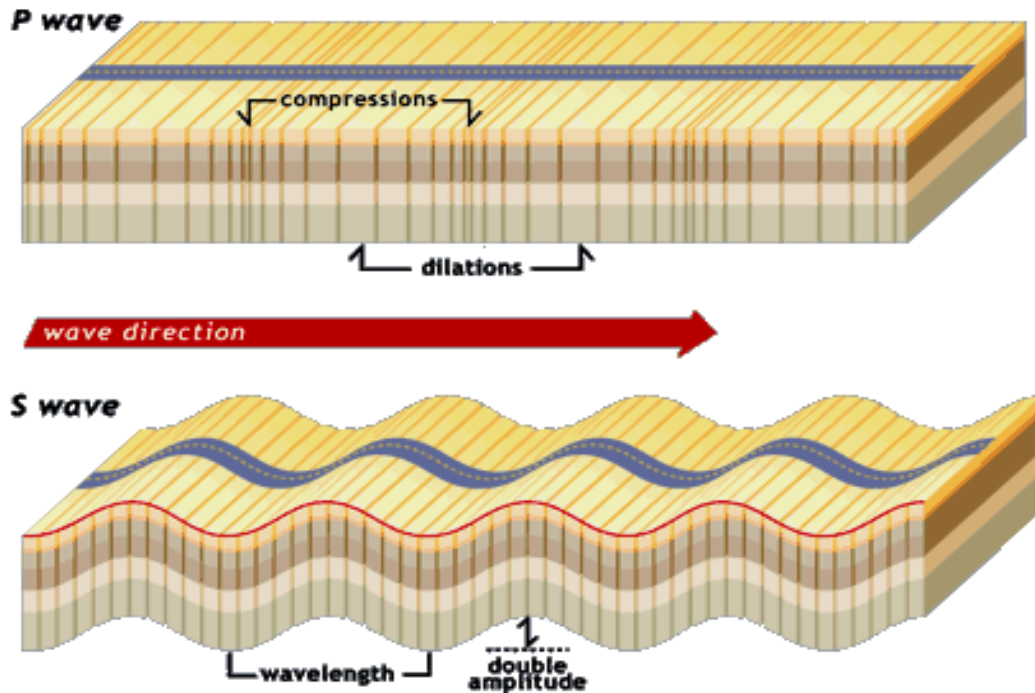


Figure 6.2. Compressive and shear waves

The measured shear wave velocity is generally considered the most reliable means to obtain  $G_{max}$ . These methods involve the creation of a transient and/or steady-state stress waves (source) and the interpretation of the arrival time and spectral response at one or more locations (receivers). The generation of the impulse wave by the source can vary from a sledgehammer blow at ground surface, to a buried explosive charge or to an active varied frequency source vibrator. Figure 6.3 shows different methods for creation of impulse waves. These sources generate p-waves, s-waves and surface waves at different relative amplitudes depending of the dominant wave in the method used.

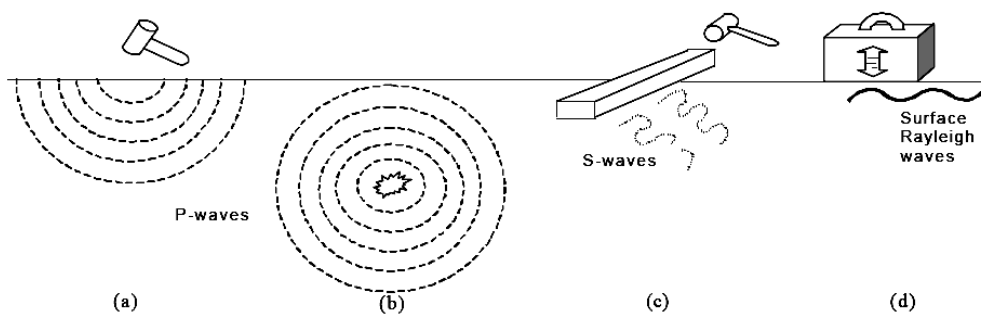


Figure 6.3 - Methods to create impulse waves: a) vertical impact, b) shallow explosive, c) horizontal impact, and (d) frequency-controlled surface waves

Several equations are used to determine soil properties employing ultrasonic apparatus or bender elements and others as follows. Assuming that the distance between an s-wave transmitter and an s-wave receiver is  $L_s$  and the time for the wave to travel this set distance is  $t_s$ , the average shear wave velocity can be calculated as [16],

$$V_s = L_s / t_s \quad (6.1).$$

Correspondingly for the velocity of the p-waves,

$$V_p = L_p / t_p \quad (6.2)$$

where  $L_p$  is the distance between the extender element transmitter and receiver and  $t_p$  is the travel time of the p-wave.

**Constrained modulus ( $M$ )** of the soil is then,

$$M = \rho * V_p^2 \quad (6.3).$$

**Shear modulus ( $G$ )** is a calculated parameter based on the  $V_s$  using the simple elastic relationship

$$G_{max} = \rho * V_s^2 \quad (6.4)$$

where  $\rho$  - mass density of the soil.

Mass density is often estimated or measured by a nearby subsurface sampling or using correlations. Advanced correlations to estimate the value of the dynamic shear modulus are available based on the standard penetration test, Atterberg limits (plasticity index) and grain size distributions. The shear modulus is used to perform more advanced soil modeling, and dynamic response of the soil-structure interactions. Shear modulus at low-strain levels as measured by geophysical techniques will provide the elastic parameter for machine foundation analysis or earthquake engineering. The important utility of this parameter is that it can be used as a varying parameter with respect to strain making the soil response represents the real modulus degradation in soil behavior. This parameter is used in defining the stiffness matrices for finite element analysis of earth structures and foundation soils.

**Maximum shear modulus ( $G_{max}$ )** is used to normalize the shear modulus ( $G$ ) vs. shear strain relationships. These normalized relationships allow the engineer to use well-established degradation curves and scale them to the measured in-situ value of  $G_{max}$ . In the absence of extensive dynamic soil testing at all ranges of shear strain these curves are used and  $G_{max}$  is used as the scaling parameter.

**Poisson's ratio ( $\mu$ )** is a fundamental parameter that is difficult to measure and it is usually estimated in engineering calculations. The ratio of horizontal to vertical strain is required to relate modules and strains in a solid body. A suggested range of values for Poisson's ratio for soils is from 0.2 to 0.5, less common values may be as low as 0.1 for loess deposits. This ratio can be calculated [ $\mu = E/(2G-1)$ ] based on laboratory tests at low strains if  $G$  and  $E$  are obtained from torsional and longitudinal vibration, respectively.

The Poisson's ratio  $\mu$  is represented also by,

$$\mu = [(M / G_{max} - 2) / (2M / G_{max} - 2)]. \quad (6.7)$$

**The elastic modulus ( $E$ )** can be determined using,

$$E = 2G_{max} * (1 + \mu) \quad (6.5)$$

For plane waves, the shear strain,  $\gamma_s$ , is defined as the ratio of peak particle velocity,  $u$ , to shear wave velocity:

$$\gamma_s = u / V_s \quad (6.6)$$

**Damping ratio ( $D$ )** is used in several dynamic analysis procedures to provide realistic motion attenuation. This ratio is based on the material damping properties. The damping ratio vs. shear strain relationships for cohesionless and cohesive soils are provided in Seed, et al. Since damping ratio is also shear strain dependent, it is required to have several values with strain. Dynamic analysis results are also influenced by the damping ratio for single and multi degree modal systems. The effects of soil-structure interaction also influence the damping of the system making it an area where recent research has focused. The utility of this parameter is based on the ability of the system to absorb dynamic energy and how this will affect the duration and modes of vibration.

## **6.2. Application of dynamic parameters in engineering practice**

Dynamic parameters of soil are determined in order to predict soil behavior under dynamic excitations. Laboratory studies will simulate past loading regimes as a consequence of the historic accumulation of debris and sediment and future loading based on a range of follow construction scenario: laboratory pile tests, blasting and rail track and several other.

**Testing of piles** in the laboratory involves the application of a sudden compressive load whose reaction is given by the high acceleration of a relatively small mass. The load duration is approximately 100 ms. This

involves the rapid loading characteristics of clays. These tests can be performed in the laboratory on the cyclic triaxial system.

**Blasting.** The blasting signature can be used for testing the foundation material. What effect does blasting have on structures in the areas surrounding the quarry or site? What effect does blasting have on the foundations of these structures?

**Rail track.** What effect does vibrations have on buildings close to railway track? Trains are becoming faster creating vibrations of greater frequency, which are transmitted into the surrounding ground. Cyclic tests on the track subbase can be performed.

Moreover dynamic tests answer on questions connected with existent problem offshore, earthquake and liquefaction. This situation we will give more details below.

**Offshore.** To investigate the wave effect on offshore, structures, waterside buildings, harbors and pipelines. Wave effect and pipeline vibrations can be recreated. The exploitation of offshore natural resources has presented engineering with the problem of dealing with in situ soil deposits on a potential slip surfaces for which few engineering data are available. Practically the initial stress state in soil beneath the offshore structures usually is of anisotropy. Moreover, the initial stress states of soil located at different parts in structural foundation are all different. Also, it is well know that the magnitude and orientation of the principal stresses acting on soil deposits constantly change for a variety of field loading conditions. Conventional triaxial monotonic testing on solid cylindrical specimens or torsional monotonic testing on hollow cylindrical specimens is a commonly used approach to study the effect of varying magnitude of the principal stresses on the behavior of soil in the laboratory, using a soil element that is subjected to an axisymmetric stress state. Liquefaction and shear failure are two main types of loss of stability of sandy seabed under wave loading. While experimental investigations have traditional focused on the conventional triaxial shear or torsional shear tests, as shown in figures 6.4 a) and b), studies have shown that more complex stress conditions are encountered in engineering. In one cycle of the wave loading, the principal stress axe in the sea soil revolves continuously.

The deviation of normal stresses ( $\sigma_v - \sigma_h$ ), shear stress  $\tau_{vh}$  and the deviation stresses composed by them vary incessantly cyclically, as shown in figure 6.4 c) and d).

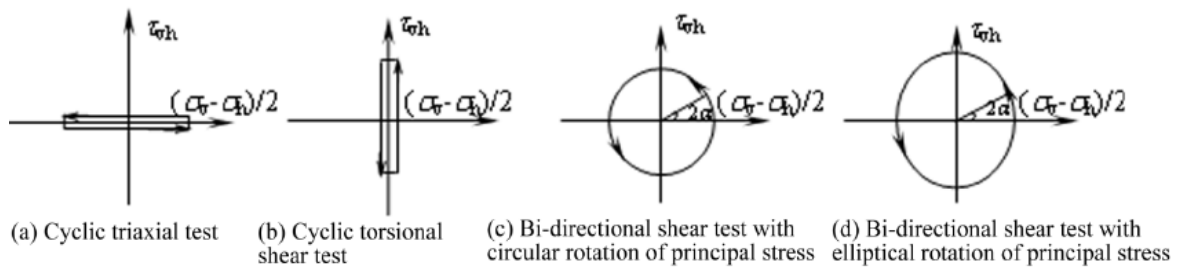


Figure 6.4. Two dimensional loading schemes

Continuous revolving of the orientation of principal stress has effect on both pore water pressure and deformation. Practically the initial stress state usually is of anisotropy. Moreover, the initial stress states of soil elements located at different parts in structural foundations are all different. Sands can behave in either a contractive or dilative manner depending on their initial conditions. The cyclic shear strength of sand is obviously influenced by the initial sustained shear stress. The orientation of initial stresses of any point on a potential slip surface strongly depends on the location of the point [11].

Therefore, as an essential issue in evaluation the stability of seabed and structural foundations, the complex anisotropic initial stress state and the complex variation pattern of cyclic stress must be taken into consideration for prediction of deformation and strength behavior of sands. True triaxial tests with independent control of the three principal stresses on cubical soil specimens have been performed to investigate primarily the effect of intermediate principal stresses. However, the initial principal stress direction cannot be acted and orientation of principal stresses can not be rotated in those studies. For this reason, the conventional triaxial shear and torsional shear tests are incapable to reproduce the above-mentioned complex initial stress condition and cyclic loading pattern. An alternative way is to use the soil static and dynamic universal triaxial and torsional shear apparatus.

An intensive and systematic experimental study for such a special issue had hardly been made due to lack of modern soil testing technology in reality, and involves many experimental difficulties.

**Earthquake and liquefaction.** The dynamic deformation characteristics of the soil are used in order to calculate seismic response of ground, earth structures and structure-ground response. Seismic loading occurs when a rupture in a fault releases energy that is propagated as a stress wave through the rock and overlying soil. The wave may either attenuate or amplify in magnitude as it travels toward the ground surface. The attenuation or amplification depends on several factors including the unit weight, shear wave velocity, damping ratio, and shear modulus associated with a specific soil. Understanding the cyclic behavior of soil allows the prediction and



calculation of the magnitude and frequency of a seismic wave at the ground surface, or at any point within a given subsurface profile.

Figure 6.5 shows schematic wave propagation from a fault to a ground surface. In the engineering point of view, the earthquake wave travels from the fault to the ground surface through the seismic bedrock where earthquake motion can be defined to be a function with respect to the distance from the fault, and the engineering seismic base layer at which earthquake motion is not affected by the existence of the surface ground, i.e., the subsoil above the engineering seismic base layer.

The earthquake wave propagates vertically in the surface ground because the ground becomes softer to the ground surface. In addition, since the soil is soft, it may exhibit nonlinear behavior under the large *cyclic loading*.

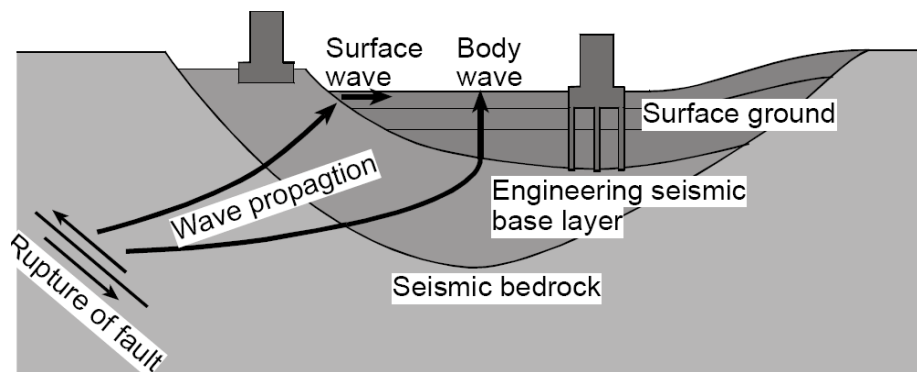


Figure 6.5. Wave propagation from fault to ground surface [31]

The term “cyclic loading” implies a regular repetition of magnitude and frequency. When applied to geotechnical earthquake engineering, “cyclic” is a misnomer because the source of cyclic loading does not consistently repeat. Earthquakes are not intrinsically regular events, and when active they do not regularly repeat in magnitude or frequency. The acceleration time history in figure 6.6 shows the irregular, but repeating, or “cyclic”, nature of seismic loading. Despite the misnomer, seismic loading includes stress reversals, time-dependant pore pressure dissipation (especially in the case of liquefaction), and dynamic effects as the earthquake propagates from rock to the ground surface.

Earthquake induced failures of slopes on shear surfaces consisting of saturated soils may result in high mobility landslides or flow type failures on the order of tens of meters. Associated with seismic risk evaluation there are many cases where limited deformations are tolerated, but the flow type of failures with long travel distances representing high mobility threat with catastrophic consequences in terms of damage and casualties are never permissible. Another type of phenomenon occurring during earthquakes known as soil liquefaction is very often directly connected with landslide

processes, especially landslide mobility, resulting in large deformations. Many earthquake-induced landslides result from liquefaction phenomena, but many others simply represent the failures of slopes that were marginally stable under static conditions.

*The phenomenon of liquefaction* is one of the most controversial topics in geotechnical earthquake engineering, and in the past almost 40-50 years it has been studied and debated by hundreds of researchers around the world. Liquefaction began to be focused on by engineers and researchers after the 1964 Niigata earthquake. During the Bhuj earthquake on 26 January 2001, a number of medium to high rise residential buildings collapsed in Ahmedabad city, which is located about 300 km away from the epicenter. The city is founded over thick recent unconsolidated sediments. The severe damages in this location are attributed to the response of such unconsolidated sediments to violent shaking. This catastrophic earthquake has provided a serious reminder that liquefaction of sandy soils and sands with non-plastic fines as a result of earthquake ground shaking poses a major threat to the safety of civil engineering structures.

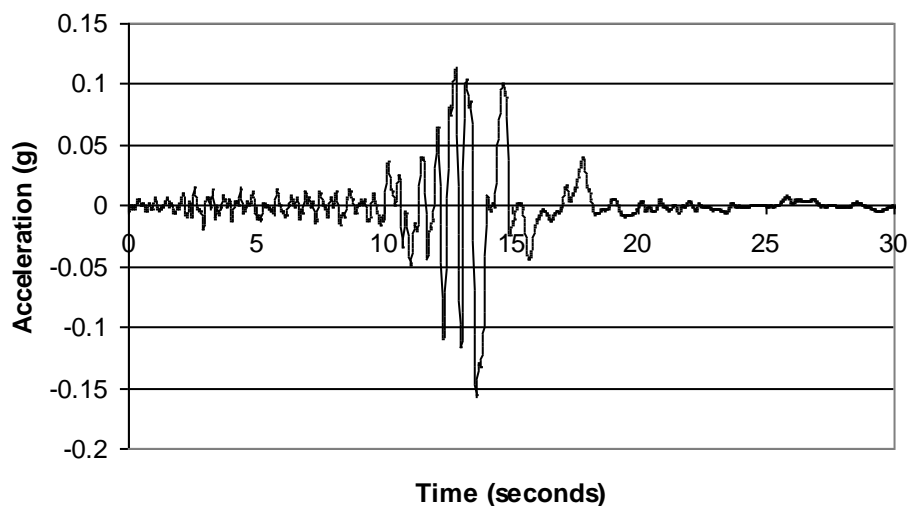


*Figure 6.6. Acceleration-Time History, Loma Prieta Earthquake [9]*

At the beginning, mechanism of the liquefaction was of primary interests, and then the interests have moved to the behavior up to or after the liquefaction. Prior to an earthquake, the water pressure is relatively low. However, earthquake shaking can cause the water pressure to increase to the point here the soil particles can readily over with respect to each other. Clean soil is the easiest soil for liquefaction to occur, but recent earthquakes showed that widespread soil from sandy silt to gravel liquefied.

There are two important features in recognizing the behavior up to and after the liquefaction. At first, effective confining stress decreases under constant shear stress amplitude loading due to negative dilatancy, resulting in

increase of shear strain or softening behavior. After stress path crossed the phase transformation line, positive dilatancy also occurs, resulting in hardening behavior when shear strain increases. Therefore hysteresis loop becomes inverse-S shape. Under the cyclic loading, effective stress gradually decreases and shear strain increases reaching liquefaction. This phenomenon is called *cyclic mobility*. Some ground failures attributed to soil liquefaction are more correctly ascribed to "cyclic mobility" which results in limited soil deformations without \* liquid-like flow.

Soil liquefaction and related ground failures are commonly associated with large earthquakes. In common usage, *liquefaction* refers to the loss of strength in saturated, cohesionless soils due to the build-up of pore water pressures during dynamic loading. A more precise definition of soil liquefaction is given by Sladen et al. (1985):

*"Liquefaction is a phenomenon where in a mass of soil loses a large percentage of its shear resistance, when subjected to monotonic, cyclic, or shock loading, and flows in a manner resembling a liquid until the shear stresses acting on the mass are as low as the reduced shear resistance."* In a more general manner, soil liquefaction has been defined as the transformation *"from a solid state to a liquefied state as a consequence of increased pore pressure and reduced effective stress"*. This water exerts a pressure on the soil particles that influences how tightly the particles themselves are pressed together. The concept behind liquefaction is simply stated as the loss of effective stress due to rapidly increased pore pressure. When loose cohesionless soils are saturated, rapid loading, such as seismic loading, occurs under undrained conditions. The pore water instantaneously supports the new load, and the effective stress decreases. After several stress reversals during cyclic loading, the pore pressure increases accumulate because the rapid loading does not allow for complete dissipation between loading cycles. Eventually, the pore pressure ( $u$ ) will equal the confining pressure, causing the effective stress to disappear  $\sigma_{\text{effective}} = \sigma_{\text{confinement}} - u = \sigma_{\text{confinement}} - \sigma_{\text{confinement}} = 0$ , and making the soil susceptible to liquefaction. Once a soil has liquefied, damage such as slope failures, foundation failures, and flotation of buried structures can occur [13].

Liquefaction susceptibility is evaluated based on several factors, however in 1936 Casagrande first attempted to evaluate liquefaction based on the critical void ratio concept. The critical void ratio concept describes how a soil will dilate or contract based on its void ratio and confining pressure in relation to the *critical void ratio (CVR)* line. Figure 6.7 shows the tendency of sand to move towards a state on the CVR line.

Casagrande originally made the argument that loose soils above the CVR line were susceptible to liquefaction while soils below the CVR line were not. Since Casagrande's original hypothesis, it has been observed and

shown that the CVR line is not a fine line between liquefaction potentials, but in fact liquefaction can even occur in soil that plots somewhere below the CVR line.

Liquefaction results from the tendency of soils to decrease in volume when subjected to shearing stresses. When loose, saturated soils are sheared, the soil grains tend to rearrange into a more dense packing, with less space in the voids, as water in the pore spaces is forced out. If drainage of pore water is impeded, pore water pressures increase progressively with the shear load. This leads to the transfer of stress from the soil skeleton to the pore water precipitating a decrease in effective stress and shear resistance of the soil. If the shear resistance of the soil becomes less than the static, driving shear stress, the soil can undergo large deformations and is said to liquefy. By the narrowest definition, true if *liquefaction* refers only to the flow of soil under a static shear stress that exceeds the undrained, residual shear resistance of a contractive soil. Liquefaction of loose, cohesionless soils can be observed under both monotonic and cyclic shear loads.

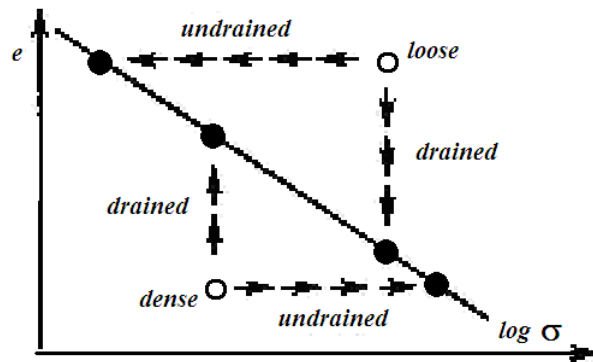


Figure 6.7. Critical void ratio line

When dense sands are monotonically sheared, the soil skeleton may first compress and then dilate as the sand particles move up and over one another. For dense, saturated sands sheared without pore water drainage, the tendency for dilation or volume increase results in a decrease in pore water pressure and an increase in the effective stress and shear strength. When a dense sand sample is subjected to cycles of small shear strains under undrained conditions, excess pore pressure may be generated in each load cycle leading to softening and the accumulation of deformations. However, at larger shear strains, dilation relieves the excess pore pressure resulting in an increased shear resistance.

Considering mechanisms of ground failure, Robertson suggested a fairly complete classification system to define "soil liquefaction" [6] :

*Flow liquefaction*, used for the undrained flow of a saturated, contractive soil when the static shear stress exceeds the residual strength of the soil. Failure may be triggered by cyclic or monotonic shear loading.

*Cyclic softening*, used to describe large deformations occurring during cyclic shear due to pore pressure build-up in soils that would tend to dilate in undrained, monotonic shear. Cyclic softening, in which deformations do not continue after cyclic loading ceases, can be further classified as:

- *cyclic liquefaction*, which occurs when cyclic shear stresses exceed the

initial, static shear stress to produce a stress reversal. A condition of zero effective stress may be achieved during which large deformations may occur.

- *cyclic mobility*, in which cyclic loads do not yield a shear stress reversal and a condition of zero effective stress does not develop. Deformations accumulate in each cycle of shear stress.

This classification system for liquefaction recognizes that various mechanisms may be involved in a given ground failure. Yet, this definition preserves the contemporary usage of the term "liquefaction" to broadly describe the failure of saturated, cohesionless soils during earthquakes.

Once the likelihood of soil liquefaction has been identified, an engineering evaluation must focus on the mode and magnitude of ground failures that might result. The National Research Council lists eight types of failure commonly associated with soil liquefaction in earthquakes:

- *sand boils*, which usually result in subsidence and relatively minor damage;
- *flow failures of slopes* involving very large down-slope movements of a soil mass;
- *lateral spreads* resulting from the lateral displacements of gently sloping ground;
- *ground oscillation* where liquefaction of a soil deposit beneath a level site leads to back and forth movements of intact blocks of surface soil;
- *loss of bearing capacity* causing foundation failures;
- *buoyant rise of buried structures* such as tanks;
- *ground settlement*, often associated with some other failure mechanism;
- *failure of retaining walls* due to increased lateral loads from liquefied backfill soil or loss of support from liquefied foundation soils.

Ground failures associated with liquefaction under cyclic loading can be broadly classified as:

- *flow failures*, occurring when the liquefaction of loose, contractive soils (that do not gain strength at large shear strains) results in very large deformations;
- *deformation failures*, occurring when a liquefied soil gains shear resistance at large strains, yielding limited deformations without loss of stability.

During the last decades progress as been made in theoretical and experimental aspects of research concerning phenomenon of liquefaction. The phenomena and problems associated with liquefaction concern saturated cohesionless soils, even if they contain considerable amount of fines. In recent years particular attention has been focused on sloping ground conditions, which although do not require earthquake loading, might result in

flow failure associated with catastrophic consequences. As a result, many researchers have attempted to describe liquefaction in the field and in the laboratory during the past approximately 40 years.

### 6.2. Methods of measurement of dynamic characteristics of soil

Various idealized models and analytical techniques may be used to represent a soil deposit and its response. Regardless of type of procedure, it is first necessary to evaluate the appropriate dynamic properties of soil. Precise measurement of dynamic soil properties is somewhat a difficult task in the solution of geotechnical earthquake engineering problems. Several laboratory and field (figures 6.8, 6.9) techniques are available to measure the dynamic properties in which many are employed in these measurements at low-strain and many are in the large strain levels.

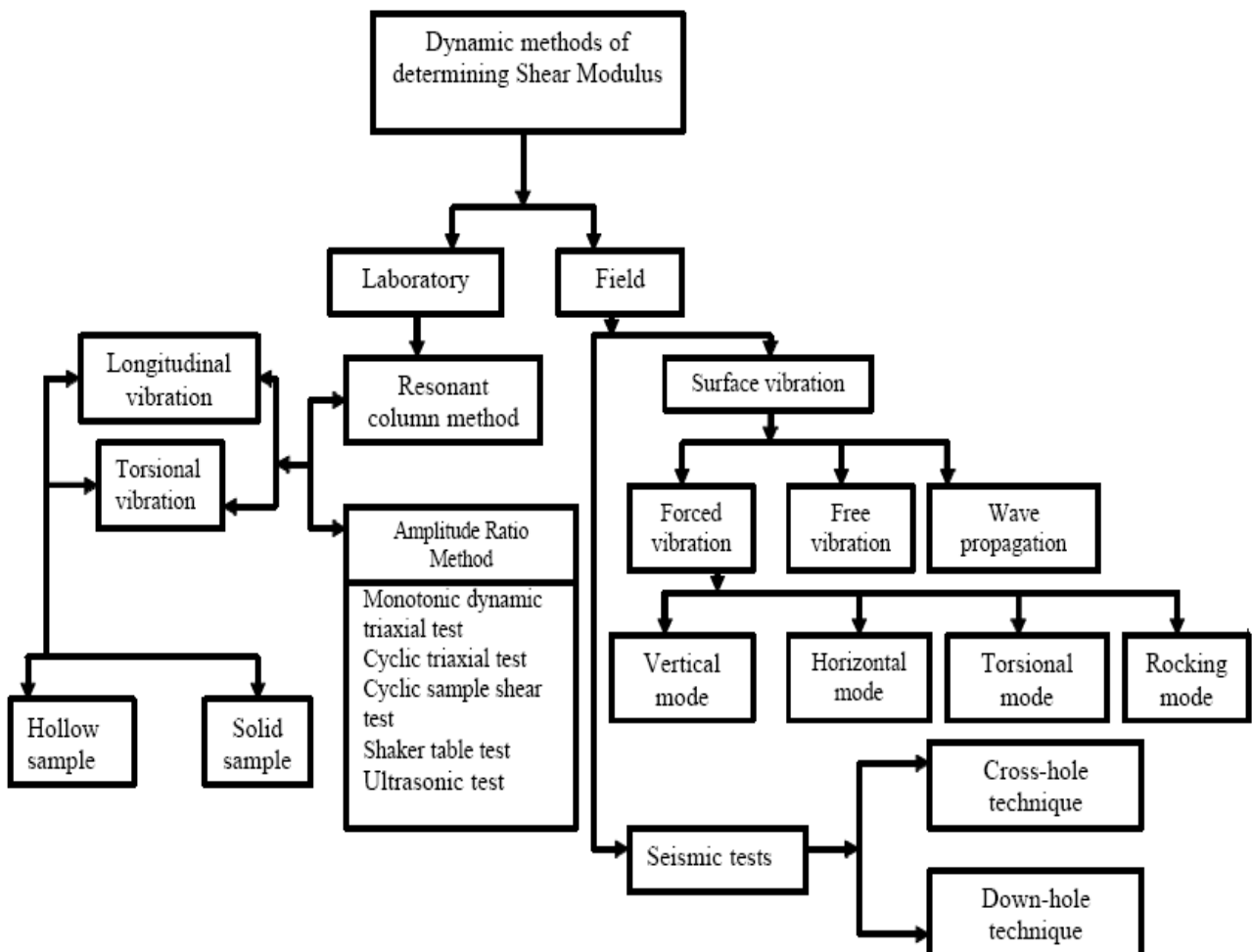


Figure 6.8. Classification of dynamic methods of obtaining shear modulus

Evaluation of dynamic soil properties by field tests has a number of advantages, as these tests do not require sampling that can alter the stress and structural conditions in soil specimens. Further, the tests measure the response of relatively large volumes of soil. However, these field tests can be again classified based on the range of magnitude of strain as low-strain and high-strain tests.

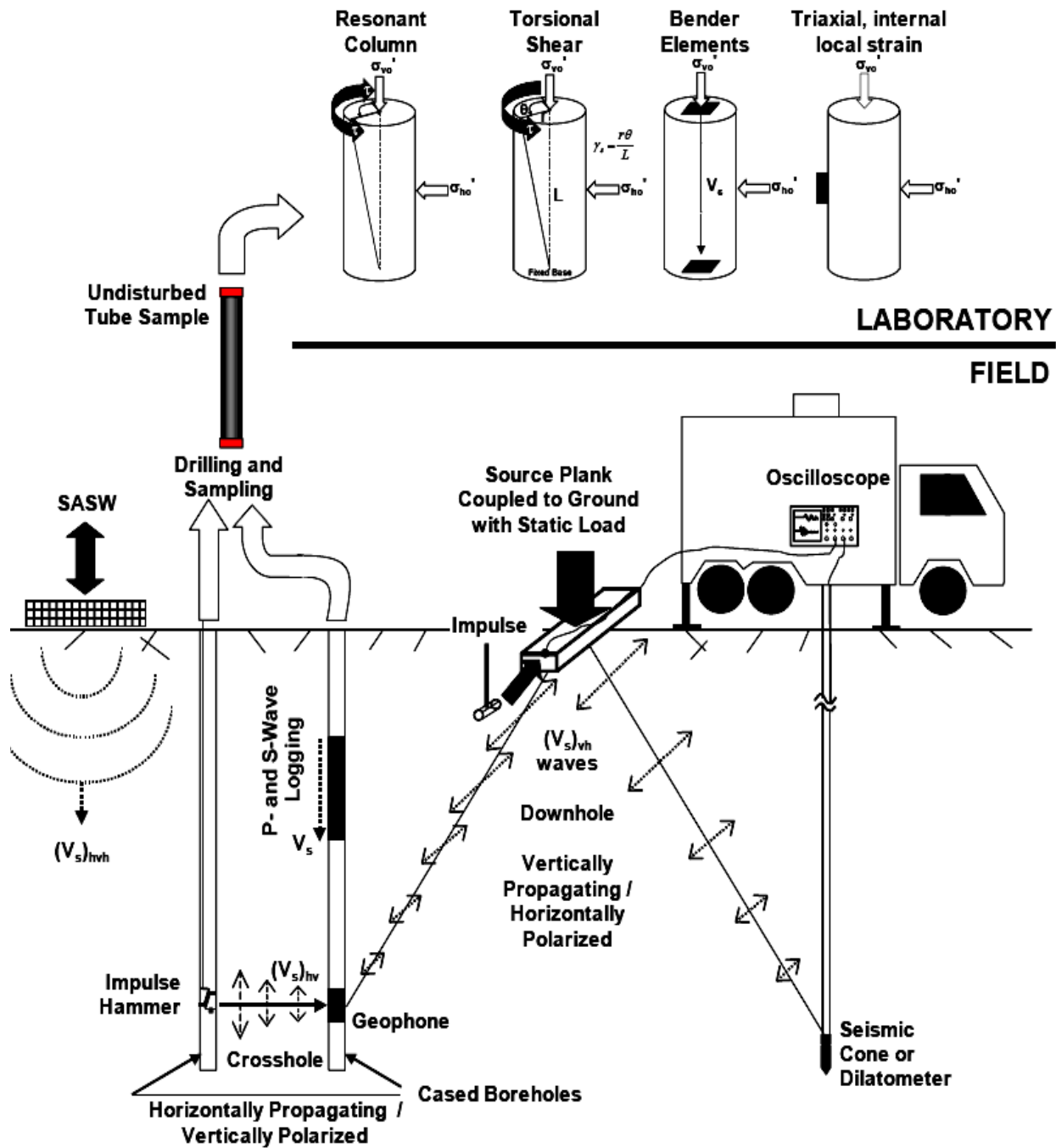


Figure 6.9. Field and Laboratory Methods for Determining Shear

**Low-strain field tests.** Dynamic soil properties depend much on the shear strain level. In the strain range below the order of 0.001%, the deformations shown by most of the soils are purely elastic and recoverable and the damping are negligible. Low-strain tests operate below the strain specified above and are based on the theory of wave propagation in the materials. Some of the low-strain field tests are seismic reflection test, seismic refraction test, suspension logging test, steady-state vibration or Raleigh wave test, spectral analysis of surface wave test (SASW), seismic cross-hole test, seismic down-hole (up-hole) test and seismic cone test.

**High-strain field tests.** At higher range of shear strains, the behaviour of soils is elasto-plastic and produces irrecoverable permanent deformations in the soil. Standard penetration test (SPT), cone penetration test (CPT), dilatometer test and pressuremeter test are of particular importance to measure high-strain characteristics of soil.

In the field (figure 6.9), seismic methods can be used for measuring the value of  $G_{max}$ . A range of seismic tests have been developed commercial including the *seismic cone penetration test* (SCPT), cross-hole and down-hole shear wave velocity measurement, and the surface wave (Rayleigh Wave) methods of SASW (spectral analysis of surface waves) that uses a hammer as the seismic source and CSW (continuous surface wave) that uses a frequency controlled vibrator as the seismic source. The field seismic methods can be divided into borehole methods and surface methods.

At small strains, particle motion resulting from propagation of shear waves is nondestructive. As  $\gamma_s$  increases past the elastic threshold shear strain,  $\gamma_{th}^e$ , the shear modulus will decrease from the maximum small strain value,  $G_{max}$ . In-situ tests have commonly been assumed to be small strain ( $\gamma_s < \gamma_{th}^e$ ), and the measurement of shear wave velocity will be directly related to the maximum shear modulus. However, at shallow depths it has been noticed that shear strains above the threshold strain may be reached during DHT, and thus a strain-based correction factor may be necessary to obtain  $G_{max}$ .

Tests are performed to assess ground motion amplification parameters and liquefaction susceptibility of soils. Many dynamic properties can be obtained through in situ tests that limit sample disturbance, which is inherent in laboratory samples. The laboratory methods have been determined with small samples and the level of displacement is very different. However, they have the advantages of controlled testing and being economical. To develop a greater confidence of the results of in-situ tests, it is helpful to compare field results to conventional laboratory tests. In the laboratory, parameters such as shear strain, confining pressure, frequency, number of loading cycles, void ratio, and **overconsolidation ratio** (OCR) can be varied to analyze soil response. In addition to these parameters, tests on undisturbed specimens provide insight into the effect of the degree of weathering for residual soils.



Analysis of in-situ test data can estimate soil parameters (such as void ratio and OCR) that will affect the maximum small-strain shear modulus,  $G_{max}$ , but the confidence in these correlated values for residual silty sands is not high without laboratory confirmation. A comparison of laboratory and in-situ measurements in soils was undertaken to better define mechanisms affecting  $G_{max}$ . The system can apply a uniquely.

The choice of a particular technique depends on the specific problem to be solved. Figure 6.10 shows the changes in soil properties with shear strain.

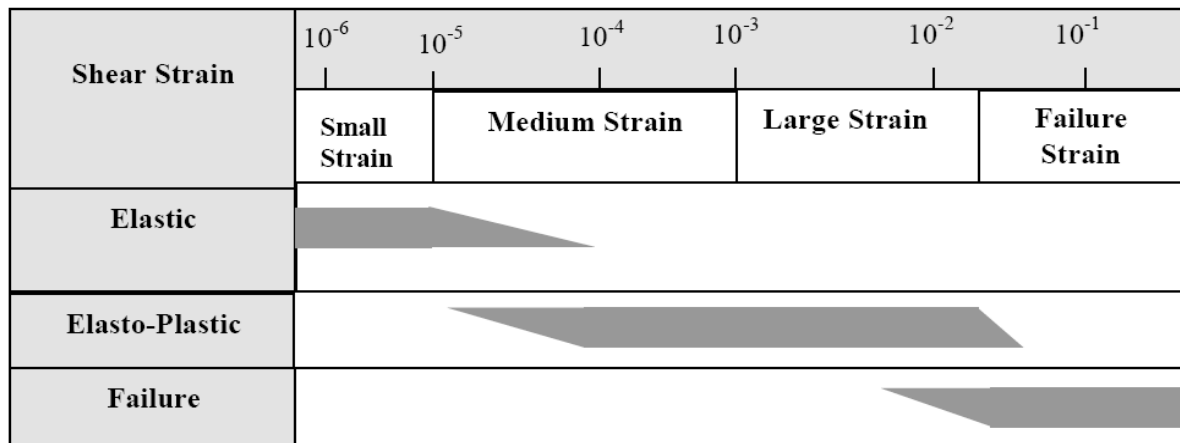


Figure 6.10. Changes in soil properties with shear strain

**Low-strain laboratory tests.** Very few laboratory tests are available to measure the dynamic properties of soils at low strain levels. For very small strain measurements *ultra-sonic, resonant column test* and *the piezoelectric bender element test* are the commonly employed techniques. Among these methods, the resonant column method is popular. There are different versions of this method using different end conditions for the sample.

**High-strain laboratory tests.** For the measurement of strain-dependent dynamic properties, several devices have been developed. Typical examples are *cyclic triaxial test* and *cyclic direct simple shear test devices*.

Figure 6.11 presents the typical variation of the normalised shear modulus  $G/G_{max}$  with shear strain  $\gamma$ . The stress-strain relationship can be expressed as a function of  $\gamma$  by:

$$G / G_{max} = 1 / [ 1 + a \gamma ( 1 + 10^{-b\gamma} ) ] \quad (6.8)$$

where the coefficients  $a$  and  $b$  are soil type dependent.

At small strains ( $\gamma < 10^{-5}$ ) the shear modulus  $G_{max}$  (or  $G_o$ ) is independent of the strain level.  $G_{max}$  can be obtained from resonant column tests in the laboratory but results are necessarily affected by sample disturbance. The most reliable measurement of  $G_{max}$  is by seismic testing (e.g. cross-hole

testing). It has been shown that in stiff to very stiff materials laboratory tests can underestimate the dynamic shear modulus by a ratio of 2 to 3.

At shear strains between  $10^{-5}$  and  $10^{-4}$  the relative decrease of the shear modulus is moderate and can be obtained from resonant column (RC) tests.

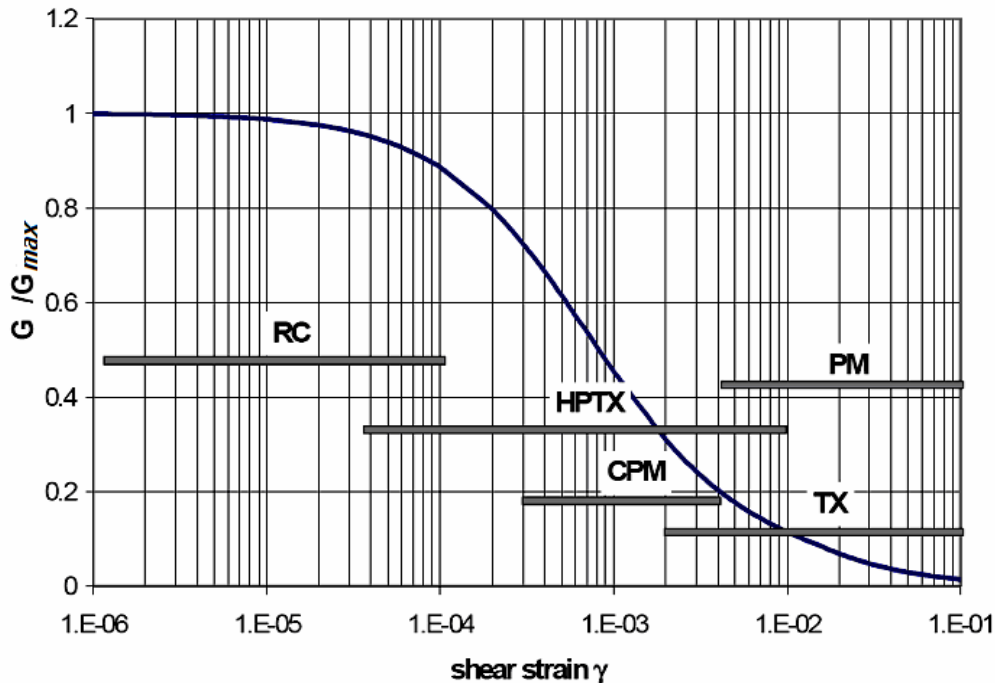


Figure 6.11. Typical variation of normalised shear modulus: RC: resonant column; TX: triaxial test; HPTX: high precision triaxial test; PM: pressuremeter test; CPM: cyclic pressuremeter test [16]

Above  $10^{-4}$  the  $G/G_{max}$  ratio drops to reach values below 0.3 beyond  $10^{-2}$ .

This latter value is representative of deformations obtained in standard triaxial (TX) testing, failure of samples being obtained for a few percent of axial deformation.

Soil deformations governing settlements of structures and soil-structure interactions are in the range  $10^{-4}$  to  $0.5 \times 10^{-2}$ . It is now recognised that a sound knowledge of the complete stress-strain relationship of the soil is required to make a realistic assessment of soil deformations under the influence of foundation loads. This has raised the need for developing high precision laboratory testing equipments (e.g. high precision triaxial controlling deformations till about  $10^{-5}$ ) and improved in-situ testing procedures (e.g. cyclic pressuremeter testing recording deformations in the range  $10^{-3}$  to  $10^{-4}$ ). There is also a consensus to call for seismic measurements of the  $G_{max}$  value which is considered as a reference property of the material (independent of strain in the quasi-elastic domain).

Table 6.1 shows the appropriate strain ranges for respective soil test methods and deformation characteristics. The most common tests are listed below.

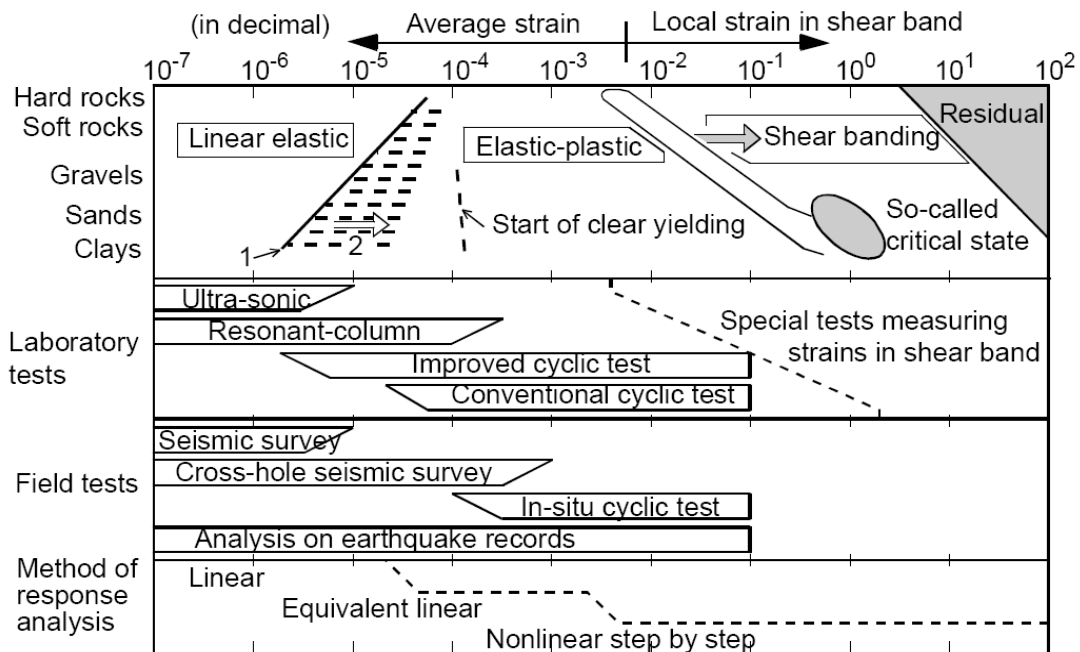
Table 6.1

Dynamic property tests [1]

METHOD		Deformation Characteristics				Strength
		Compression Modulus, E	Shear Modulus, G	Poisson's Ratio, $\mu$	Damping Factor, D	Dynamic Shear Strength
Laboratory Test	Cyclic triaxial compression	○	□	○	○	○
	Cyclic simple shear test		○		○	○
	Ultra sonic Pulse test	○	○	□		
	Resonant column test	○	○	□	○	
	Torsion Shear test		○		○	○
	Ring Shear test		○		○	○
Field survey	Seismic Survey Refraction, Reflection, Crosshole, Downhole, Surface Wave Methods	□	□	□		
	Resonant footing	□	□	□	□	
	Cyclic Pressuremeter	□	□	□		
	Standard Penetration Test	△	△		△	

- : The property is directly determined
- : The property is indirectly determined
- △ : The property is estimated based on many experimental data.

Figure 6.12 shows strain dependent characteristics of rock and soil, laboratory and field tests, methods response analysis. As shown in the figures 6.12 and 6.13, soil exhibits nonlinear nature even at small strains.



1. For normally consolidated soils subjected to monotonic loading
2. Increases as OCR increases and with cyclic loading

Figure 6.12. Strain dependent soil properties, measurement, and analysis [31]

During the late 1980s and early 1990s, dynamic soil stiffness was measured in the laboratory using small strain resonant column apparatus. Investigators were struck by the similarity of these dynamic modules to static module back-analysed from movements around real static structures like retaining walls and excavations. They then realised the differences in moduli measured in the past between static tests (like the conventional triaxial) and dynamic tests (like the resonant column) were related to strain level- i.e. one test measured small strain module and the other large strain module, not to the fact that one test was "dynamic" and the other "static". More recently, the value of  $G_{max}$  (the value of the shear modulus at very small strains) has been treated as a fundamental soil property that is particularly useful in finite element modelling. This means there is much interest in the measurement of  $G_{max}$  both in the laboratory and field.

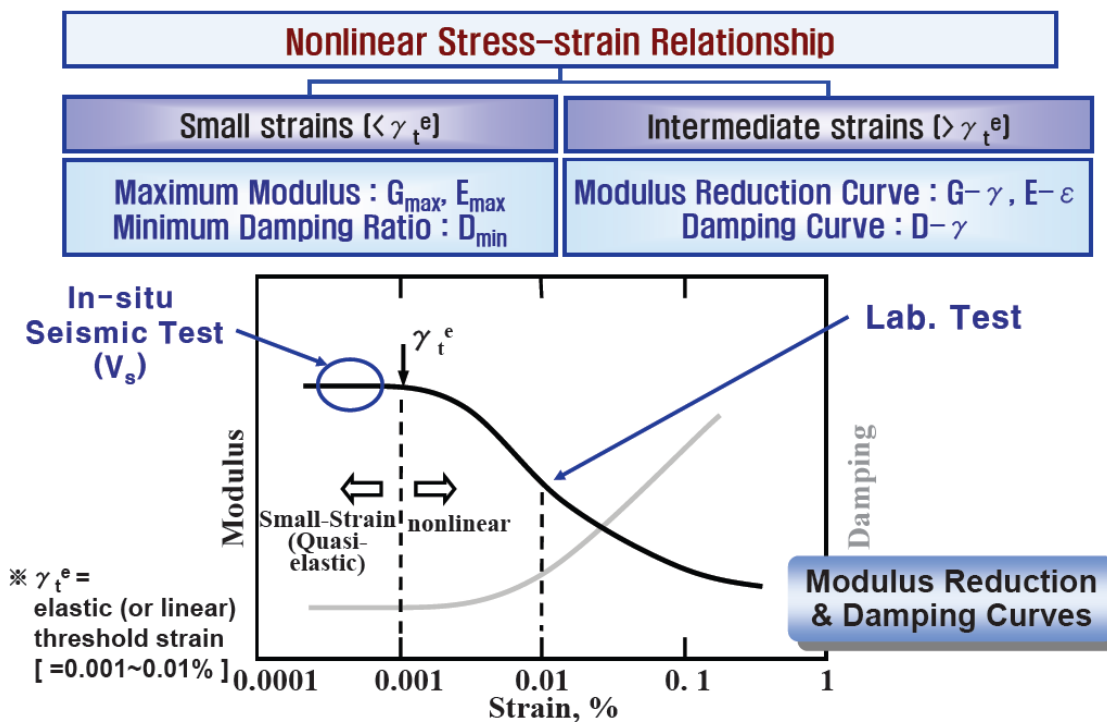


Figure 6.13. Deformational characteristics of soils

The difference between static and dynamic loading conditions is in the term of time of loading and is expressed in terms of speed of loading or rate of straining (speed effect or rate effect). If load application last more than 0.1 sec then we have "static problems" and if load application have a shorter time of application we have "dynamic problems". *Cyclic tests* are low-frequency (<0,1 Hz), *dynamic tests* are high frequency spectra are in the 0,1-10 Hz range (figure 6.14).

• **Modulus by Testing Condition**

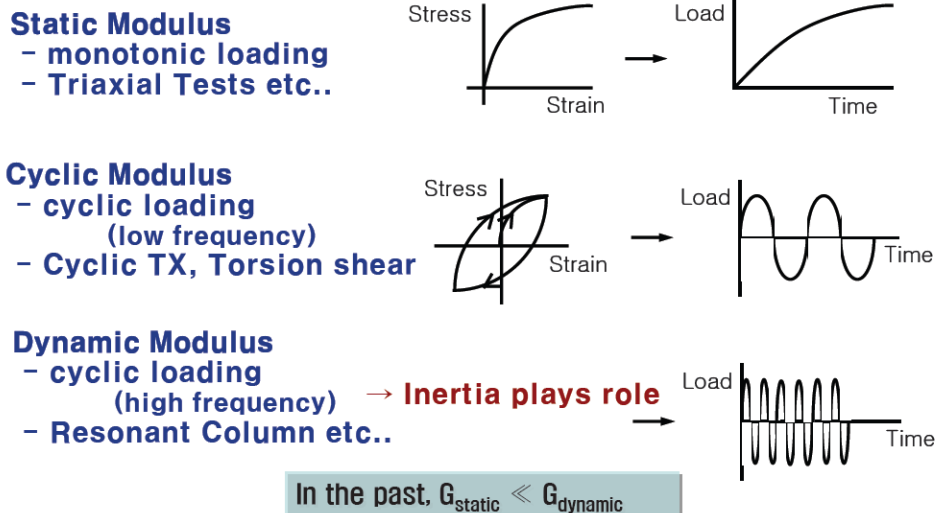


Figure 6.14. Static, cyclic, dynamic soil properties

**6.3. Laboratory tests of soil**

**6.3.1. A brief introduction to experimental laboratory devices**

The analysis and the understanding of the mechanical behaviour of soils cyclically and/or dynamically loaded can be considered up till now among the most stimulating subjects of soil mechanics, in particular, when large strains as well as a large spectrum of frequencies are taken into consideration and the problem of the coupling between volumetric and shear irreversible strains is analysed.

Usually, this subject is studied by starting from two opposite points of view. The cyclic mechanical behaviour is highlighted by means of sophisticated constitutive models capable of reproducing the volumetric-deviatoric coupling and the irreversibility of the constitutive relationship, and by disregarding at all the time factor. On the contrary, the dynamic mechanical response is tackled by means of elasto-viscous approaches that are linear and allow us to solve boundary value problems in the frequency domain. Solely in the last decade non-linear numerical analyses of dynamic problems have been performed, but, as far as constitutive modelling is concerned, according to the authors, a great effort of synthesis of the different experiences must still be done.

These few following part will be devoted to enumerate the experimental devices that are usually employed, to describe the experimental results and finally to critically analyse some constitutive approaches conceived to highlight some aspects of the problem and suggest new research items.

In the last thirty years many experimental test series were performed with the aim of describing and highlighting the mechanical behaviour of soils under cyclic and dynamic loads both in drained and undrained conditions. When cyclic tests are considered, a quasi-static evolution of the material microstructure is assumed, inertial forces are negligible but the time factor can play a role because of the time dependency of the material mechanical behaviour. When dynamic and impulsive tests are taken into consideration, the interpretation of the mechanical problem becomes more complex *because the time dependency of the mechanical behaviour is superimposed to the inertial effects.*

Finally, even the number of cycles as well as the amplitude that characterise the loading disturbance are important peculiarities of the problem. When seismic actions are taken into consideration, the number of cycles is quite small but the cyclic load amplitude can be considerable. On the contrary, when wind actions, travelling loads or vibrating machine foundations are considered, the loading cycle amplitude is smaller but the representative number of cycles is enormous.

The most widespread experimental test apparatus to study the cyclic mechanical behaviour of soils are the triaxial cell, the simple shear and the torsional shear device. Whereas, the resonant column and more recently the torsional shear device are employed to study the dynamic mechanical response.

1. Triaxial cyclic experimental test series are usually performed to analyse the problem of cyclic liquefaction of saturated granular materials. Both compression and extension cycles in the effective triaxial plane ( $q-p'$ , where  $q = \sigma_a - \sigma_r$ ,  $p' = (\sigma_a' + 2\sigma_r')/3$ ,  $\sigma_{ij}' = \sigma_{ij} - u\delta_{ij}$ ,  $u$  is the pore pressure and  $\delta_{ij}$  is the Kroneker symbol) are usually performed. The number of cycles necessary to reach in undrained conditions the material liquefaction is evaluated and the effective stress path is recorded. Usually, the total stress path is imposed, the axial load is cyclically varied and both pore pressure and axial strain are recorded. The type of consolidation (oedometric or isotropic), the consolidation pressure, the relative density of the specimen, the initial stress level, the strain history are usually varied.

When soil specimens are tested in drained conditions, a viscoelastic approach is usually assumed to interpret the material mechanical response. The single loop in the  $q - \varepsilon_a$  plane is taken into consideration and the pseudo-elastic stiffness  $E$  as well as the damping ratio  $D$  are directly evaluated from the stress-strain curve. A more detailed definition of these parameters is introduced here below.

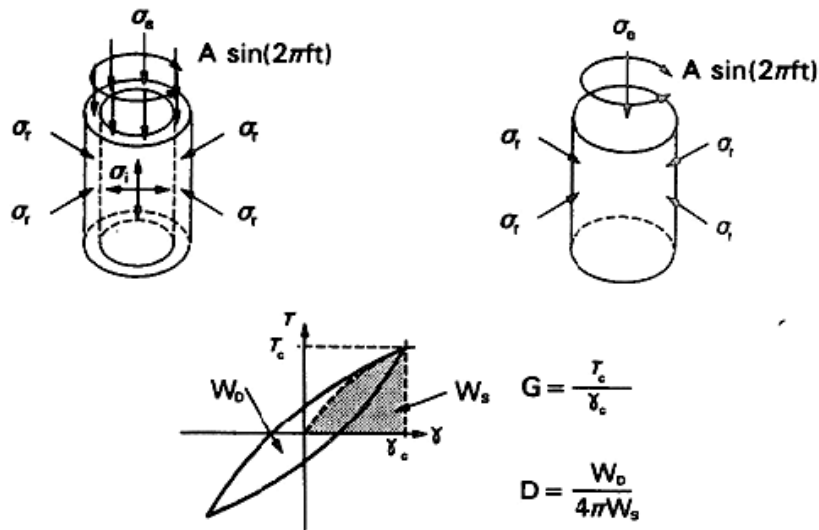


Figure 6.15. Stress state and schematic interpretation of results in a cyclic torsional shear test

2. Conversely to the triaxial cell, the simple shear test is conceived to reproduce the stress paths followed by soil layers during seismic ideal events. The initial state of stress is imposed to be oedometric and the cyclic perturbation is characterised by the change in the value of the shear stress  $\tau$ . Analogously to the triaxial apparatus, as is synthetically illustrated in figure 6.15 with reference to the torsional shear device, these tests allow the direct evaluation both of the shear stiffness  $G$  and of the shear damping  $D$ .

3. The torsional shear test puts together some peculiarities of the two previously cited laboratory experimental apparatus. Cyclic shear stresses (it is worth noting that in this case the cylinder is hollow) imposed by means of a torque moment applied along the vertical axis (figure 6.15) are superimposed to a general triaxial state of stress. By recording the applied torque moment and the relative rotation, it is possible to evaluate the corresponding stress paths within the soil specimen. If the internal and external pressures are independently controlled the principal axis rotation of the state of stress can be uncoupled of the change in the stress level.

In all the three test apparatus cited above the loading history is assumed to be quasistatic and inertial forces are disregarded. Sometimes, to evaluate the stiffness of a soil at very small strain levels, impulse tests are performed. The perturbation frequencies are largely higher than those characterising the natural frequency of the soil sample. The state of stress is a priori imposed by means of the test apparatus employed and the propagation rates of  $p$  and  $s$ -waves within the soil specimen are recorded.

4. The resonant column is a triaxial apparatus equipped with a cyclic torsional loading system (figure 6.16). It is based on the theory of wave propagation in prismatic rods. The axial and radial stresses are usually kept constant during the test and they define the initial state of stress. On the

contrary, the torsional loading frequency is changed continuously to obtain the soil specimen resonance. Sometimes, compression waves instead of shear waves are propagated through the soil specimen. The resonant frequency is a function of the soil specimen mass and of the material shear stiffness  $G$ . Damping is determined by switching off the driving power at resonance and recording the amplitude of the decaying vibrations.

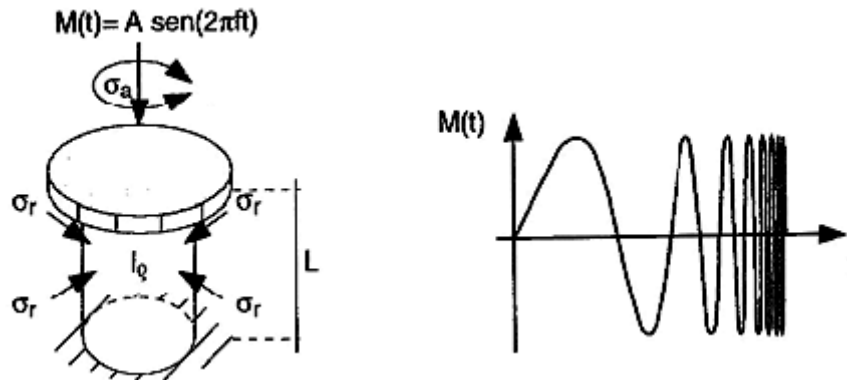


Figure 6.16. Stress state in a resonant column apparatus

### 6.3.2. Resonant Column Test

Resonant column technique is the most common method for measuring  $G_{max}$  in the laboratory. It involves in a special device where a cylindrical or hollow specimen is excited torsionally or axially and turned to resonance.

The Resonant column test is used to determine the shear modulus ( $G_{max}$  or  $G_0$ ), young's module  $E$  and damping  $D$  characteristics of soils at small strains for cases where dynamic forces are involved, particularly seismic ground amplification and machinery foundations. The values obtained in the torsional resonant column apparatus are normally associated with shear strains of  $10^{-6}\%$  to  $10^{-2}\%$ . These tests are usually performed on cohesive soils to determine the ground motion amplification parameters. Recent research has shown the results are also applicable to static loading at very small strains; for example. At measurements of shear modulus and damping can be done at any consolidation stage under isotropic or anisotropic stress conditions.

The resonant column apparatus (figure 6.17, a) gives the capability of measuring the shear modulus and damping ratio for a cylindrical test specimen. Prepared cylindrical specimens are placed in a special triaxial chamber and consolidated to ambient overburden stresses. One end of the test specimen is fixed and the other end is excited with a very small sinusoidal rotational displacement (figure 6.17, b). Very low amplitude torsional vibrations are applied to one end of the specimen by use of a special loading cap with electromagnetic. The resonant frequency, damping, and strain amplitudes are measured by the use of motion transducers.



From a knowledge of the specimen and the resonant frequency, the value of the wave propagation velocity and hence shear modulus can be found.

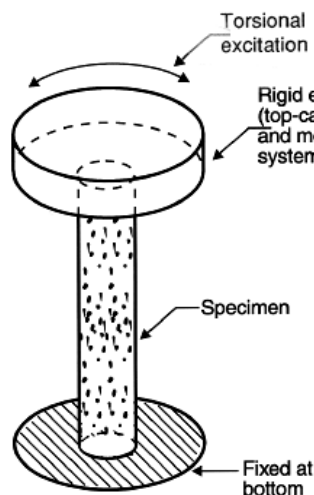
Resonant column test readings are taken at time similar to that of a consolidation test (i.e. 1, 2, 4, 8, 15, 30, 60, 120 min. etc.) and at times well into secondary consolidation. The resonant column measurements are normally made at constant shear strain level,  $10^{-3}\%$  or lower, with an accuracy of  $\pm 10\%$ . At the end of each consolidation phase, a series of readings at increasing levels of shear strain starting at the lowest possible level are taken.  $G_{max}$  is checked after measurements taken at larger shear strains.

There are two types of resonant column equipment, *the Drnevich and the Stokoe apparatuses*. In the Drnevich apparatus, isotropic and anisotropic consolidation can be applied and it is possible to shear the specimen to failure after testing as in a standard triaxial test. In the Stokoe apparatus, only isotropic consolidation is possible, and the specimen can not be sheared to failure. However, larger torque can be applied than in the Drnevich apparatus.

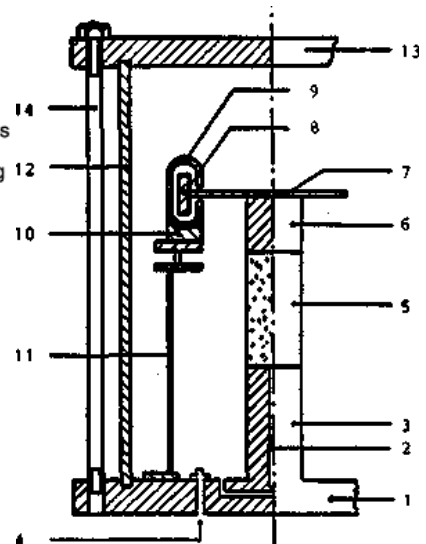
The Stokoe Apparatus is shown in cross-section in figure 6.17, c [5]; numbers in brackets refer to the numbered components. The sample (5) is enclosed in a rubber membrane placed between a lower platen (3) and a top cap (6), both of which were roughened to provide torsional coupling. A cruciform loading arm (7) carries permanent magnets (8) which can oscillate freely within coils (9). The coil assembly is mounted on an adjustable holding ring (10) supported by an outer sleeve (11). All this, is enclosed within a pressure sleeve (12) and end plates (1 and 13), retained by tension bolts (14). Cell pressure is provided by compressed air. Pore pressures may be measured by connecting a line (2) through the base.



a)



b)



c)

Figure 6.17. Resonant column test: a) resonant column apparatus, b) scheme of fixed free resonant column tests, c) scheme of Stokoe apparatus

The frequency of the input vibration is changed until the resonant (frequency) condition is determined. There resonant frequency, the geometry of the sample, and its conditions of end restraint provide the necessary information for calculating the velocity of wave propagation in the soil under the given conditions. From this, the small strain shear modulus,  $G_{max}$ , can be computed.

GUS Instruments has developed a novel resonant column apparatus enabling tests to be carried out at a range of confining pressures from low to very high (up to 25 MPa). The apparatus also has the option of temperature control from  $-30^{\circ}\text{C}$  to  $+50^{\circ}\text{C}$ . In addition to the normal torsional mode of excitation the GUS resonant column can also use a vertical bending mode of excitation. The system is fully supported by software to allow the selection of excitation mode under computer control.

Results from resonant column testing of light castle sand are showed in figure 6.18. Also the presentation of results test are normally in the form of:  $G_{max}$  vs. log time;  $G$  vs. log shear strain; damping ratio vs. log time; damping ratio vs. log shear strain. Generally, the RCT is considered a nondestructive test and the material properties are essentially unchanged during the small-strain torsional loading. Therefore, it is common that the same specimen can be subjected to several levels of effective confining stress. Experience with the RCT on soils indicates that  $G_{max}$  is a function of void ratio and mean effective confining stress, as well as cementation, aging, saturation, and other factors. A well-known expression is:

$$G_{max} = (625/e^{1.3})(\sigma_{ATM} \sigma_0')^{0.5} OCR^k \quad (6.9)$$

where  $k=(PI^{0.72})/50$  and  $\sigma_{ATM}$  = atmospheric pressure (1 bar =100 kPa = 1 tsf).

The resonant frequency is a function of soil stiffness, sample geometry, and boundary conditions of the device. For the case of fixed base and free top, shown in figure 6.17, b , the frequency at first resonance is either [19]:

$$f_s = \frac{v_s}{4h} = \frac{\sqrt{\frac{G_{max}}{\rho}}}{4h} \quad (6.10)$$

in the torsional mode, or

$$f_L = \frac{v_L}{4h} = \frac{\sqrt{\frac{E}{\rho}}}{4h} \quad (6.11)$$

where  $h$  is the height of the sample and  $E$  is the Young's modulus of the soil.  $E$  is relevant to  $G_{max}$  by  $E=2(1+\nu)G_{max}$ .

For a solid cylindrical specimen of height  $h$ , the shearing strain  $\gamma$  at radius  $r$  is calculated from

$$\gamma = \alpha r / h \quad (6.12)$$

where  $\alpha$  is the angle of twist in radians. In the resonant column test, the angle of twist is calculated using measurements of the resonant frequency and acceleration levels.

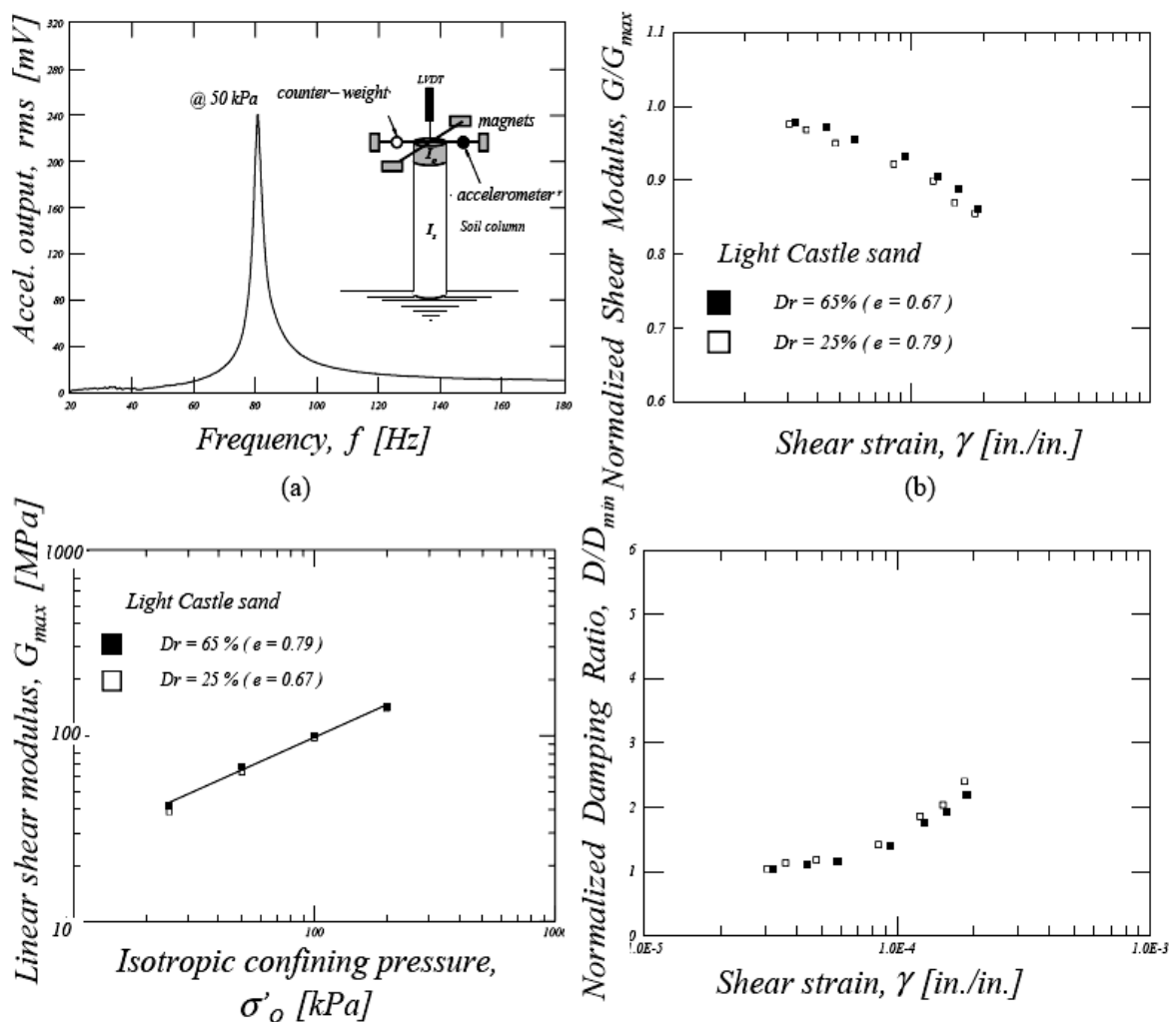


Figure 6.18. Results from resonant column testing of sand: a) measured resonance at a given effective confining stress and shear strain; b) normalized modulus reduction ( $G/G_{max}$ ) with shear strain; c) variation of small-strain shear modulus ( $G_{max}$ ) with effective confining stress level; d) damping ratio  $D$  increase with shear strain [15]

The dynamic shear modulus of the soil is determined from the resonant frequency, specimen dimensions, and system constants. The shear wave velocity,  $V_s$ , from resonant column tests is calculated on the basis of the theory elasticity as

$$V_s = 2 \pi h / (\beta \rho) \quad (6.13)$$

where  $\beta$  is a function of mass polar moment of inertia  $c$  both soil specimen and resonant-column drive system an is found from

$$I/I_0 = \beta \tan(\beta) \quad (6.14)$$

where  $I$  is the mass polar moment of inertia of soil specimen, and  $I_0$  is the mass polar moment of inertia of the resonant-column drive system (figure 6.19). The shear module,  $G$  is calculated from formula 6.4.

The damping ratio is determined from the free-vibration decay curve, which is generated by shutting off the input signal at resonance. A typical free-vibration decay curve from a resonant-column test is shown in figure 6.20. The damping ratio  $D$  is calculated from the logarithmic decrement 5 of the decay curve as follows:

$$D = \frac{\delta}{4\pi^2 + \delta^2} \cdot 100 \quad (6.15)$$

where

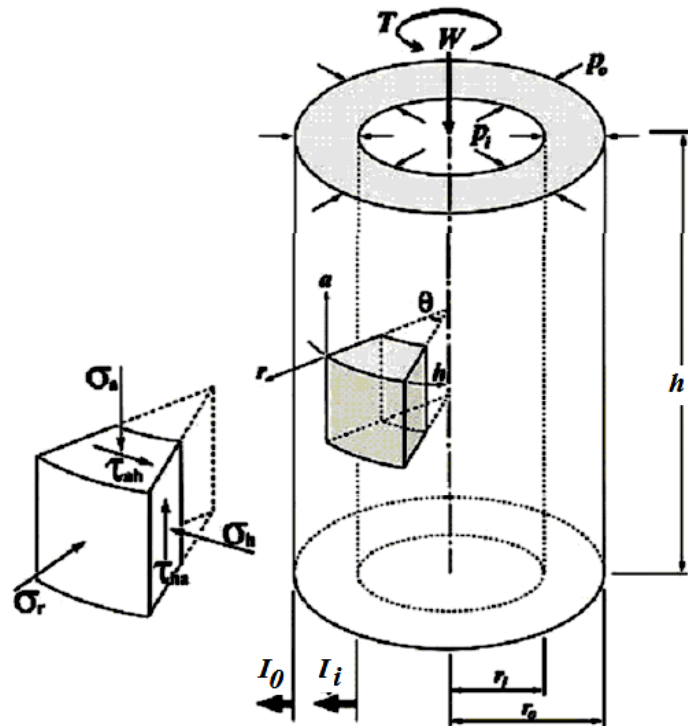


Figure 6.19. Sample characteristics: Sample dimensions:  $H$  - sample height,  $r_i$  - sample inner radius,  $l_i$  - radial movement of inner wall (mm),  $r_o$  - sample outer radius,  $l_o$  - radial movement of outer wall (mm), applied force and pressures:  $W$  - applied axial load (N),  $T$  - applied torque (N B·m),  $P_i$  - confining inner cell pressure (kPa),  $P_o$  - confining outer cell pressure (kPa), applied stresses :  $s_a$  - axial (vertical) stress,  $s_r$  - radial stress,  $s_h$  - horizontal (circumferential) stress,  $t_{ah}$  - shear stress

$$\delta = \frac{1}{n} \ln\left(\frac{z_1}{z_{n+1}}\right) \quad (6.16)$$

where  $z_1$  and  $z_{n+1}$  are the amplitudes of cycles 1 and  $(n+1)$ , respectively.

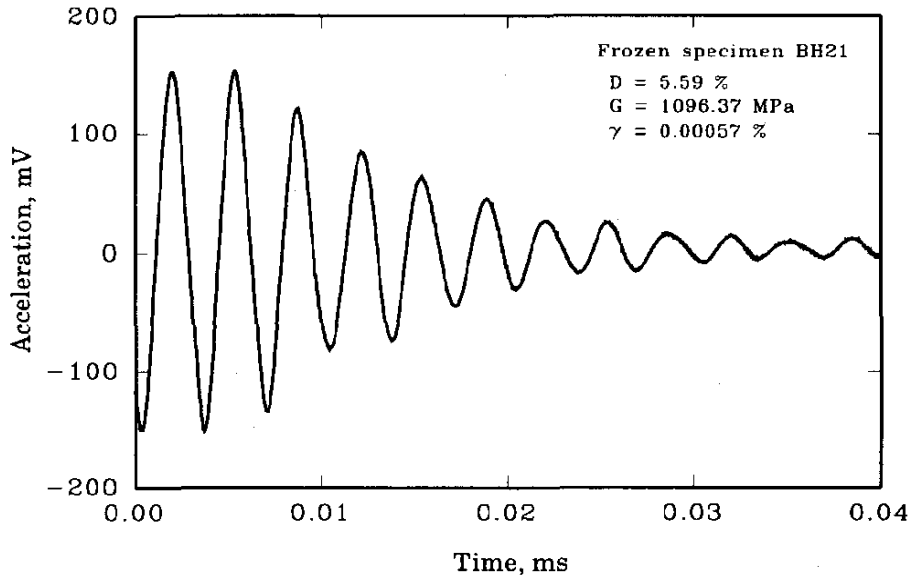


Figure 6.20. Typical free-vibration decay curve

Although field methods such as the crosshole, downhole, surface wave, and suspension logging techniques provide direct in-situ measurements of  $V_s$ , the RCT is *advantageous* in that it can evaluate the variation (decrease) of  $G_{max}$  with increasing shear strain  $\gamma_s$ , as well as the increase of damping  $D$  with  $\gamma_s$ . There are however significant time (soil aging) effects, which can lead to lower values than obtained in the field.

### 6.3.3. Cyclic Triaxial Test

The most widely used of the cyclic loading laboratory tests is the cyclic triaxial test. In this test a cyclic load is applied to a column of soil over a number of cycles slowly enough that inertial effects do not occur. Cyclic load is usually applied as cyclic axial load by mechanical, hydraulic or pneumatic actuator. This test is usually performed on sands to determine liquefaction susceptibility although it can also be used to obtain ground motion amplification parameters. Normally these tests are carried out in the undrained state to study the build-up of pore pressure with number of cycles and the consequent reduction in stiffness and strength.

One of the first pieces of equipment designed to test cyclic triaxial loading was the pendulum loading apparatus by Casagrande and Shannon in 1948. This apparatus utilizes a weight on a pendulum to apply regular loading and unloading cycles to the triaxial test. Several other apparatus

have been developed since 1948 that can apply cyclic loads, but the goal of any cyclic triaxial test is to model cyclic shear stress conditions.

According to Das, 1983, the specimen is first loaded with a total normal stress of  $\sigma_3$ . The stresses on the specimen are then altered to an axial stress of  $\sigma_3 + \frac{1}{2}\sigma_d$  and a radial stress of  $\sigma_3 - \frac{1}{2}\sigma_d$ . Next, the specimen is loaded so that the axial stress is  $\sigma_3 - \frac{1}{2}\sigma_d$  and the radial stress is  $\sigma_3 + \frac{1}{2}\sigma_d$ . According to this loading series, the shear stresses on the X-X and Y-Y planes oscillate between  $\pm\frac{1}{2}\sigma_d$ . For saturated sands, Das explains that undrained laboratory tests can be performed by applying the same all around normal stress of  $\sigma_3$  and a cyclic load of  $\sigma_d$  in the axial direction only. Measurements can be made for axial strain, pore water pressure, and the number of cycles of  $\sigma_d$ . In order to achieve the loading conditions, a pore pressure  $u = \frac{1}{2}\sigma_d$  must be subtracted from the observed loading condition and added to the loading condition [8].

Seed studied liquefaction using the cyclic triaxial apparatus with the stress conditions described by Das above. As with the cyclic shear tests, the sample liquefied when the pore pressure equaled the confining pressure, increasing the cyclic shear stress caused liquefaction in a fewer number of cycles, and increasing the confining pressure caused liquefaction in a greater number of cycles.

The cyclic triaxial test is typically performed using conventional triaxial testing equipment that has been modified to allow application of a cyclic deviator stress (figure 6.21). The cyclic deviator stress is usually applied harmonically at periods of 1 to 60 sec. Test specimens are consolidated isotropically (occasionally anisotropically) and subjected to a series of cycles of constant amplitude loading.

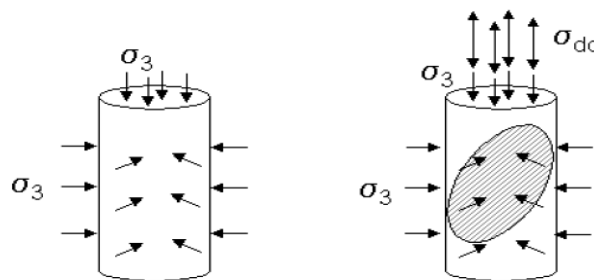


Figure 6.21. Stress conditions on cyclic triaxial test specimen: a) before cyclic loading and b) during cyclic loading. Shaded region indicates orientation of plane of maximum shear stress.

The deviator stress, axial strain, and porewater pressure are recorded during the test; test results are most commonly expressed in terms of stress-strain loops, stress paths, and compilations of numbers of cycles to initial liquefaction (i.e., pore-pressure ratio,  $r_u = 1.0$ ) or, in the event that initial liquefaction is not reached, to some limiting axial strain (e.g., 3%).

The electromechanical dynamic triaxial testing system (figure 6.22). is a combined triaxial cell and dynamic actuator, the axial force and axial deformation being applied through the base of the cell. The cell itself is screw-driven from an integral base unit housing the motor drive. Where an optional dynamic radial actuator is not chosen, the cell is provided with a balanced ram to eliminate disturbance to constant cell pressure during dynamic testing. Data is saved and displayed in real-time for any number of cycles.

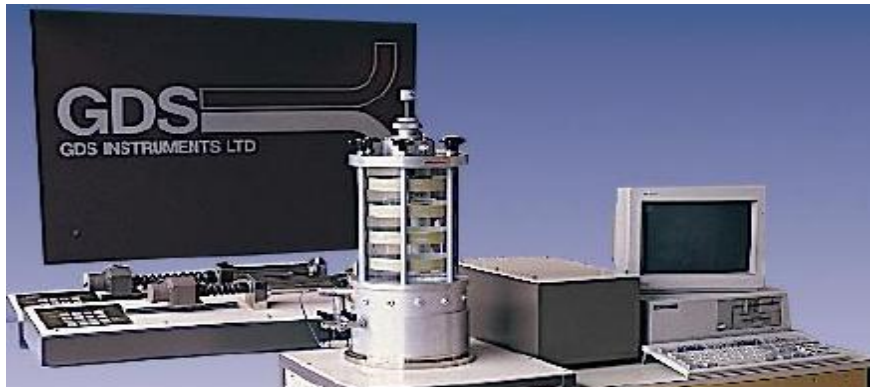


Figure 6.22. Electromechanical dynamic triaxial testing system [28]

The cyclic triaxial test allows specimens to be tested under relatively uniform stress and strain conditions, at least at low strain levels. This test has historically been the most commonly used for measuring liquefaction behavior in the laboratory, so a considerable amount of data exists. The limitations of the cyclic triaxial test, however, influence its use for measuring liquefaction behavior, most significantly in the following ways:

In a triaxial test specimen, shear stresses do not exist on horizontal planes. Schematic of triaxial apparatus and system with bender element are illustrated in figures 6.23 and 6.24. In the conventional cyclic triaxial test, maximum shear

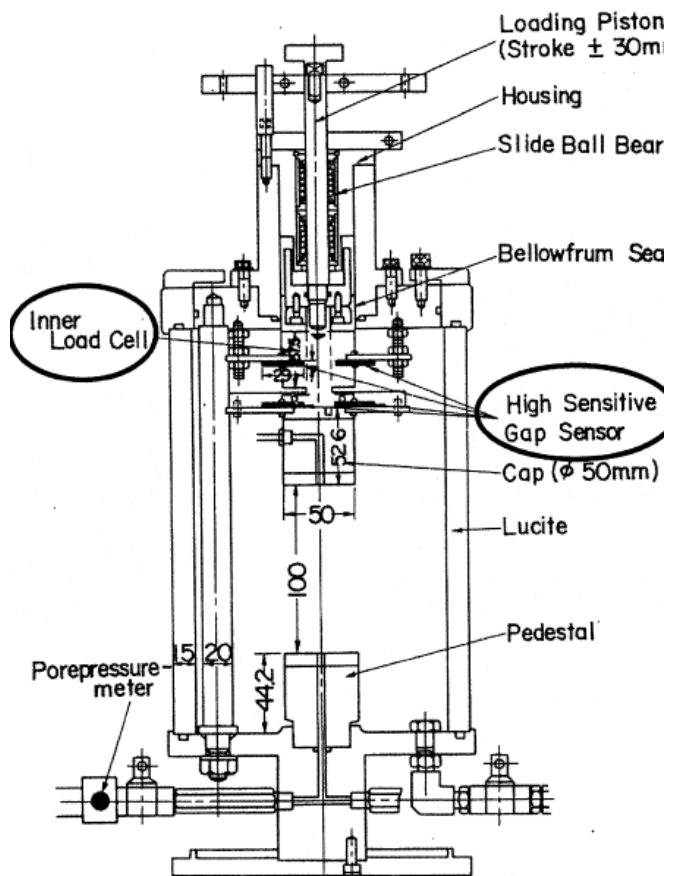


Figure 6.23. Cyclic triaxial test apparatus with inner load cells and high sensitivity sensors

stresses are imposed on planes oriented at  $45^\circ$  to the horizontal. Because most of the energy in earthquake ground motions at shallow depths is in the form of vertically propagating s-waves, shear stresses in the field act primarily in the horizontal direction. Therefore, the cyclic triaxial test does not impose shear stresses on the planes upon which they are imposed in the field. For soils with inherent or induced anisotropy, the response in the cyclic triaxial test may be different than that which would occur in the field.

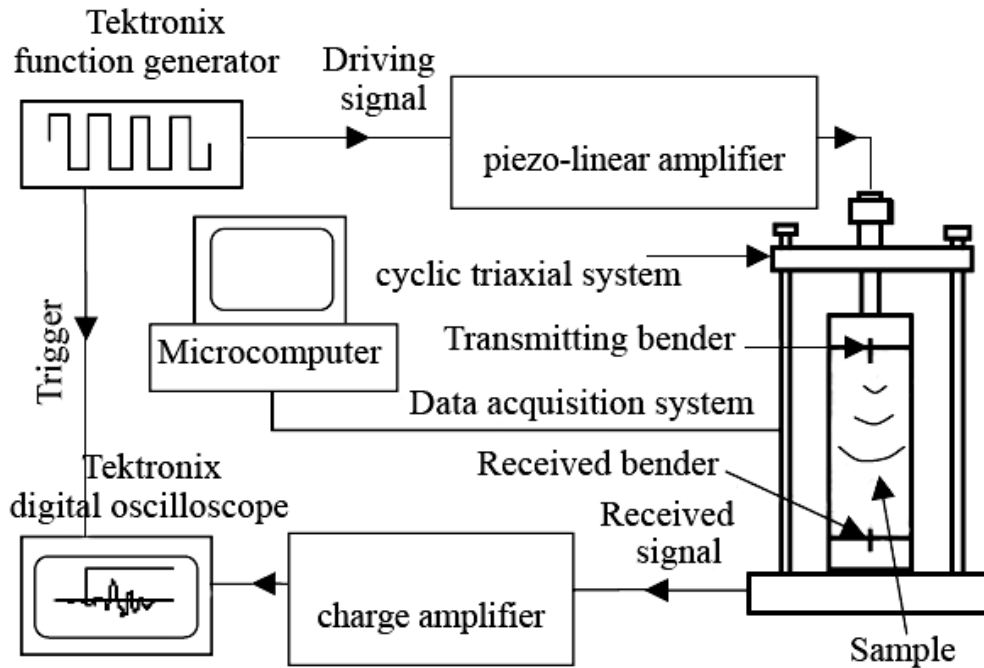


Figure 6.24. Schematic of triaxial system with bender element [10]

*Principal stress axis rotation is not realistic in the cyclic triaxial test.* In the field, the propagation of vertical SH-waves produces continuous rotation of principal stress axes. In the cyclic triaxial test, the principal stress axes remain unchanged until a stress reversal occurs; then they rotate instantaneously by  $90^\circ$ .

*Mean stress and shear stress are not applied independently.* In the conventional cyclic triaxial test, the cell pressure is held constant while the deviator stress is changed. As a result, the mean stress acting on the specimen changes during cyclic loading. At level ground sites in the field, the mean stress remains constant when subjected to vertically propagating shear waves. Cyclic triaxial testing can be performed by cycling the deviator and confining stresses simultaneously to maintain constant mean stress, but it is not common to do so.

*Stresses and strains become non-uniform.* At strain levels above 15% – 20%, changes in the shape of a cyclic triaxial specimen prevent accurate determination of the stresses and strains associated with its response. The



problem can be alleviated to some degree by the use of lubricated ends, but even these measures increase the uniform range to axial strain levels of perhaps 25% or so. Important properties of liquefiable soils, particularly the residual strength, may not be fully mobilized at these strain levels.

*Bedding errors can prevent the accurate measurement of small strain behavior.* Bedding errors occur with conventional strain instrumentation (external measurement of axial strain). Alternative instrumentation schemes, such as those that measure deformations across the central third of the test specimen, can alleviate this problem.

With the *cyclic triaxial testing device* it is possible to apply dynamic stress conditions to the sample through axial cyclic loading in vertical direction. In combination *bender element tests* are performed on the same sample allowing the analysis of results from two different tests on the same sample under identical test conditions.

Using CTTD the option of cyclic loading in vertical direction is added. The used apparatus has a very wide range of loading options, namely in axial deformation (0.01%...10%), cyclic load (+/- 5 kN), loading frequency (0...70Hz), waveshapes, drained or undrained testing, the number of applied cycles, and standard and nonstandard testing, respectively. Therewith the dynamic behavior of soil samples can be investigated under numerous cyclic loading conditions.

To measure local strains an on-specimen transducer set (LVDT's) is used. Simple external deformation measurements may be influenced by clearance of the loading device. Also deviations at the edge of the soil sample are supposed to be minimized using these local strain measurements. One further advantage is the possibility of measuring radial deformations directly at the soil sample. The application of on-specimen transducers improves the accuracy of measurements in axial direction compared to the single application of external deformation measurements.

Vertical arrival time Bender Element (BE) tests are performed with separate equipment. A single sinusoidal electrical signal, generated by using the soundcard of a PC, causes bending of the top cap BE. This bending generates a shear wave propagating towards the bottom of the sample where the arriving wave generates bending of the bottom BE.

The resulting electrical signal is recorded with a PC oscilloscope. The time delay between sender and receiver signal allows calculating shear wave velocity and shear modulus of the specimen.

Every test contains several test phases outlined in the following (figure 6.25.). Tests are performed on reconstituted sand samples at different loading conditions to investigate the dynamic parameters (damping ratio and shear modulus) as well as the long term behavior of the soil (accumulation of residual deformation).

*During saturation* all air inside voids of the soil is replaced by deaired water or driven into solution. Therefore a flushing procedure is applied to the sample by letting deaired water passing from the bottom to the top of the sample. While most of the void air is replaced by water during this procedure, eventually remaining air is driven into solution applying back pressure to the sample subsequently.

*During consolidation* the sample is set to the required stress conditions (according to the field conditions being simulated) applying confining pressure in axial and lateral direction. Both, isotropic (lateral = axial pressure) and anisotropic (lateral  $\neq$  axial pressure) consolidation is possible. Once the sample is set to the requested test conditions, BE test and/or cyclic loading is applied.

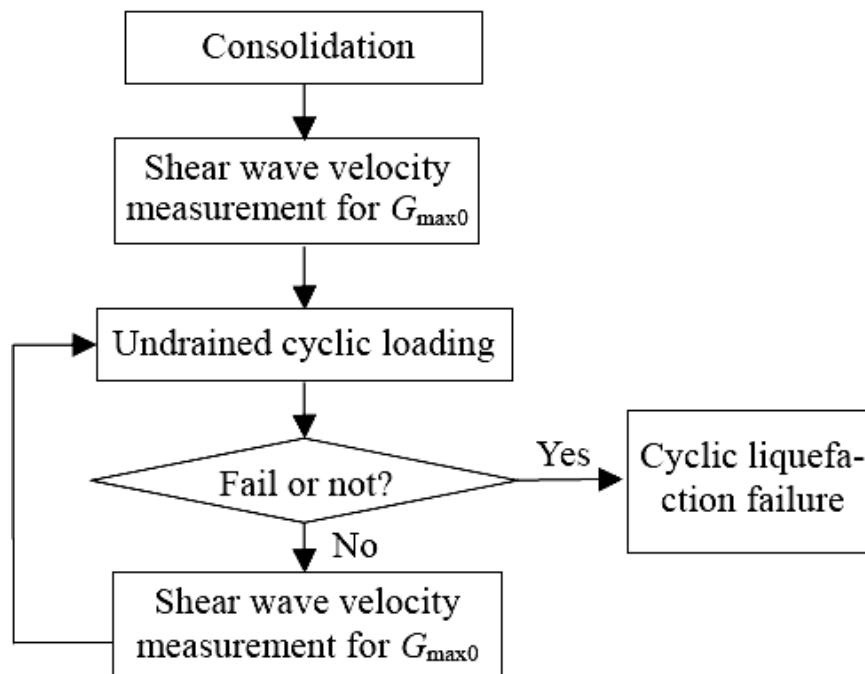


Figure 6.25. Cyclic test procedure

*Standardized cyclic tests* are performed to determine damping ratio and shear modulus of the soil or the liquefaction potential. Non-standard tests may widen the range of applications for example in the field of long term testing, where the accumulation of strain in dependence of different parameters may be investigated.

*After consolidation* bender element tests are performed to determine the stiffness of the sample. One of the essential features of the used equipment is the possibility of combination of cyclic loading and BE-testing – applying BE tests after the cyclic loading as well, structural changes may be detected by changes in time delay.

During the whole test procedure enormous amount of data is recorded. Much effort is done to program analysis tools especially for the cyclic part of the test, namely the analysis of recorded hysteresis loops for determination of damping ratio and shear modulus [10].

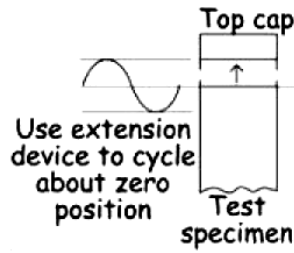
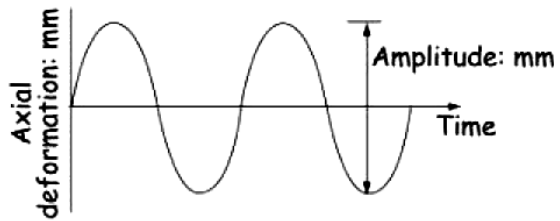
A highly automated advanced CTTD is set up to investigate cylindrical soil samples on their dynamic properties and long term behavior (high number of loading cycles), respectively.

Therefore local strain measurements and BE tests are employed in combination with a very wide range of cyclic loading options. Data analysis tools are programmed for standardized cyclic triaxial tests to determine shear modulus and damping ratio. An extensive program of non-standard long term tests is defined. Data analysis tools for these tests will be developed in the near future. From these test results parameters of an explicit accumulation model will be determined to adapt the model to the tested soil. The model will be implemented in numerical calculations and used for prediction of test results. In a further step prediction of settlements caused by low level vibrations will be possible using the found constitutive laws.

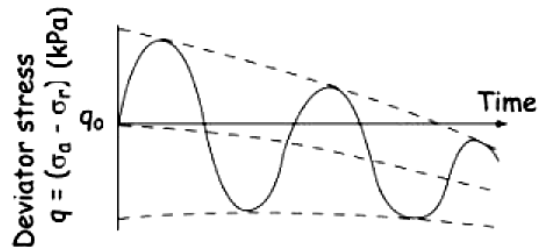
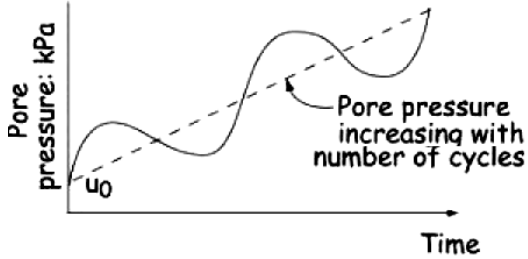
A cylindrical soil specimen with diameter of 36, 54, 72 or 80 mm is used. Other diameters are available upon request. A typical height of twice the diameter is enclosed in a rubber membrane inside the triaxial cell. Equipment and techniques are available to handle a range of soil types, including sample preparation, trimming and mounting of the specimen inside the triaxial cell. Special care is given to very soft soil by the "untouched by hand method" - which makes it possible to push the sample directly from the sample tube into the rubber membrane. Method of reconstitution of sand specimens is chosen according to desired density and structure.

After applying the back-pressure the specimen is consolidated isotropically or anisotropically before undrained or drained shearing. Cyclic loading can be performed as either stress-controlled or strain-controlled. The specimen can be subjected to varying cyclic stress or strain levels and frequencies. Typical dynamic triaxial test results are presented on figures 6.26 and 6.27.

Input: Test control by sinusoidal variation of deformation

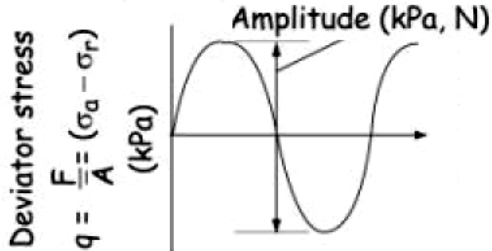


Output: Test results



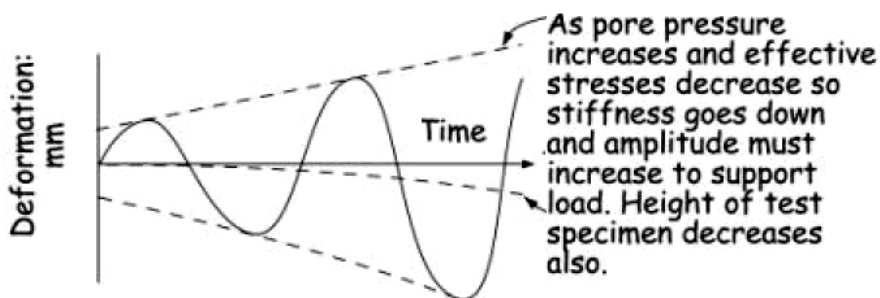
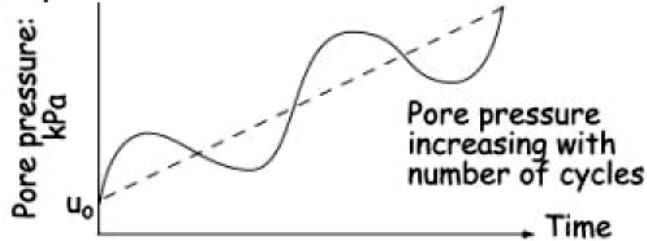
Figures 6.26. Results of strain control

Input: Test control by sinusoidal variation of axial force or deviator stress



Actual stress depends on soil stiffness. If stress chosen cannot be achieved (e.g. large amplitude on soft soil) then reduce amplitude

Output: Test results



Figures 6.27. Results of stress control

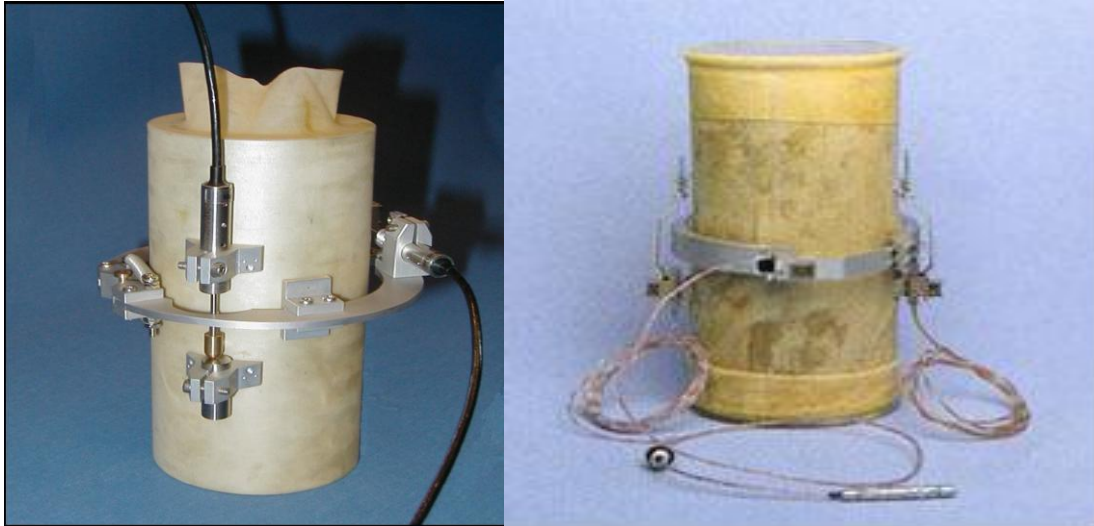


Figure 6.28. Hall effect and local strain transducers (LVDT)

Any triaxial system also may be upgraded to perform Local Strain measurement using either Hall Effect or LVDT transducers (figure 6.28).

Both device types enable axial and radial deformation to be measured directly on the test specimen via lightweight aluminum holders. Hall effect transducers may be used in water up to 1700 kPa. LVDT transducers come in 2 versions: low pressure (up to 3500kPa) version for use in water, high pressure (up to 200MPa) version for use in nonconducting oil. On sample transducers consist of radial and axial strain belts. In conventional triaxial testing the determination of axial stiffness is based on external measurements. This method brings errors due to sample bedding effects of the porous stones on either end of the sample and to the loading system and load measuring system. Furthermore the two ends of the specimen are subjected to restraint, differently from the middle third of the sample, where the strain transducers are mounted and where the realistic deformations occur. Axial and radial strain transducers give the opportunity to measure with high accuracy the deformations directly on the triaxial test specimen.

#### ***6.3.4. Cyclic direct simple shear test***

The cyclic simple shear test is a preferred experiment for research into dynamic soil behavior because of its simplicity and its ability to model many types of field loading conditions that are difficult to achieve with other laboratory equipment. The ability to simulate principle stress rotation is common to many geotechnical problems, including earthquake loading. A soil element, as shown in figure 6.29, a, b may experience deformations due to the upward propagation of shear waves from the underlying soil layers.

The cyclic simple shear test is a modified version of a test commonly used to measure shear strength and stress-strain behavior under static loading conditions. In the cyclic simple shear test, a specimen is placed within a container that allows no lateral strain, and then subjected to a static vertical stress. Horizontal shear stresses are then applied to the specimen. As in the cyclic triaxial test, the shear stresses are typically harmonic with constant amplitude, and are applied at periods of 1 to 60 sec. stress and strain conditions in cyclic simple shear test are showed in figure 6.29, c.

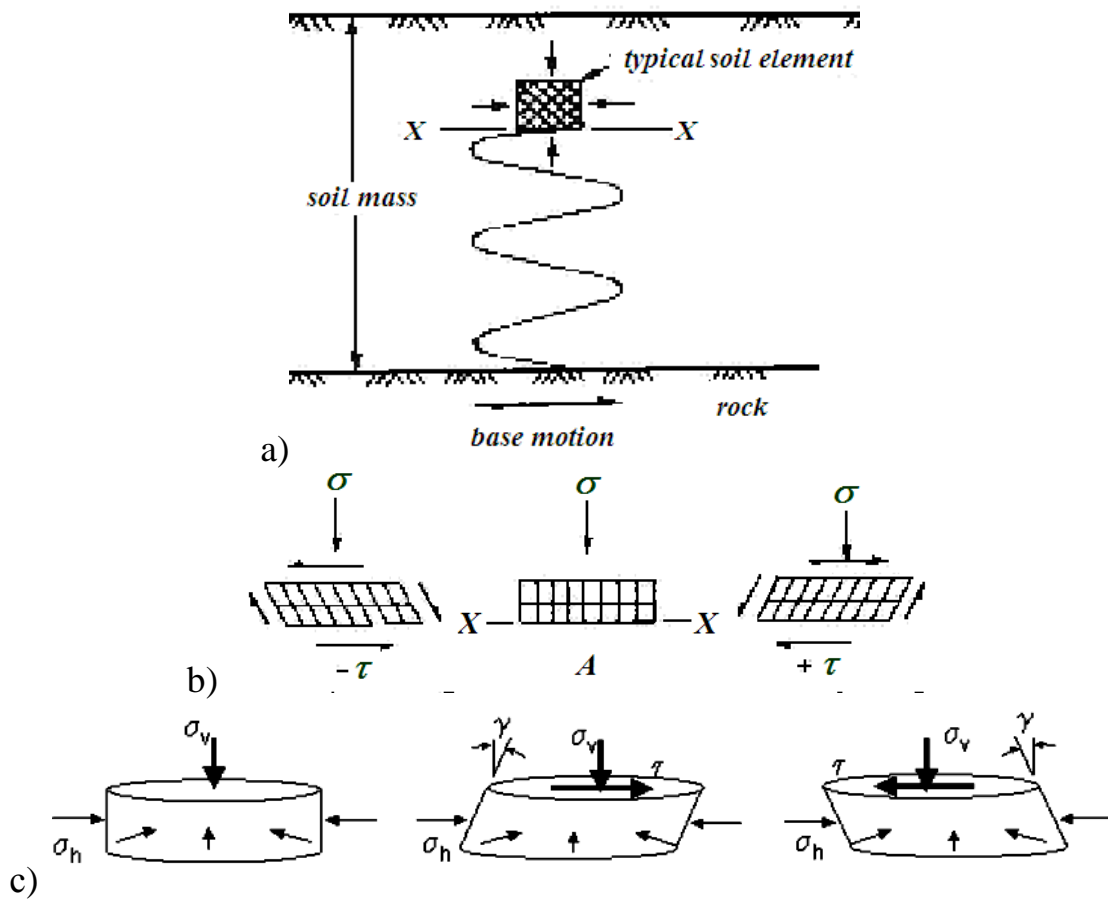


Figure 6.29. a) Typical soil element exposed to upward propagating shear, b) idealized cyclic stress conditions, c) stress and strain conditions in cyclic simple shear test

Stress concentrations, and potential for arching in the corners of cyclic simple shear test specimens limit the range of uniform shear strains to levels of perhaps 15% to 20%. Important properties of liquefiable soils, particularly the residual or steady-state strength may not be fully mobilized at these strain levels.

The cyclic simple shear test has a few advantages over the cyclic triaxial test. Because it applies cyclic shear stresses on horizontal planes and permits

continuous rotation of principal stress axes, it replicates field loading conditions much more accurately than the cyclic triaxial test.

The cyclic simple shear test also has some limitations for liquefaction testing, however, which include:

*Lack of complementary shear stresses on the vertical sides of the specimen.* Because shear stresses are applied only horizontally and the devices make no provisions for applying complementary shear stresses on the sides of the test specimen, the internal stress distribution is non-uniform. The degree of nonuniformity is most pronounced near the sides (and corners) of the test specimen. Previous research has shown that minimum test specimen aspect ratios of approximately 8:1 (width:thickness) are required to make the effects of non-uniformity insignificant. Most cyclic simple shear devices have aspect ratios on the order of 3:1.

*Unknown stress state.* Because a zero-displacement boundary condition is imposed upon the lateral boundaries of the test specimen, the lateral stress is not known. As a result, the actual stress state within the test specimen is not known. Some simple shear devices have been instrumented to measure lateral stresses, but the accuracy of the stress state inferred from those measurements is not clear.

*Low strain behavior not measured accurately.* Because of friction in the loading systems of conventional cyclic simple shear devices, the magnitudes of small shear stresses transmitted to the test specimen cannot be accurately measured. This prevents the determination of low-strain properties from conventional cyclic simple shear testing.

*Constrained, unidirectional loading.* In a conventional cyclic simple shear apparatus, unidirectional loading is applied to the specimen in a predetermined direction. In the cyclic triaxial test, shearing can occur in an infinite number of directions. Because earthquake shaking produces three-dimensional ground motions which induce three-dimensional cyclic shear stresses in the soil, conventional simple shear apparatuses may not reflect the range of response that can be exhibited by the soil.

The *combined dynamic cyclic simple shear (DCSS)* apparatus (figure 6.30, b) uses a cylindrical test specimen. The specimen is supported laterally by a stack of low friction constraining rings. The top of the test specimen is connected to an actuator which is free to move vertically but is rigidly fixed in the horizontal direction by means of high quality linear guides. The base of the test specimen is connected to an actuator that is free to move horizontally but is rigidly fixed in the vertical direction by high quality pre-loaded linear guides.

A cylindrical soil specimen is laterally confined by Teflon coated low friction retaining rings, ensuring a constant cross sectional area. A shear force loading is then applied (figure 6.30, a). Vertical displacement may be

prevented; therefore constant volume conditions are enforced (i.e. simple shear). The apparatus allows for a smooth and continuous rotation through 90 degrees of the principal stress directions.

Both horizontal and vertical actuators are 5kN capacity electro-pneumatic actuators with closed-loop control of force and displacement by means of the digital control system, or DCS.

The cyclic shear apparatus (figure 6.31) is connected to an electronic data acquisition system and the hinged end walls provide deformations to simulate seismic loads. It is necessary to be careful when performing an undrained cyclic shear test to control the volume. Errors of up to 100 percent have been reported when system compliance of the boundary conditions has allowed a positive volume change causing the test to not be truly undrained.

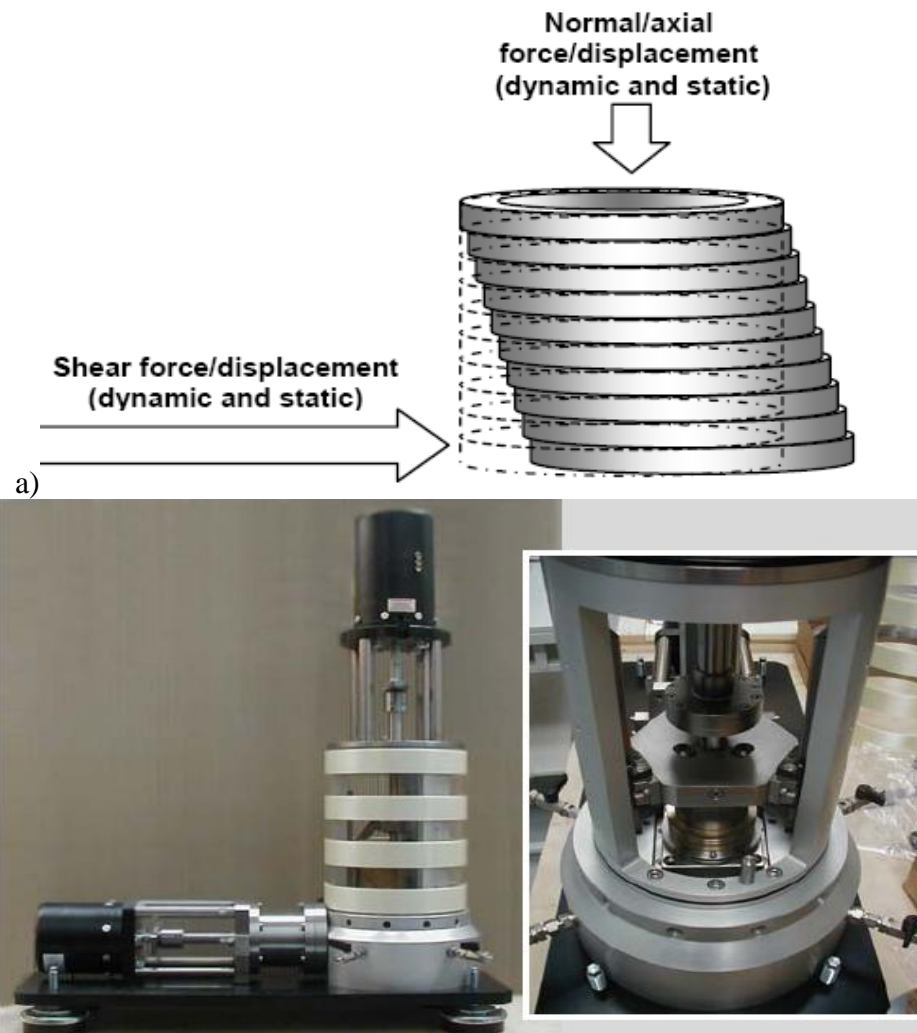


Figure 6.30. Cyclic direct simple shear test : a) Simplified view of laterally constrained sample under simple shear conditions; b) the combined dynamic cyclic simple shear (DCSS) apparatus [27]



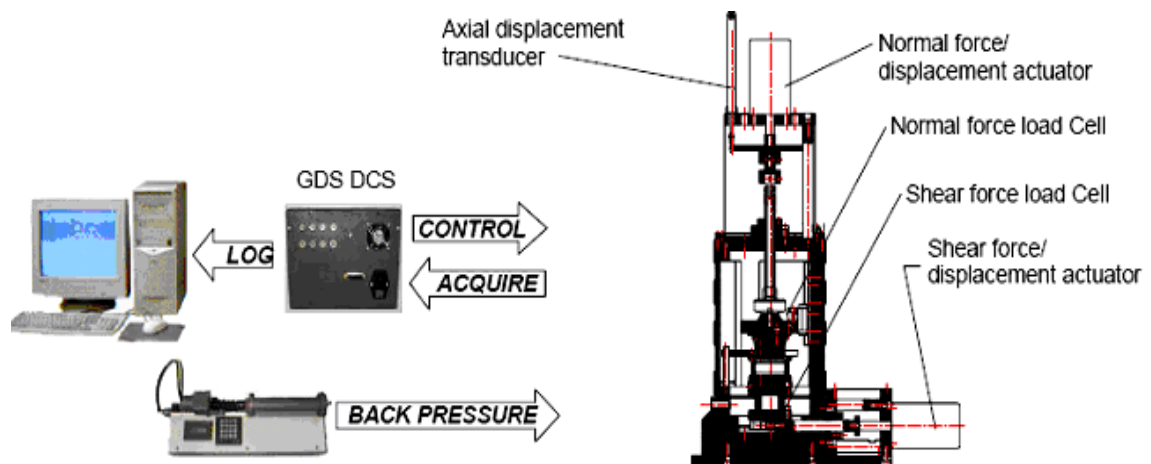


Figure 6.31. DC System Schematic [27]

The simple shear device allows direct investigation of the shear stress versus shear strain in drained and undrained situations. In addition, the dynamic cyclic capability allows investigation of damping ratio and liquefaction. Typical cyclic shear load test data is shown in figure 6.32.

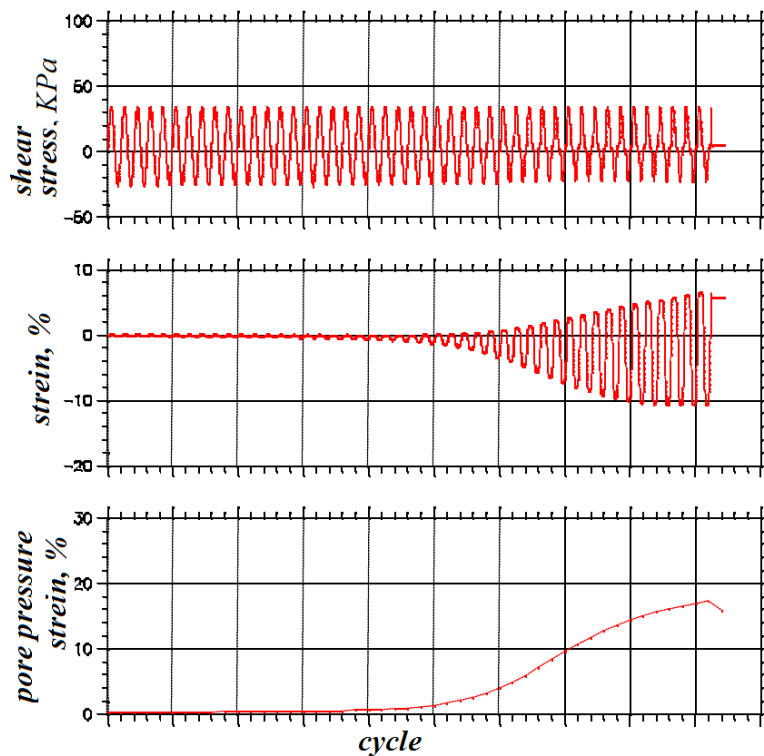


Figure 6.32. Typical cyclic shear data

**The ring shear apparatus** (figure 6.33) was used to examine dynamic characteristics in rapid shear. Ring shear apparatus was initially developed to investigate residual shear resistance mobilized along the sliding surface following large shear displacements in landslides of high mobility. The test configuration for the ring shear device was introduced by Hvorslev (1939) in.

This principle was adopted and improved by Bishop et al. (1971), Bromhead (1979), Savage and Sayed (1984), Hungr and Morgenstern (1984), Tika (1989) and Garga and Sendano (2002) as stated in Sassa (2004).

A series of ring shear apparatus has been developed and improved; the version DPRI Ver.5—intelligent, undrained, torque-controlled ring shear apparatus. The general purpose of the DPRI ring-shear testing program is to use apparatus that can quantitatively simulate the entire process of failure of a soil sample, from initial static or dynamic loading, through shear failure, pore-pressure changes and possible liquefaction, to large-displacement, steady-state shear movement.

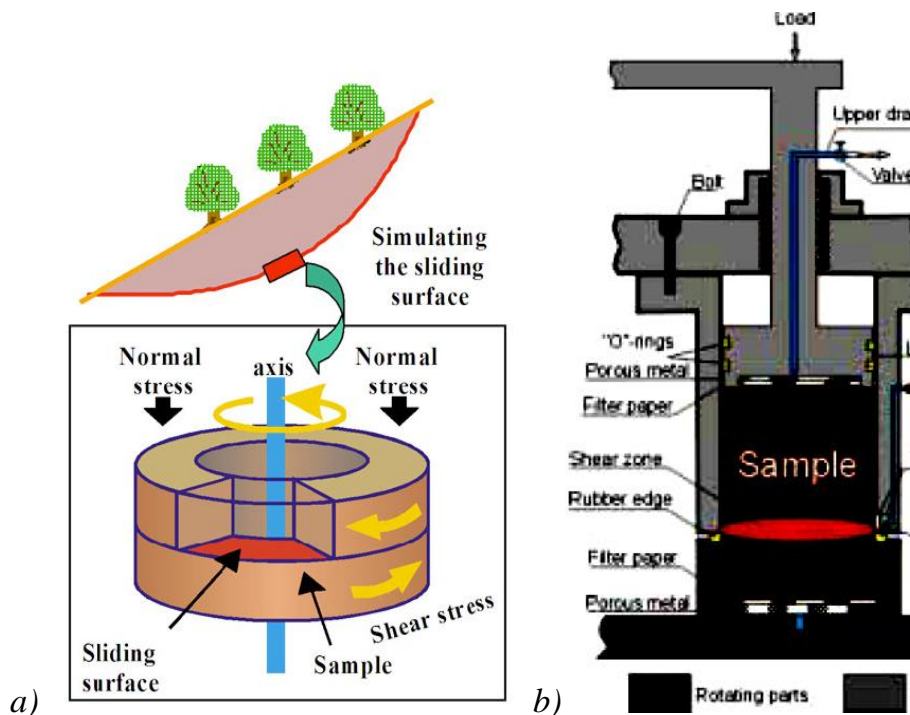


Figure 6.33. a) concept of using ring shear apparatus, b) scheme of the DPRI-Ver.5

The concept of ring shear landslide simulation test is illustrated in figure 6.33, a. Shear/normal stresses along a sliding surface in place are realized in the interior of the shear box, and necessary physical quantities of the soil sample in shear (resistance, pore water pressure, shearing velocity and accordingly the mobilized apparent friction angle) are monitored in real time. An upright cross-section of the shear box with the pore pressure measuring system built in is shown in figure 6.33, b.

Current undrained ringshear apparatus simulates the formation of the shear zone and the post-failure mobility of high-speed landslides and observes the consequence of mobilized shear resistance, as well as the post-failure shear displacement and generated pore-water pressure. It is proved that undrained torque-controlled ring shear apparatus is capable to simulate

and observe all the parameters in terms of stated goals of this investigation. A scheme of the DPRI-Ver.5 ring shear is shown in figure 6.34.

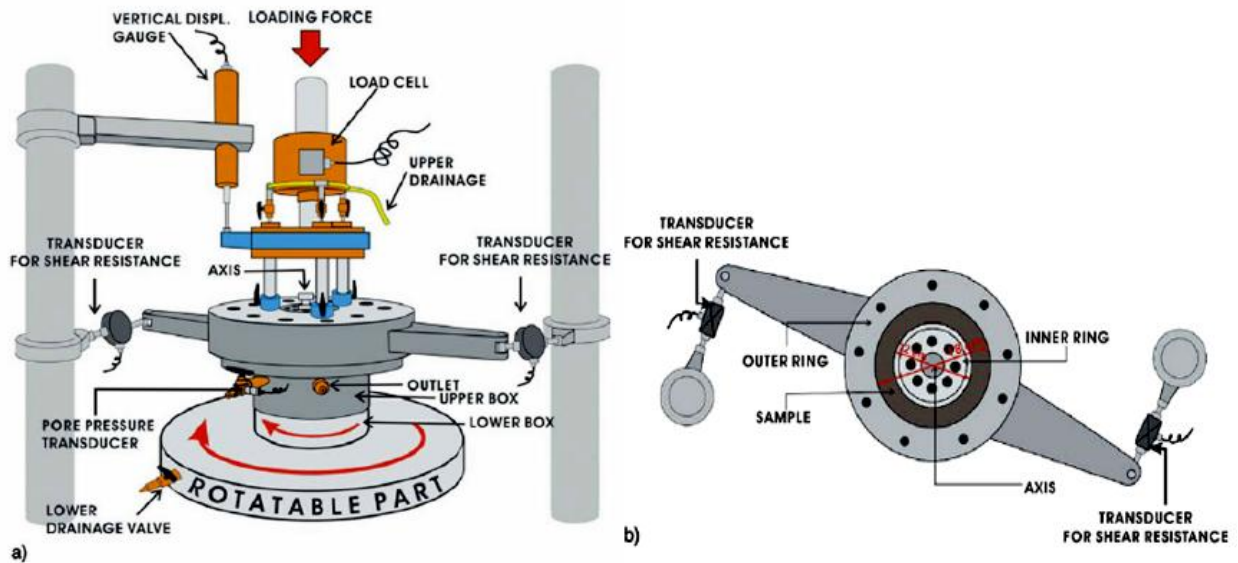


Figure 6.34. Scheme of DPRI-Ver.5 ring shear

The specimen is placed in the donut-like (circular) form between the inner and the outer stainless steel shear boxes. The outer diameter of the shear box is 18.0 cm and the inner diameter is 12.0 cm, therefore the area of shear surface is approximately 141.4 cm<sup>2</sup>. The specimen is sheared by rotating the lower half of the shear box (rotatable part in figure 6.34, a), while two resistance transducers restrain the upper half of the shear box (in the left and right arms of the ring shear box in figure 6.34, b) with which shear resistance is measured. Both of speed-controlled and torque-controlled tests are possible with this apparatus. A rubber edge is bonded to the upper surface of the lower half of the shear box in order to prevent leakage of water and specimen during consolidation and undrained shearing.

The dry deposition method was used in this study to place the sample into the shear box. After oven dried sample was placed into the shear box, CO<sub>2</sub> was supplied to remove remaining air. All samples were normally consolidated under the effective normal stress of 200 kPa for non-plastic silt and 150 kPa for silt-clay mixtures respectively. After consolidation at the initial effective normal stress, the initial driving shear stress was increased reaching value in accordance with calculated and simulated static conditions on the sliding surface. Afterwards, the shear box was switched to undrained conditions, the driving cyclic shear stress with constant amplitude was applied corresponding to CSR = 0.5 with a loading frequency of 0.5 Hz [17].

In 1968, Peacock and Seed performed the first comprehensive study on liquefaction in the laboratory using the cyclic shear apparatus (Prakash, 1981). Peacock and Seed observed that for the confining stress of 5.00

kg/cm<sup>2</sup>, a sudden increase in strain occurred after the 24<sup>th</sup> cycle. Up until the 24<sup>th</sup> cycle, the pore pressure increased. Not coincidentally, when the pore pressure reached the initial confining pressure, the soil liquefied. Peacock and Seed then varied the magnitude of the cyclic shear stress and recorded the number of cycles required to cause liquefaction. Their last step was to investigate the effect of different confining pressures. In summary, Peacock and Seed found that the sample liquefied when the pore pressure equaled the confining pressure, increasing the cyclic shear stress caused liquefaction in a fewer number of cycles, and increasing the confining pressure caused liquefaction in a greater number of cycles [8].

The loose sands tested by Seed in the 1960's exhibited similar behavior in both cyclic shear and triaxial tests: the sample liquefied when the pore pressure equaled the confining pressure, increasing the cyclic shear stress caused liquefaction in a fewer number of cycles, and increasing the confining pressure caused liquefaction in a greater number of cycles. However, the cyclic stress required to cause liquefaction under simple shear conditions was considerably less than under triaxial conditions, as shown in figure 6.35.

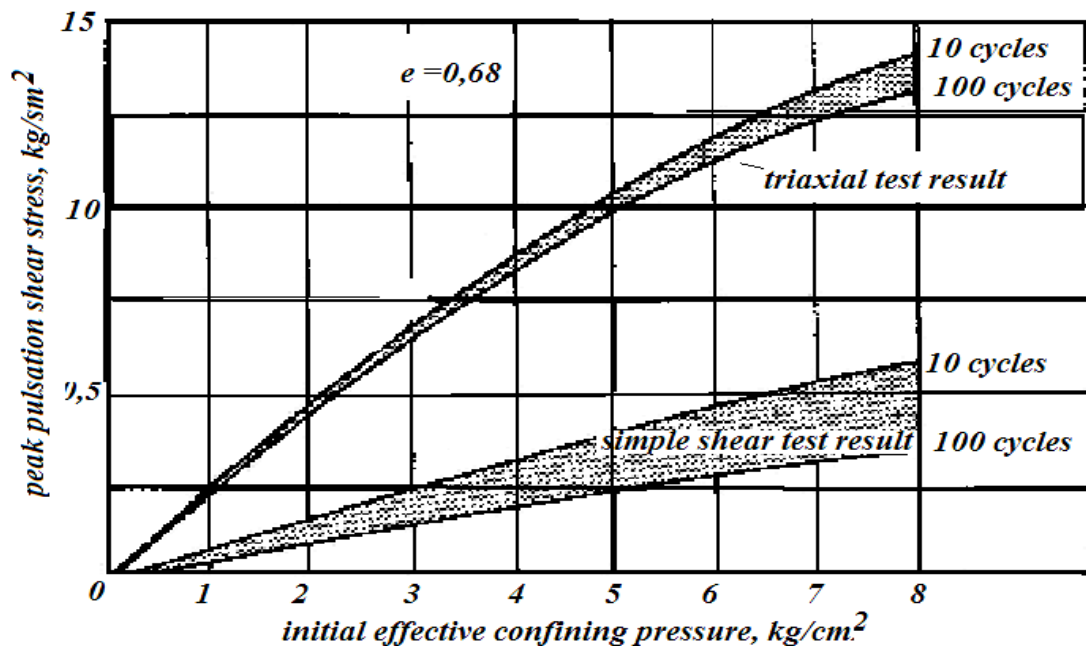


Figure 6.35. Comparison of cyclic simple shear and triaxial test results

In fact, the cyclic shear stress required to cause liquefaction under simple shear conditions was about 35% less than that required under triaxial conditions. The direct shear apparatus tests loads one single plane, while the inclined shear stress planes in the triaxial apparatus will change inclination with different applied compressive stress. This results in a more concentrated load on the shear plane during the simple shear test and a less concentrated load on the shear plane during the triaxial test. While both tests are necessary

to model different loading conditions, the cyclic shear test best imitates the in situ shearing experienced by a seismic shear wave as shown in figure 6.5 and is probably the better test to understand the liquefaction susceptibility of a soil.

### **6.3.5. Hollow cylinder torsional shear test**

Advanced soil constitutive models that incorporate the non-linearity and anisotropic (i.e. directional dependence) behaviour are increasingly being used in the analysis of geotechnical structures. The successful application of these models requires careful site characterizations and laboratory tests, as well as appropriate modelling of the construction sequences and the super-structures. Recent advanced laboratory studies have improved understanding on major aspects that influence the soil behaviour: shearing mode, stress/strain dependency, geological history, soil fabric and structure, temperature and time. However, the commonly used triaxial cell can only apply compression or extension shearing modes under the axi-symmetric condition. In this respect the *Hollow Cylinder Apparatus* (HCA) offers the best solution for a full control of imposed anisotropy by changing angle of major principal stress to vertical direction, and intermediate principal stress parameter ( $b = [\sigma_2 - \sigma_3] / [\sigma_1 - \sigma_3]$ ).

The hollow cylinder apparatus (figure 6.36, a, b) allows for rotational displacement and torque to be applied to a hollow cylindrical specimen of soil (figure 6.36, c). Using this device it is possible to control the magnitude and direction of the three principal stresses. Studies can for example be made of the following: the anisotropy of soil samples; the effects of principal stress rotation; the effects of intermediate principal stress.

In addition to the hollow cylinder torsional shear test, it can be used for carrying out triaxial shear test by changing a pedestal. Moreover, triaxial shear apparatus is available both for saturated soil test and unsaturated soil test. Hollow cylinder torsional test & triaxial test (for saturated soil) is applied for strain-controlled monotonic torsional test; strain-controlled cyclic torsional test; strain-controlled monotonic triaxial test; strain-controlled cyclic triaxial test.

References to the existence of hollow cylinder torsional devices go back as far as 1965, (Broms and Casbarian, 1965). After that landmark a long list of hollow cylinder torsional apparatuses have been described, the most recent references are: (Hight et al., 1983), (Alarcon et al., 1986), (Ampadu and Tatsuoka, 1993), (Huang et al. 1994).

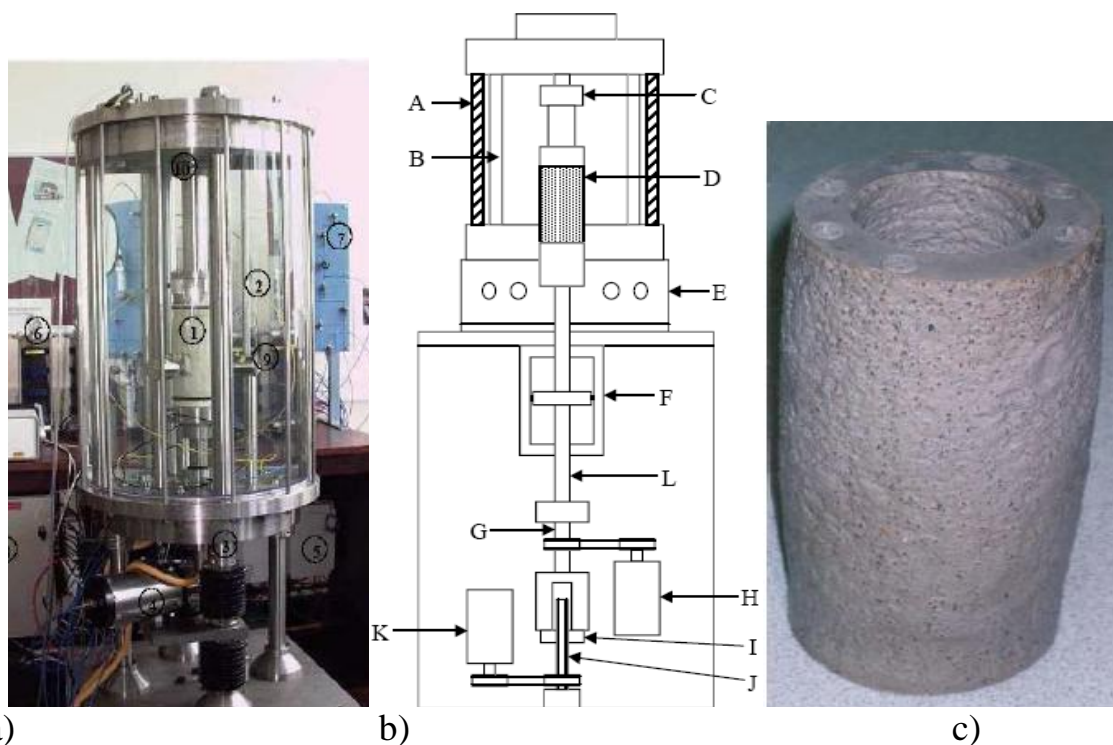


Figure 6.36. Hollow cylinder torsional shear test: a) hollow cylinder apparatus, b) scheme and c) example of hollow cylinder specimen after testing [13, 28]

A new hollow cylinder torsional shear apparatus, it is a fully automated system combining advanced triaxial testing features with advanced torsional shear capabilities.

This advanced apparatus enables to simultaneously impose and individually control axial pressure  $W$  and torque  $M$  as well as outer chamber pressure  $p_o$  and inner chamber pressure  $p_i$ . And different combinations of these components can be fulfilled. Therefore the consolidation and loading paths under different complex stress condition of soils can be implemented. In addition, cyclic shear stress induced by cyclic torque and cyclic stress difference caused by cyclic axial force can be simultaneously imposed on soil samples, and the phase lag between them can also be controlled, therefore complex variation patterns of stress or stress paths such as continuous rotation mode of dynamic principal stress axis, as shown in figure 6.37, can be accomplished. These complex stress conditions were focused to approximate the loading conditions of site ground subjected to vertical and horizontal motions, induced by water wave or earthquake. A typical stress state of soil element in hollow cylindrical sample is shown in figure 6.38.

It is a matter of fact that test devices and test methods are not currently available to satisfy the broad range of requirements related to those situations of interest in geotechnics which may produce shear strains varying by more than five orders of magnitude.

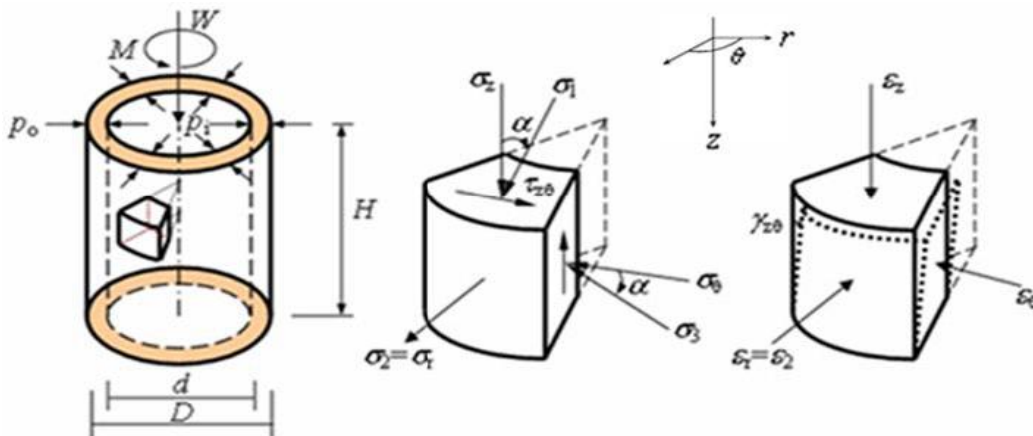


Figure 6.37. Stress condition of soil element

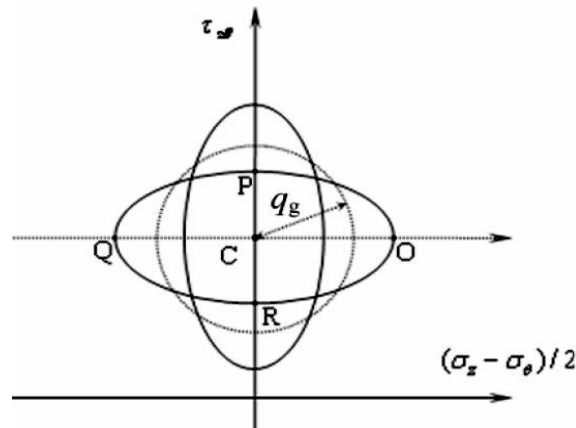


Figure 6.38 Loading scheme

Torsional shear testing devices have become the devices of choice to study the monotonic and cyclic behaviour of soils especially when used with a hollow cylinder specimen.

The arguments for hollow cylinder specimens torsional testing include: minimal effects of end platens, ease of testing with anisotropic stress conditions, and complete definition of the state of stress, which can be accurately measured.

As a consequence, in recent years, increasing attention has been given to the laboratory testing of soils in torsional shear, particularly with regard to cyclic behaviour. Given the recognized limitations of the cyclic triaxial test, the benefits of torsional shear testing make it clear that performing tests with torsional shear devices has much to offer the practice of geotechnical engineering and soil mechanics.

A computer-automated closed-loop feedback system provides accurate and independent control of the load, torque, vertical displacement, rotations, pressures and calculated stresses and strains.

Anisotropy in granular materials is caused either by the arrangement of particles, such as occur in natural deposits in which the grains may have their major axis on the bedding plane, or by spatial distribution of contacts and contact forces. Further to this so-called inherent anisotropy (induced anisotropy is caused in the specimen by the non-reversible strain increments during the follow up of stress path. Only through carefully designed and controlled tests is it possible to clarify the influence of the stress path followed by the soil on the strength and deformability. The importance of experimental studies is further emphasized by the path dependence of strain behaviour.

With the HCA fully automated control of generalized total stress path, i.e. in the stress space, is made possible. Several imposed strain path tests such as the simple shear test and the plane strain test may also be carried out in this apparatus.

In addition to the tests on hollow cylindrical test specimen described above the system can also be used for carrying out advanced triaxial compression and extension tests. These triaxial tests can be executed under stress or strain control with independent control of the axial and torsional modes of operation.

The use of this apparatus is illustrated by a stress controlled undrained torsional shear test of a sand specimen. The specimen was prepared using a new automatic sand pluviator. During the test four stress cycles of low amplitude were followed by four extra cycles of medium amplitude thus enabling two distinct patterns of stress-strain behaviour to be observed: the first is in the small strain domain with no pore pressure build-up and the second occurs in the medium amplitude range in which the joint effect of dilatancy and compaction tendency causes the pore pressure to increase with an oscillatory pattern and the shear strain amplitude to rise.

In a torsional shear apparatus the combination of axial and torsional loadings leads to principal stresses that are inclined on the axes of symmetry of the material. The use of different inner (inside the hollow cylinder test specimen) and outer pressures causes a general average state of effective stress described by the following effective stress tensor:

$$\sigma' = \begin{bmatrix} \sigma'_r & 0 & 0 \\ 0 & \sigma'_\theta & \tau_{\theta z} \\ 0 & \tau_{z\theta} & \sigma'_z \end{bmatrix}$$

Each component in this tensor represents the average value over the sample volume of the corresponding stress field. While  $\sigma'_r$  and  $\sigma'_z$  are deduced based on equilibrium conditions, the definition of the remaining components depends on the basic assumptions about the stress field. In the present paper the definitions as in were used.  $\sigma'_z$  and  $\tau_{z\theta}$



The ability to control each of the components is only possible by independent advanced control over the axial force, torque, inner and outer pressures. These features are available in the present apparatus thus making possible generalized stress path testing.

The assumed average strain tensor is given by

$$\varepsilon = \begin{bmatrix} \varepsilon_r & 0 & 0 \\ 0 & \varepsilon_\theta & \varepsilon_{\theta z} \\ 0 & \varepsilon_{z\theta} & \varepsilon_z \end{bmatrix}$$

On the one hand, controlling the axial strain  $\varepsilon_z$  and the off-diagonal component may be straightforward, since they are, respectively, expressed as a direct function of the axial displacement and of the torsional rotation, respectively. On the other hand, advanced strain path testing (e.g. plane strain testing mode) requires very precise servo-control of the confining pressures.

The HCA consists of a combined cell and actuator. A schematic drawing of the HCA is shown in figure 6.36, b. The cell, containing the test specimen and the confining fluid, is designed to be very strong, both axially and rotationally. This strength is achieved by the use of three large section tie rods (A) between the cell top and the cell base. These tie rods are rectangular with the longest side facing the test specimen. This arrangement ensures high stiffness to torque. The cell chamber (B) is made from a transparent plastic material and is rated at 1700 kPa. A submersible load/torque cell (C) is attached rigidly to the cell top. The load/torque cell can be easily changed. A counterweighted lifting system (not shown) is used to allow the cell top to be raised, lowered and balanced in any intermediate position as an aid to test specimen set-up. Exchangeable base platens can be attached to the ram (L) to allow for two sizes of test specimen (100 outer diameter/60 inner diameter (100/60) and 70/30).

The ram (L) passes into the cell chamber via the balanced ram chamber (F) and the cell base. The balanced ram is designed to ensure that there is no disturbance to confining pressure under dynamic axial loading conditions. This is achieved by ensuring that when the ram enters the cell a matching volume of water leaves the cell and enters the balanced ram chamber. An associated effect is that changes in cell pressure cause a zero resultant force on the ram (L).

Axial load and displacement is generated by a high power brush less dc servomotor (K) attached to the base of the ball screw (J) by means of a high stiffness, zero backlash toothed belt drive. Rotation of the ball screw (J) causes the ball nut (I) to move axially, this motion is transferred to axial motion in the ram (L). The ball nut (I) is prevented from rotating by means of a linear guide (not shown). Rotational motion is added to the axial motion by means of the splined shaft (G). A second brushless dc servomotor (H) is

attached to the splined shaft (G) by means of a high stiffness, zero backlash toothed belt drive and is used to generate torque or displacement as required. Control of load/displacement and torque/rotation is provided by specially designed High-Speed Data-Acquisition And Control (HSDAC) cards. These cards are resident on the pc ISA bus and provide facilities for both static and dynamic control of load/displacement and torque/rotation. Feedback for load/torque is derived from the combined load/torque cell and feedback for displacement/rotation is derived from high resolution rotational encoders attached to the motors (H & K).

There are three pressures to control in the hollow cylindrical test specimen, these are: outer pressure, inner pressure and the back pressure. If it is necessary to maintain low pressure differences between the inner and outer pressures or between the outer pressure and the back pressure, then advantage is taken of the ability of the pressure controllers to control via a second transducer – in this case low range wet/wet differential pressure transducers. The back pressure controller is used to measure volume change in the test specimen and the inner pressure controller is used to measure volume changes in the inner space of the hollow cylinder test specimen. The ability to accurately control these pressures and volume changes is vital for carrying out specialised low speed tests such as stress paths in the stress space or simple shear.

The HSDAC cards are used for data acquisition at both high and low speeds. Each card is capable of acquiring data from up to eight channels. The parameters normally acquired are as follows: axial load, axial deformation; torque, rotation, local external axial strain during triaxial tests (two channels), local external radial strain during triaxial tests, pore pressure (two channels), inner pressure, outer pressure, back pressure, inner volume change, specimen volume change, small strain external displacement, small strain external rotation. The local external axial and radial strain devices are Hall Effect local strain transducers.

Pore pressure can be measured using an external pore pressure transducer connected to the base pedestal, additionally provision is made for the measurement of pore pressure using a mid-plane pressure transducer that is attached directly to the test specimen at its mid height. Inner pressure, outer pressure and back pressure are measured using the output of the GDS digital pressure/volume controllers. In addition inner, outer and back pressures are measured using separate transducers attached to the cell to enable dynamic as well as static measurements to be made [6].

The following table (table 6.2) shows those parameters that can be independently controlled; this means that a hardware based controller exists to directly control that parameter, to match a target sent by the computer, without the computer being involved in the control process. There are five

independent axes of control. Where more than one parameter is assigned to an axis this means that only one item in the list can be controlled at any one time, for example either torque can be controlled or rotation can be controlled but both cannot be controlled independently at the same time.

Table 6.2

Independent axes of control

Axis	1	2	3	4	5
Static variable	Axial force	Torque	Outer pressure	Inner pressure	Back pressure
Kinematical variable	Axial displacement	Rotation	Outer volume change	Inner volume change	Specimen volume change

All of the above parameters can be controlled in quasi-static tests. In dynamic tests at frequencies up to 5 Hz only parameters one and two can be controlled. The requirement for dynamic control over outer pressure, inner pressure and back pressure is not necessary because for a typical dynamic test the test specimen is undrained, the outer pressure is equalised with the inner pressure and the dynamic balanced ram ensures that the outer pressure is not disturbed by motion of the loading ram.

If the computer is used to execute some control algorithm it is possible to carry out more complex control for quasi-static tests. Options exist to control the derived parameters for hollow cylinder test specimens listed in table 6.3.

Table 6.3

Derived control parameters.

Axis	1	2	3	4	3,4
Variable	$\sigma_z$	$\tau_{z\theta}$	Constant outer diameter	Constant inner diameter	Constant wall thickness

Generalised HCA control is achieved by allowing the control path for each axis to be independently selected according to some time based reference. The control paths offered are: constant value, ramped value (from a start value to and end value), cycled value (sine, square or triangle).

This ability for HCA generalised control allows the user to perform a range of tests from simple to very complex. Simple tests could be modulus tests (Young's or shear) performed by keeping the inner pressure and outer pressure constant and ramping or cycling either deformation or rotation. Examples of more complex tests could be cycled  $\sigma_z$  or  $\tau_{zz\theta}$ , constant  $\sigma_z$  with cycled outer pressure or back pressure, and simple plane strain tests. The degree of control means that complex tests like simple shear can be routinely carried out in a number of ways. For example, by specifying constant wall thickness the simple shear requirement is established, it is then possible to add to this other control parameters such as cycling rotation, torque or  $\sigma$ .

The full control capabilities of the new HCA are mobilized in the implementation of the generalised stress path capability. The hardware design

and ease of control means that it is relatively straightforward to implement complex control algorithms. The stress path control capability allows a number of linear paths to be defined in terms of the controlled parameters. Each linear path is defined in terms of its end-points in the stress space. Any number of paths can be executed sequentially thus allowing complex geotechnical processes to be modeled.

The degree of control and ease of control provided by this new piece of apparatus means that one can carry out tests previously requiring many different systems. The system can be used to replace triaxial systems (static and dynamic), true triaxial systems, simple shear systems and of course it is a complete hollow cylinder apparatus for both static and dynamic work.

This new equipment has been designed to give an extensive range of element testing capabilities. The equipment can perform both quasi-static and dynamic tests with sinusoidal waveforms up to 5Hz at both small and large strains. The hardware implementation has been designed to remove computing load from the host computer and thus simplify the control software. The supporting applications software is designed to give the user flexibility in the use of the equipment with both hollow cylinder and solid cylinder (triaxial) tests supported. The combination of intelligent hardware, comprehensive systems software and flexible applications software means that even highly complex procedures, such as stress paths defined in stress space, can be routinely carried out. The equipment represents the ultimate single piece of advanced laboratory soil testing equipment capable of carrying out tests normally requiring many separate testing systems – advanced triaxial, true triaxial, shear box, and simple shear apparatus [6].

Figure 6.39 schematically shows dynamic deformation characteristics test to compute them by *triaxial and torsional shear test apparatus*. Usually, hysteresis loop at the 10<sup>th</sup> cycle of loading is used to compute them. Because behavior at small strains was

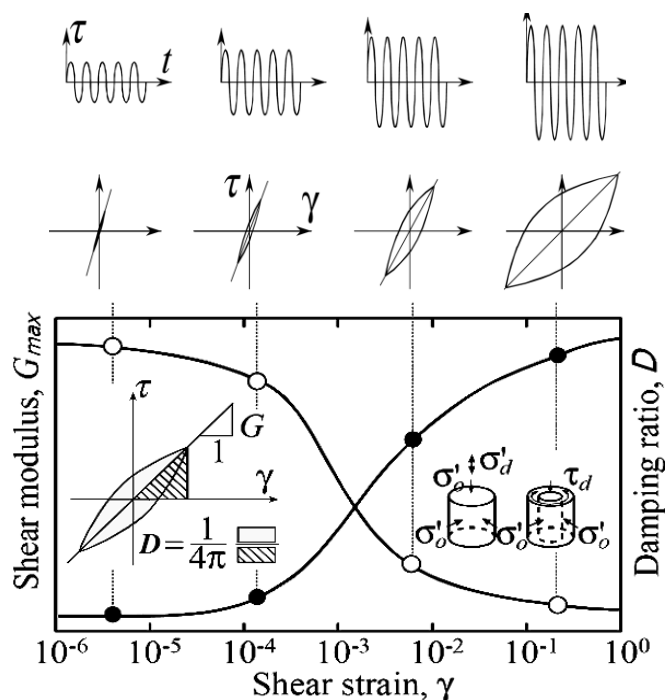


Figure 6.39. Schematic figure showing the data processing in dynamic deformation characteristics test [31]

difficult to measure at the beginning, other tests, such as a resonance column test, were used to measure the property at small strains. Improvement of the loading system and the measurement enabled it to use from very small strains to large strains up to failure.

### 6.3.6. Ultrasonic test, shaking tables and centrifuge devices

The purpose is to determine the pulse velocities of compression and shear waves in intact *rock* and the ultrasonic elastic constants of isotropic *rock*.

Procedure ultrasound waves are transmitted through a carefully prepared rock specimen. The ultrasonic elastic constants are calculated from the measured travel time and distance of compression and shear waves in a specimen. Figure 6.40 shows a schematic diagram of typical apparatus used for ultrasonic testing.

The primary advantages of ultrasonic testing are that it yields compression (p-wave) and shear (s-wave) velocities, and ultrasonic values for the elastic constants of intact homogeneous isotropic rock specimens. Elastic constants for rocks having pronounced anisotropy may require measurements to be taken across different directions to reflect orthorhombic stiffnesses and moduli, particularly if pronounced foliation, banding, layering, and fabric are evident.

The ultrasonic evaluation of elastic rock properties of intact specimens is useful for rock classification purposes and the evaluation of static and dynamic properties at small strains (shear strains  $< 10^{-4}$  %). Older equipment only provides ultrasonic p-waves measurements, while new designs obtain both p- and s-wave velocities. When compared with wave velocities obtained from field geophysical tests, the ultrasonics results provide an index of the degree of fissuring within the rock mass. This test is relatively inexpensive to perform and is nondestructive, thus may be conducted prior to strength testing of intact cores to optimize data collection.

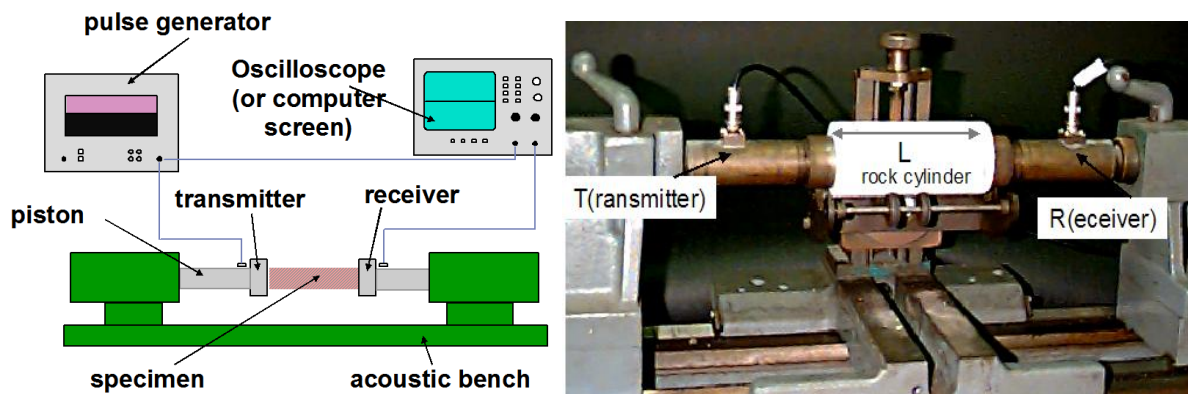


Figure 6.40. Measuring shear velocities in the laboratory

For earthquake engineering purposes, geotechnical models are usually well instrumented and then tested using shaking tables or centrifuge devices. Shaking tables offer the advantage of testing larger models, but centrifuge devices are capable of modeling in situ stresses more accurately. Centrifuge devices are also available in different sizes, ranging from small drum centrifuges with radii less than 1 m to large centrifuges with radii of several meters. Very large geotechnical centrifuge is available at Davis (figure 6.41).

Shaking tables are available in many different sizes, from those capable of testing models with dimensions of tens of centimeters to those capable of testing models several meters in height. The shaking table at the Public Works Research Institute (PWRI) in Japan, for example, has a base that measures 7.6 m by 7.6 m. This shaking table has been used for testing large specimens of saturated soil with lateral spreading deformations.



*Figure 6.41. Geotechnical centrifuge at UC Davis. Note laminar box in centrifuge bucket for testing models under seismic loading conditions*

A unique liquefaction box was designed and built that has two of its walls hinged at the bottom of the box thus allowing rotation and inducing simple shear in the sample. A shaking table is utilized with the box to induce controlled shear strains in the sand specimen.

Electrolysis technique was used to generate oxygen and hydrogen gases uniformly within the specimen without causing any change in the density of the loose sand.

Experimental test results demonstrate that partially saturated sands have larger strength against liquefaction than fully saturated sands. Induced partial saturation can be a liquefaction mitigation measure.

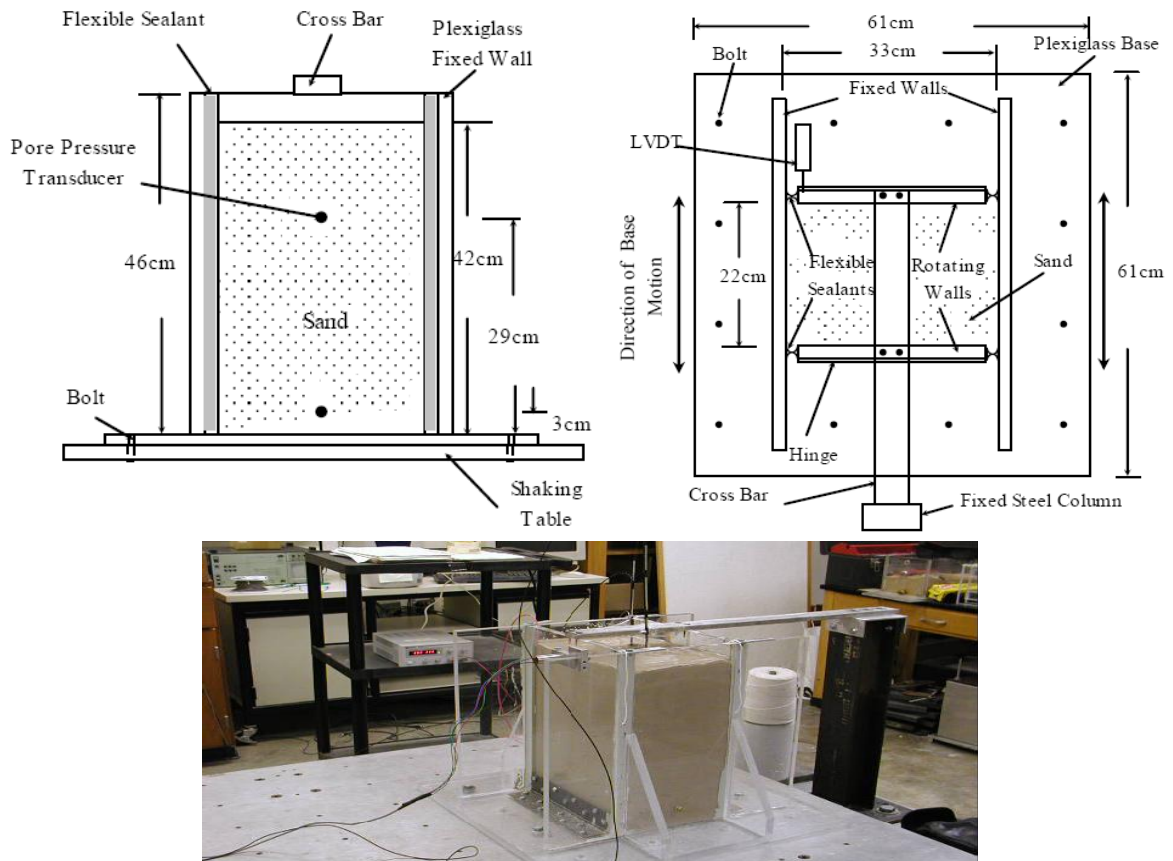


Figure 6.42. Details of the rotating-wall liquefaction box for testing fully and partially saturated sands

A special Plexiglas box was built that has two rotating walls that induce simple shear strains in a large specimen of sand. Flexible sealant connects the rotating walls of the box with the fixed walls, which makes the joints water tight and allows movements between the rotating and fixed walls of the box. The experimental results demonstrate that small reduction in the degree of a fully saturated specimen can lead to significant reduction in excess pore pressures generated in loose liquefaction susceptible sand. Induced partial saturation can be a potential inexpensive liquefaction mitigation measure at sites where using conventional mitigation techniques are prohibitive.

## 6.4. Measurement of dynamic soil stiffness by piezoelectric sensors

### 6.4.1. The structure of piezoelectric ceramics

The measurement of soil stiffness at small strains is assuming greater importance in the study of soil mechanics and its application to geotechnical design. Routine estimations of stiffness have traditionally been made in a stress path triaxial apparatus using local displacement transducers fixed directly on the sample. However, recent research has brought about the

development of dynamic methods for the measurement of soil stiffness at very small strains using piezo-ceramic plates (bender elements).

The piezoceramic bender element (BE) is an electro-mechanical transducer, which is capable of converting mechanical energy (movement) either to or from electrical energy (figure 6.43). The single bender element consists of two thin piezoceramic plates, which are rigidly bonded together with conducting surfaces between them and on the outsides. The polarisation of the ceramic material in each plate and the electrical connections are such that when a driving voltage is applied to the element, one plate elongates and the other shortens. The net result is a bending displacement, which is greater in magnitude than the length change in either of the two layers. On the other hand, when the bender element is forced to bend, one layer will go into tension and the other into compression: this will result in an electrical signal, which can be measured.

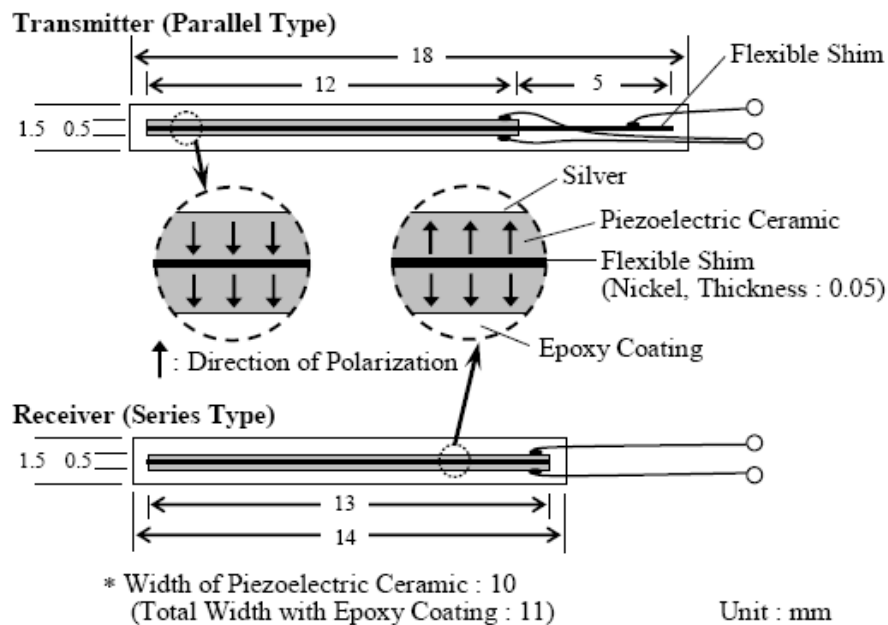


Figure 6.43. An example of bender element (BE)

In the soil application the bender elements are encapsulated and mounted into inserts, which are fixed into the pedestal and top cap of a triaxial cell. Any triaxial system may be upgraded to perform *s*- and *p*-wave bender element testing (figure 6.44) with the addition of the following items: bender element pedestal with new inserted element, bender element top-cap with new inserted element, high-speed data acquisition card, optional horizontal bender elements, signal conditioning unit, amplification of source and received, signals with user-controlled gain levels (via software).

Three different types of element pairs are available: *s*-wave only, *p*-wave only (high power) and combined *s*- and *p*-wave. Each set of element pairs comprises a "source" and a "receiver" element.



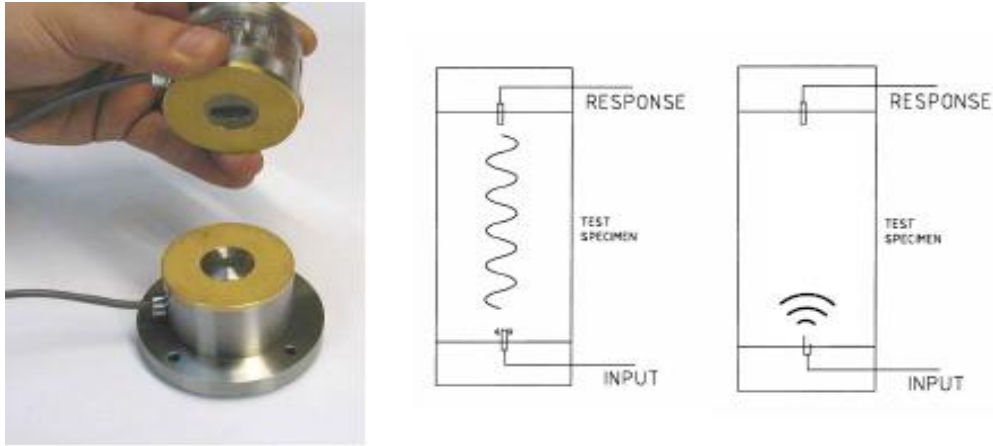


Figure 6.44. *p- and s-wave elements* [28]

Piezoelectric elements distort or bend when subjected to a change in voltage. Two such elements are placed opposite one another and inserted a small distance into a soil sample (typically 3mm). The voltage in one element is varied creating shear waves through the sample, which are received by the opposite element. The system consists of a transmitter, which is energized to produce the shear waves through the soil sample, and the receiver that generates the electrical signal. The travel time of the shear wave from the transmitter to the receiver is determined via a specific software that allows the user to quickly and easily calculate the shear wave velocity.

When excited the bender element bends from side to side pushing the soil in a direction perpendicular to the length of the element and thus having a large coupling factor with the soil. This produces a shear wave, which propagates parallel to the length of the element into the soil sample. On the other end of the soil sample another bender element is forced to bend and produces an electrical signal that can be measured. Theory on shear wave propagation in an elastic body tells us that the value of the shear modulus  $G_{max}$  of the soil from measurement of shear wave velocity  $V_S$ .

The input voltage, (created using a function generator) and the received signal are recorded continuously using an oscilloscope, allowing the travel time of the shear waves to be measured from which the dynamic elastic shear modulus ( $G_{max}$ ) can be determined.

Piezoelectric ceramic material generally consists of a group of perovskite crystals, individually consisting of a tiny, tetravalent metal ion, such as titanium or zirconium, surrounded by a lattice of larger, divalent metal ions, normally lead or barium, and  $O^{2-}$  ions. The general crystal structure can be thought of as a face centered cubic (FCC) lattice with a  $B^{4+}$  ion at the center surrounded by six  $O^{2-}$  ions, each at a face center, and eight  $A^{2+}$  ions, each at the corner (figure 6.45).

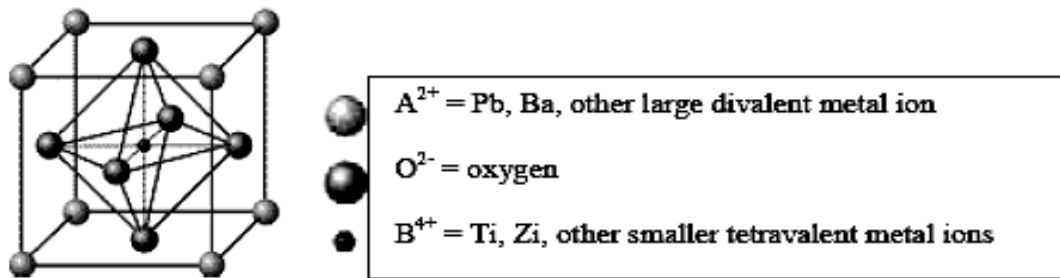


Figure 6.45. Crystal structure of a traditional piezoelectric ceramic [9]

To create a piezoelectric ceramic, fine powders of the component metal oxides are mixed in specific proportions, and then heated to form a uniform powder. The powder is mixed with an organic binder and is formed into structural elements having the desired shape. The elements are fired according to a specific time and temperature program, during which the powder particles sinter and the material attains a dense crystalline structure.



Figure 6.46 a) cubic lattice, symmetric arrangement of positive and negative charges. b) tetragonal (orthorhombic) lattice, crystal has electric dipole.

The elements are cooled, then shaped or trimmed to specifications, and electrodes are applied to the appropriate surfaces. At a specific temperature called the Curie temperature the crystal structure transforms from a non-symmetrical (tetragonal piezoelectric) to a symmetrical (cubic nonpiezoelectric) form. At temperatures higher than the Curie point, each crystal element portrays a simple cubic symmetry with no dipole moment (figure 6.36, a). At temperatures lower than the Curie point, each crystal contains tetragonal or rhombohedral symmetry along with a dipole moment (figure 6.46, b).

Adjoining dipoles forming regions of local alignment are known as “domains.” The alignment gives a net dipole moment to the domain, which in turn causes a net polarization. However, the direction of polarization among adjacent domains is random. This means that in essence, the ceramic element has no global polarization (figure 6.47 a).

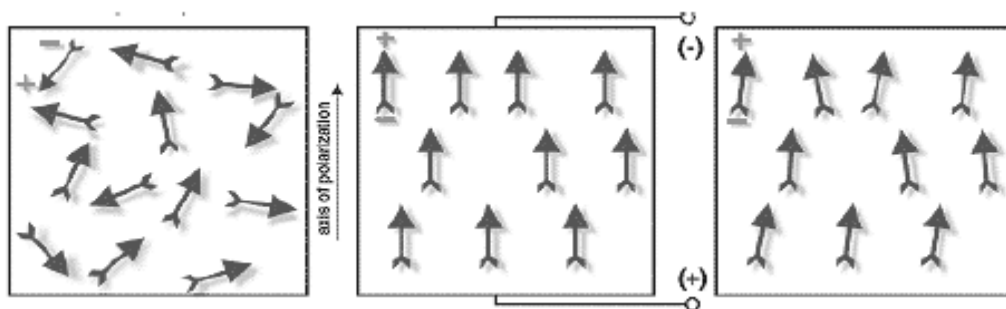


Figure 6.47. a) random orientation of polar domains prior to polarization, b) polarization in electric field, c) remanent polarization after electric field removed

The domains in a ceramic element can be aligned by exposing the element to a strong, direct current electric field (figure 6.37 b). Through this polarizing (poling) treatment, domains most nearly aligned with the electric field expand at the expense of domains that are not aligned with the field, and the element lengthens in the direction of the field. When the electric field is removed most of the dipoles are locked into a configuration of near alignment (figure 6.47 c). The element now has a permanent polarization, the remanent polarization, and is permanently elongated.

The number of domains that become aligned depends upon many variables. These include the poling voltage, temperature, and the amount of time the voltage is held on the material. During polarization the material permanently increases in dimension between the poling electrodes and decreases in dimensions parallel to the electrodes. The material can be depoled by reversing the poling voltage, increasing the temperature beyond the material's Curie point, or by inducing a large mechanical stress.

There are many different shapes and sizes of piezoelectric sensors, each created for a specific application. All piezo transducers (which convert one form of energy to another) can either exist as single sheets or two-layer elements. Single sheets can produce motion in any direction (thickness, length, and width directions) by a small excitation. These sheets produce electrical output when stretched or compressed.

Two-layer (figure 6.48) elements are more resourceful and can be used in a multipurpose fashion. They can be treated as single sheets made up of two layers or they can be used to bend (bender elements) or extend (extender elements). Although they are called out as "two-layer," these elements actually consist of nine layers. The layers of a two-layer element include four electrode layers followed by two piezoceramic layers bonded with two adhesive layers all strengthened by a center shim.

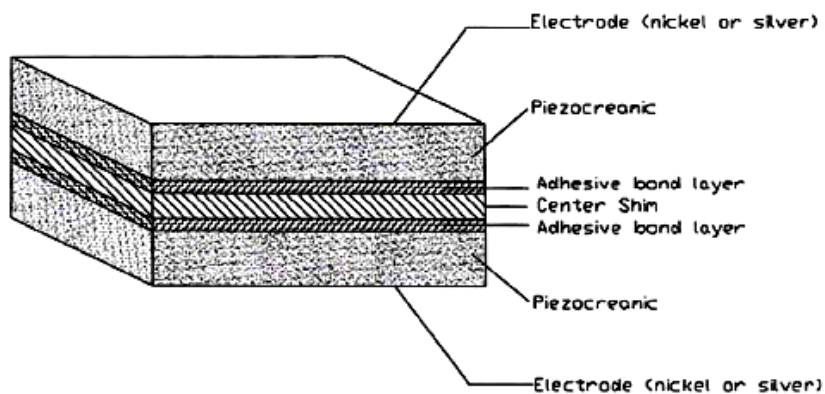


Figure 6.48. Various layers of a typical "two-layer" element

The piezoceramic bender element is made up of two slender piezoceramic plates (sheets) which are inflexibly bonded together with conducting surfaces between them and on the outsides. Because of the specific polarization of each plate a driving voltage applied to the element causes one plate to elongate and the other plate to shorten. This causes the element as a whole to bend, which means that one layer will go into tension while the other goes into compression. An electrical signal is the result of this phenomenon, which can be measured through the wire leads to the element. Figure 6.49 shows the bending displacement caused by an applied driving voltage.

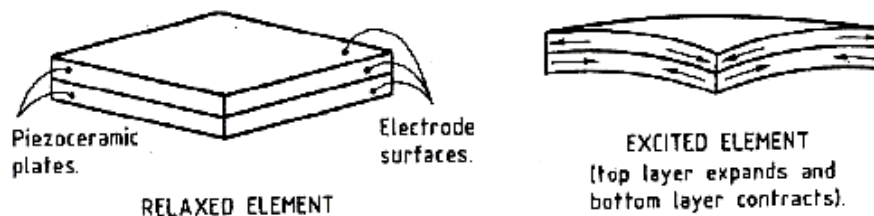


Figure 6.49. Shape of piezoceramic bender elements with and without applied excitation voltage

Piezoelectric sensors are used in a fashion that converts force and motion to voltage and charge. There are two different types of sensors known as axial sensors and flexional sensors (refer to figure 6.50).

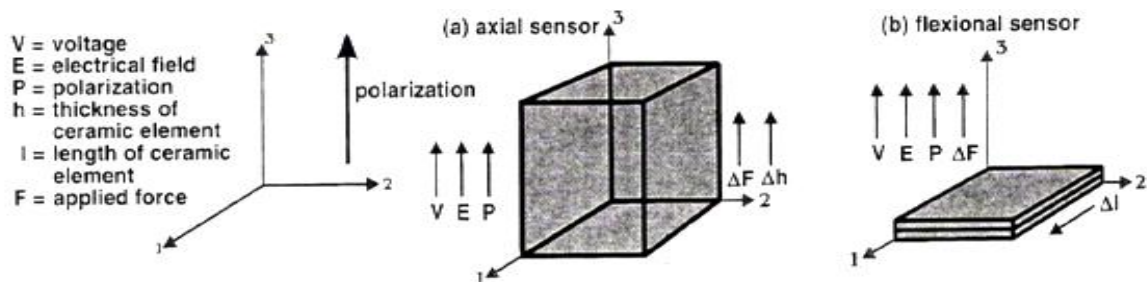


Figure 6.50. Relationship between mechanical input and electrical signal output by sensors

When a force is applied to a sheet of piezoceramic in a direction parallel to polarization a voltage is produced. This voltage attempts to return the piece to its original thickness (figure 6.51, a). This type of application involves the use of axial sensors. In the same fashion, when a force is applied to a sheet in a direction perpendicular to the polarization, a voltage is created which attempts to return the piece to its original length and width (figure 6.41, b). A single sheet fixed to a structural member which is deformed in some fashion will stimulate an electrical output.

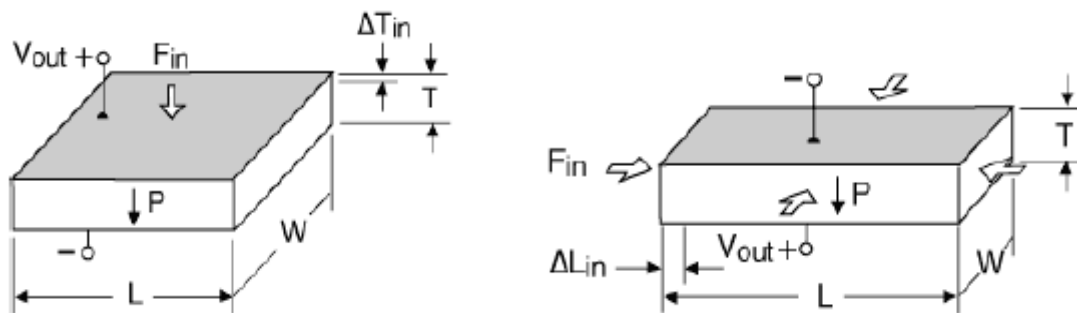


Figure 6.51. a) longitudinal generator, b) transverse generator [9]

Flexional sensors which are more common than axial sensors consist of two strips of piezoceramic bonded together to form a bilaminar element. Bender and extender elements are forms of flexional sensors. Usually these elements are fixed at one end and free on the other end where the input to be measured will act. This is known as a cantilever mounting system. An extension generator is created by bonding two single sheets of piezoceramic in such a way that an applied mechanical stress results in electrical generation. The applied force causes both layers to deform in a similar fashion and a voltage is created which in turn tries to restore the element's original configuration. A bending generator operates in a similar mode. However, in this case each layer of the two-layer element deforms in an opposing fashion. One layer is compressed and the other layer is stretched. The following figure 6.52, a depicts a bending generator while figure 6.52, b provides the common mode of vibration.

Piezoceramic sensors work well with dynamic inputs as opposed to static inputs. They work extremely well as strain gauges in the determination of dynamic strains in structures. In fact, the use of piezoceramics as strain gauges results in signal/noise ratios on the order of 50 times that of wire strain gauges.

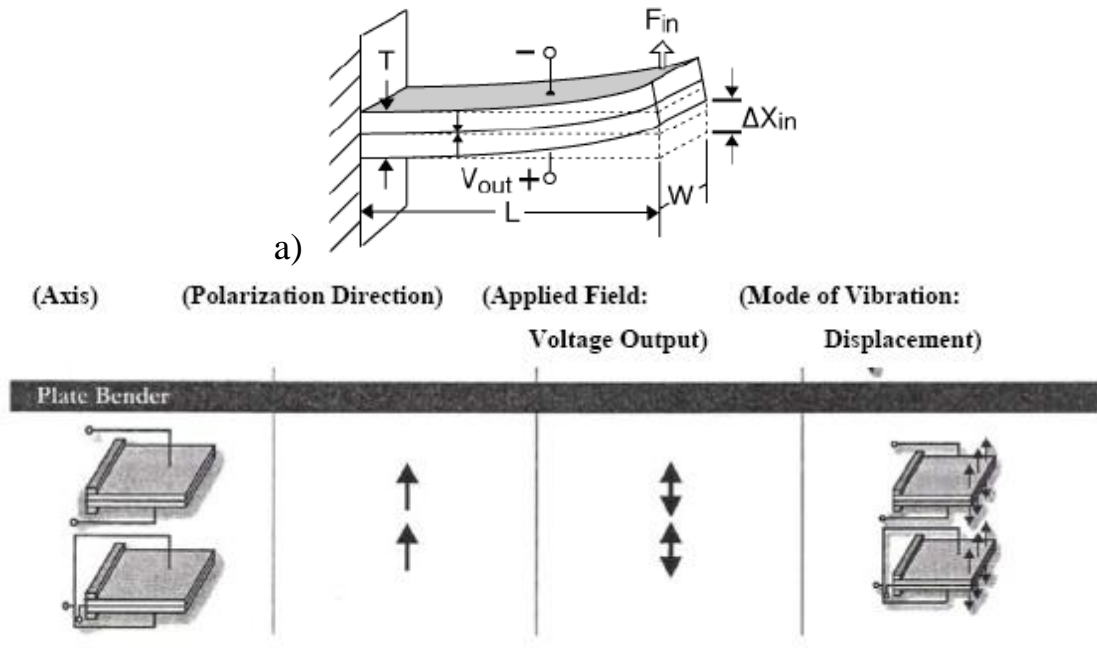


Figure 6.52. a) bending generator of cantilever mount, b) common mode of vibration for piezoceramic plate bender [9]

The ability to tailor a material to a specific application makes the use of piezoceramic sensors very attractive to the world of geotechnical engineering. Many experimental techniques have been recently introduced employing bender and extender elements for the determination of soil properties. The procedure used is quite simple. An electrical excitation is applied to a transmitter element which leads to mechanical vibrations and in turn generates shear s-waves (for a bender element). In a similar fashion, primary p-waves are produced by extender elements. The s- and p-waves produced by the transmitter elements then result in an electrical output produced by receiving elements. The velocity of the s- and p-waves can then be determined by measuring travel time and distance between the wave transmitter and receiver. This technique has been successfully used by a number of researchers including Dyvik and Madshus in 1985, Thomann and Hryciw in 1990, Jovicic in 1996, Viggiani and Atkinson in 1995, Hryciw and Thomann in 1993, Jovicic and Coop in 1998, and Zeng and Ni in 1998 and 1999 to measure the stiffness of sands and clays in the laboratory.

#### 6.4.2. Application of piezoelectric sensors in soil property determination

Pierre and Jacques Curie gave birth to the world of piezoelectricity. They were the first, in the year 1880, to demonstrate a connection between macroscopic piezoelectric phenomena and crystallographic structure. The experiment that demonstrated this connection consisted of specially prepared crystals such as tourmaline, quartz, topaz, cane sugar, and Rochelle salt which were subjected to mechanical stress. An irrefutable measurement of

surface charges appeared on these crystals. In essence the crystals became electrically polarized. If one of these voltage-generating crystals was exposed to an electric field it lengthened or shortened (in tension and compression) according to the polarity of the field, and in proportion to the strength of the field. At the time, this phenomenon was regarded as a huge breakthrough, and was quickly termed “piezoelectricity”, from the Greek word “piezen”, meaning to press or squeeze.

In 1881 the “converse effect” was mathematically deduced from fundamental thermodynamic principles. More specifically, it was determined that not only did the crystals exhibit a direct piezoelectric effect (electricity from applied stress), but they also exhibit the converse effect (stress in response to applied electric field).

In 1910, a benchmark was reached when Voigt’s “*Lehrbuch der Kristallphysik*” was published. This became the standard reference work embodying the understanding of the framework underlying piezoelectricity.

However, the first developmental work on the application of piezoelectric devices did not take place until World War I in 1917. It was during this time that Langevin and French co-workers began to create and refine an ultrasonic submarine detector made of piezoelectric material. More specifically, their transducer was a medley of slender quartz crystals bonded between two steel plates. This device was secured and mounted in a watertight housing suitable for submersion. After the war’s end, they ultimately achieved their goal of emitting a high frequency “chirp” underwater. Thus they were able to measure depth by timing the return echo. The success of Langevin and his co-workers in the development of sonar began a shockwave of activity on many types of piezoelectric devices.

During and after World War II (1940-1965), in the United States, Japan, and the Soviet Union, it was discovered that certain ceramic materials exhibited dielectric constants hundreds of times higher than common cut crystals. Not only that, but the composition, shape, and dimensions of the ceramics could be “cut-to-fit” the requirements of a specific application.

This discovery unsurprisingly began a resurgence of concentrated research and development of ceramic devices. The advances in materials science that were made during this phase of discovery fall into three main categories:

1. Development of the barium titanate family of piezoceramics and later the lead zirconate titanate family.
2. The development of an understanding of the correspondence of the perovskite crystal structure to electro-mechanical activity.
3. The development of a rationale for doping both of these families with metallic impurities in order to achieve desired properties such as dielectric constant, stiffness, piezoelectric coupling coefficients, ease of poling, etc.

Geologists and seismologists were among the first to study elastic waves in granular materials in order to better understand the behavior of seismic waves in the loose materials comprising the earth's crust. In 1939, a researcher named Iida studied compression and torsional shear wave velocity in granular materials. Gassman and Brandt then advanced the theoretical work begun by Iida. In their studies, they included both uniform packings of like spheres and random mixtures of different spheres.

Previously in 1950, Paterson showed that unlike a classical solid material that could only support a dilatational and a shear wave disturbance, porous granular materials could support three waves: a dilatational wave through both the mineral skeleton and through the pore fluid, and a third, shear wave, through the mineral skeleton. Following Paterson's work, in 1962, Biot proposed a comprehensive theory relating all three disturbances. He pointed out that the frame wave speed must be influenced by the presence of the pore fluid and cannot solely reflect the properties of the mineral skeleton.

Piezoelectric crystals were first introduced as one of two methods used at this time as a means to measure elastic wave velocities in the laboratory. The first method was introduced by Ishimoto and Iida in 1936. The method consists of vibrating one end of a cylindrical sample at various frequencies, until the frequency which gives maximum response is found. This frequency is the resonant frequency of the sample. If the mode of vibration is known the wave length may be determined from the height of the sample, and the relation,

$$c = f * \lambda$$

Where  $f$ , the frequency of the response and  $\lambda$ , the wavelength, may be used to calculate the wave velocity ( $c$ ).

The second method involving piezoelectric ceramics consists of initiating a shear wave at one point within a sample and detecting its arrival at a second point. If the distance between the two points is known, the velocity characteristic of the disturbance can be calculated directly from the required transit time using the formula where distance equals rate times time.

Paterson in 1956, Lawton in 1957, and Lawrence in 1963 were among the first to employ this technique. This technique is generally more attractive than the resonant column method due to the fact that it only requires very minute disturbances ( $5.75 \times 10^{-16}$  cm or  $10^{-6}$  inches) as compared to the  $6.92 \times 10^{-11}$  cm ( $10^{-4}$  inches) required by the latter method. Thus, the pulse technique is, in essence, the more successful form of non-destructive testing.

The first major experiment performed by Lawrence using piezoelectric crystals occurred in 1963 and was conducted on two granular materials including Ottawa sand and spherical glass beads. The equipment used in the



study consisted of an electronic pulse generator, a pair of barium titanate piezoelectric transducers, and an oscilloscope capable of observing both the voltages impressed on the sending transducer and the voltage resulting from the arrival of the stress pulse in the receiving transducer. The goal of using this type of transducer was to produce waves of minimum amplitude which would not affect the basic "soil fabric." In other words, it would remain well within the elastic range of the material. Piezoelectric crystals were the then obvious choice for producing these high frequency elastic waves of small amplitude.

The experimental technique consisted of measuring the time delay between the voltage impressed on the sending transducer and the voltage from the receiving transducer. From the delay time and the measured separation of the crystal faces, the velocity of the propagation of the stress wave was computed. With this apparatus, the shape of the received wave forms and their characteristic frequencies were also observed.

In conclusion to this study on non-saturated granular systems, it was determined that measurements of dilatational wave speed taken by the pulse method proved satisfactory. However, using these low sensitivity crystal receivers, difficulty was experienced in clearly determining the first elastic-wave arrival.

Soon after, several other complications were discovered in using this type of crystal transducer, the main difficulty being an opposition between the characteristic impedance of the crystal element and that of a soil specimen. More simply put, "The mechanical motion that is transferred to the soil is small because the element exhibits a small movement with a large force and the soil exhibits a large movement with a small force. The problem with these elements was overcome with the development of piezoceramic bender bimorph elements for use as shear-wave generators and receivers, developed by Shirley and Anderson and Shirley and Bell in 1977. This element is composed of two crystals bonded together in a sandwich-type arrangement. It is essentially a plate element which juts into the soil specimen in a cantilevered fashion. The bimorph bends side to side displacing the soil in a direction perpendicular to the length of the element. A considerable coupling factor is created with the soil. In turn, a shear wave is produced which promulgates perpendicular to the motion of the soil particles. The displacement created by a bimorph element is much greater than that of the single crystal as used in Lawrence's experiment in 1963. This element was successfully used by Shirley to measure the shear wave velocity in kaolinite clay.

In 1980, Dominic F. Howarth used ultrasonic piezoelectric transducers in a triaxial cell in fundamental studies investigating the mechanical properties of rock and the effect of rock fabric/texture on these properties. In

general, he developed equipment enabling the determination of the dynamic Young's modulus of triaxially loaded rock cores.

In 1981, Strachan studied the relationship between liquefaction resistance and shear and fluid wave velocities using bender elements and compressive disks secured in triaxial cell end caps. In this experiment, samples could be subjected to dynamic loads after measuring the elastic-wave behavior. The equipment used in this experiment involved the use of bender elements projecting directly into the soil sample. This type of setup was apparently suitable for laboratory purposes, but could not be used in-situ. Strachan also noted that problems and possible damage to the benders themselves developed when bender motion was inhibited by high effective stresses. Shultheiss and Hamdi and Taylor Smith in 1981 and 1982, respectively, have also successfully used bender elements mounted in various laboratory apparatus to measure the shear wave velocity in a soil specimen.

DeAlba conducted liquefaction tests in 1984, using a cyclic triaxial device equipped with piezoelectric bender elements. The tests conducted were used to confirm an immediate relationship between liquefaction resistance and shear or compressive wave velocities in saturated sand. Six characteristically different sands were tested and results showed that relationships between elastic-wave velocities and liquefaction resistance could indeed be established for each material. These results allowed for the conclusion that in-situ measurements of elastic-wave velocities can be used to recreate laboratory samples to their field liquefaction resistance. It should be noted that simple measurements of elastic-wave velocities alone will not put a figure on liquefaction resistance, since the resistance-velocity relationship is also material dependent.

As can be seen, bender elements have historically been installed and used in an assortment of traditional laboratory testing equipment. Not only have they been included in triaxial testing, but they have also been useful in direct simple shear and oedometer devices. From this, several significant advantages have been created in that:

“The quality of each individual specimen in these different tests can be evaluated, the need to run parallel resonant column tests is eliminated,  $G_{max}$  and the other geotechnical parameters from the test (i.e. shear modulus at large strains from triaxial or shear) can be determined and compared for the same specimen, and  $G_{max}$  measurements can be a useful guide during consolidation (i.e. to determine the rate of application of the drained deviator stress in an anisotropically consolidated triaxial test). The only disadvantage of these new techniques is that there is no direct or convenient method to determine the dampening ratio of the soil and  $G$  at high strain levels.”

In 1985, Dyvik and Madshus installed bender elements in the Drnevich resonant column device (Hardin oscillator) at NGI. Their goal was to take

$G_{max}$  measurements simultaneously by both methods (bender elements and resonant column) on the same soil sample and compare the results. Figure 6.53 depicts the setup for integrating bender elements in the resonant column device. Tests were performed on three different offshore clays, a sample of Drammen clay and a specimen of Haga clay.

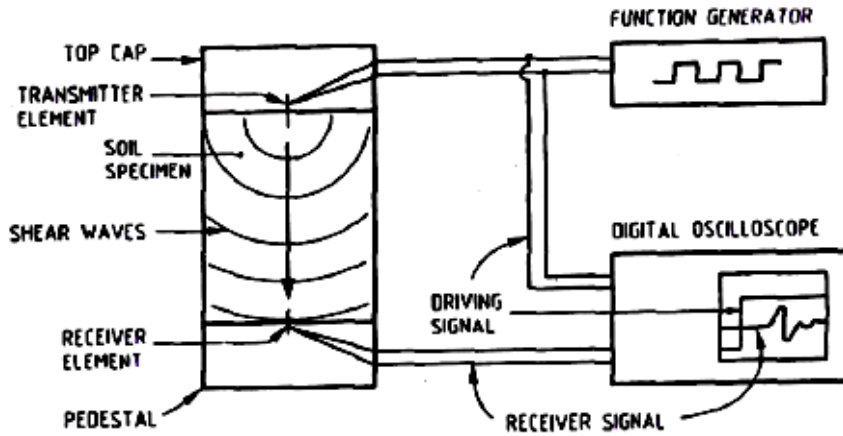


Figure 6.53. Setup for the integration of bender elements in the resonant column apparatus [9]

The outcome as shown by figure 6.54 encompasses a vast array of soil  $G_{max}$  values. Generally, the two different techniques concur. As can be seen from the graph, the best results are at a stiffness value of approximately 75 MPa (10.9 kip/in<sup>2</sup>). “Although the resonant column technique is a well established method for determining  $G_{max}$  in the laboratory, there is nothing that says these results are exactly correct, so these two techniques actually serve as a check on each other”. One simple advantage of using the bender element over the resonant column method is that the test procedures and computations for bender elements are much easier.

In 1990, Thomas Thomann and Roman Hryciw presented a new laboratory device capable of measuring the *small strain shear modulus*

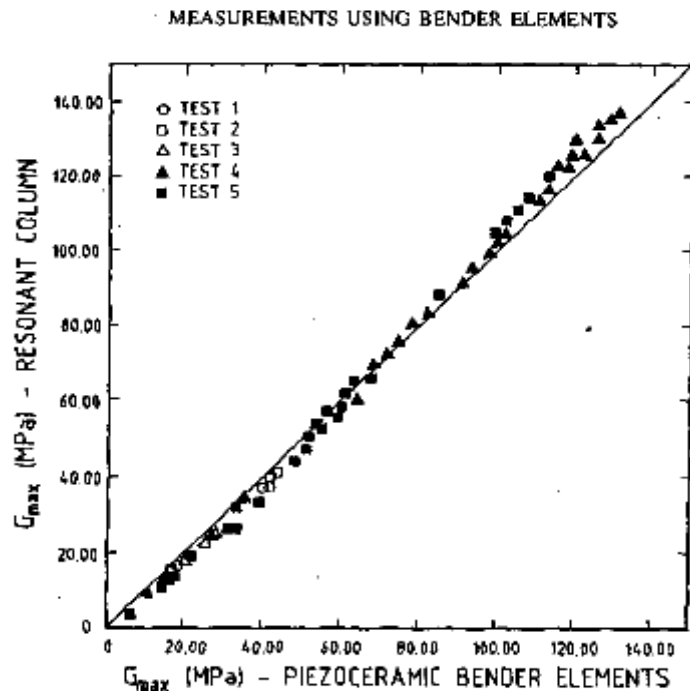


Figure 6.54.  $G_{max}$  results

under a no lateral strain ( $K_o$ ) condition. Measurement of shear wave velocity, as previously mentioned, is ordinarily performed in a resonant column device under isotropic confinement. This presents a problem though, as soils in the field are usually under a  $K_o$  condition during vertical loading, unloading, and reloading. Thus, the vertical and horizontal stresses in-situ are going to be quite different from the isotropic conditions created in resonant column testing. The new testing device is comparable to an oedometer and utilizes bender elements to measure the shear wave velocity (figure 6.55 below). The device can also be used to determine the effects of aging and secondary consolidation. This is due to the fact that the change in void ratio can be measured more accurately than in a standard resonant column device. The following figure shows the bender element oedometer (BEO) device setup as proposed by Thomann and Hryciw.

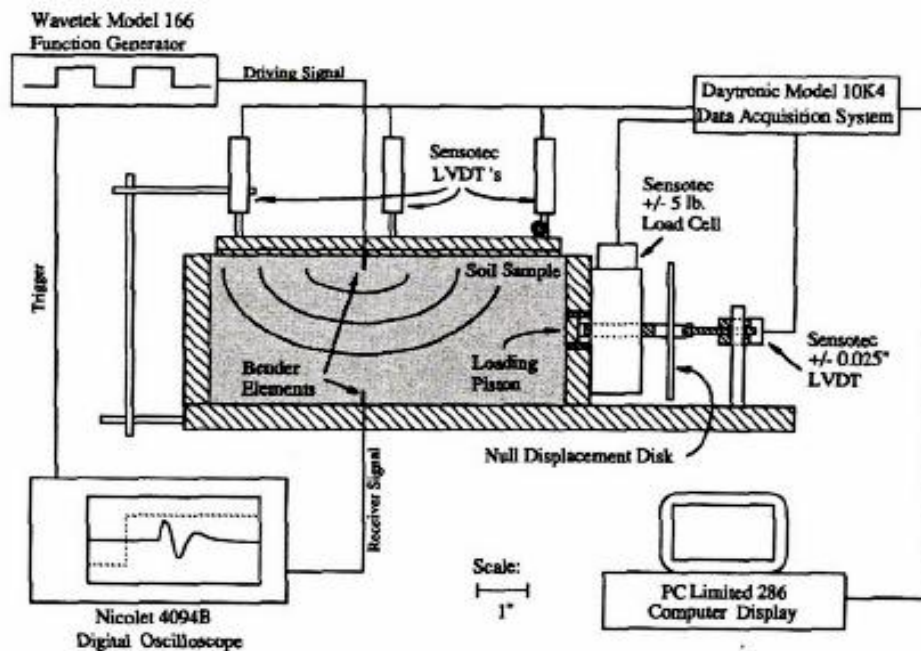


Figure 6.55. Bender element-oedometer [9]

A compilation of tests on Ottawa sand were executed to assess the performance of this BEO device.

The results of the testing eventually indicated that the device is capable of successfully measuring the lateral stresses and the shear wave velocity.

In 1998, Zeng and Ni developed a new application of bender elements to measure the small strain shear modulus of sand in four different shear planes under anisotropic loading conditions. Then in 1999, Zeng and Ni applied the bender element technique to investigate the stress-induced anisotropy in  $G_{max}$  of sands. The general focus of the work follows a basic study of the technique itself, a hypothetical framework for stress induced anisotropic  $G_{max}$  of sand and its authentication by experimental data.

In 2001, Lings and Greening created a single “crossbreed” element called the “bender-extender” element. This element can transmit and receive both *shear* (s-waves) and *primary* (p-waves) using a single pair of elements. These elements were mounted and tested using a dry sand sample. A 10 kHz 20 VPP (volt peak to peak) sine wave was used as the impulse signal. Results showed that the received bender-extender signals were clear and concise.

### 6.3.3. Problems connected with the Bender Element application

*The most common problems* in a bender element test are related to the determination of shear wave travel time. Shear wave velocity is calculated using the distance  $L$  and travel time of shear waves between the ends of a transmitter and a receiver.

In essence, distance equals rate multiplied by time. The distance can be measured quite accurately using a simple ruler or tape measure, but the most difficult part is the determination of the wave travel time from the transmitter to the receiver. The travel time of shear waves in a bender element test as defined by Zeng is, “The time interval between the instant when a transmitter initiates vibration and the time when the shear waves reach a receiver. Generally speaking, the initial vibration of a transmitter is considered to take place at the instant when an electrical signal is applied, whereas the arrival of shear waves at a receiver is taken as the instant when an electrical output is recorded from the receiver. However, finite element analysis shows that there exists a phase lag between the electrical signal and the initial vibration of a transmitter.”

In addition, there can be great difficulty in determining the arrival time of the shear wave when interference is created by other waves. It has been shown that a great disturbance is created when other waves arrive before the shear wave itself.

There can also be problems even when the shear wave arrives first. This is due in part to the strength of the signal. In both cases according to Zeng, “The first arrival of the shear wave is masked so that an accurate determination of the arrival of shear waves is not possible.” The problem in these experiments is the ability to positively determine the arrival of the s-wave. In 1981, Abbiss suggested that this be accomplished by using a source which is rich in s-waves. In addition, the polarity of the s-waves can be reversed thus reversing the signal produced on the seismograph trace and positively identifying the shear wave arrival.

Another factor affecting bender element test results lies in the rising time ( $T_r$ ) of the source signal. Zeng and Ni discovered in their 1999 experimental explorations that when the rising time is increased, the maximum electrical output from the receiver can be appreciably diminished. To study the effect

of rising time on test results, Zeng and Ni placed a receiver approximately 2.5 centimeters away from a transmitter and used three different electrical pulses as input signals. The results showed that the change in rise time was independent of the travel time for shear waves. However, the definition of the first arrival seemed to be affected by the size of the Tr. If the rising time was too large, the vibration of the transmitter was too weak causing a poorly defined shear wave. Therefore it was determined that, a square pulse can only be used as the input signal for bender element tests in the situation that the rising time is small.

The size of bender elements plays a large role in the strength of the signal acknowledged by a receiver.

In cases of high stress levels, the movement of a bender element is greatly impeded and cannot vibrate at a strong enough intensity to produce a strong signal for the receiver to pick up. Therefore, the sizes of transmitters and receivers need to be determined to measure accurately the shear-wave velocity at high stresses. Generally speaking, the intensity of the vibration of a bender element increases as its size and flexibility increase. The size plays a more important role for a transmitter, whereas it is the flexibility that is important for a receiver.

Most properties of piezoelectric ceramics are not permanent and will gradually diminish over a period of time. A logarithmic relationship with time has been developed to represent the degradation of the ceramic element after the time at which it was initially polarized. The equation is as follows:

$$\text{Rate of Aging} = (\text{Par}_2 - \text{Par}_1) / (\text{Par}_1 (\log t_2 - \log t_1))$$

Where,  $t_1$  is the time one after polarization in days,  $t_2$  is the time two after polarization in days,  $\text{Par}_1$  is a value for the parameter Par at  $t_1$ , and  $\text{Par}_2$  is a value for the parameter Par at  $t_2$ . However, the exact rate of aging is dependant upon the composition of the ceramic and the process used to manufacture the element.

It has been observed that ceramics age at two different rates. Within the first 24 to 50 hours after the polarization of the element, piezoelectric properties are rapidly lost. After this short period, the degradation of the ceramic occurs at a much slower rate throughout the lifetime of the element. The rate of aging can be increased by mishandling the elements in such a way that they could potentially be depolarized. This includes exceeding the electrical, mechanical, or thermal limitations of the element itself. The following graph shows that for a particular element, the initial aging rate (for capacitance) 1,000 to 4,000 minutes after polarization is approximately -2.4% per decade. Following this initial period an aging rate of -0.9% was approximated per decade from then on [9].

## CONCLUSION

Every building or structure which is founded in or on the earth imposes loads on the soil that supports the foundations. The stresses set up in the soil cause deformation of the soil. As in other materials, stresses may act in soils as a result of an external load and the volumetric weight of the material itself.

Soils are controlled by the effective stress strength envelope and therefore the proper determination of these parameters is paramount. The strength envelope is best determined by a series of tests - consolidated undrained triaxial shear tests with porewater pressure measurements (CU); consolidated drained triaxial tests at slow strain rates (CD); or (3) drained direct shear tests (DDS).

For clays, commonly used laboratory tests include the *unconfined compression (UC)* and *unconsolidated undrained tests (UU)*, however, these do not attempt to replicate the ambient stress regime in the ground prior to loading and therefore can only be considered as index strengths. Preferably, *the consolidated triaxial shear and direct shear box tests* can be used in conjunction with consolidation/oedometer tests in a normalized stress history approach.

To reproduce in the laboratory the same vibration, shock and cyclic forces to the soil sample, to give engineers a better understanding of how a soil material behaves under these unique situations. Dynamic, or cyclic, loads on soils exhibit three main characteristics: the effect of stress reversals, rate-dependent response of the soil, and dynamic effects where static analyses become inapplicable. Seismic loading is a form of cyclic loading that is caused by earthquakes. The most widely performed tests for evaluating the soil behavior under dynamic, or cyclic loading are the cyclic simple shear and cyclic triaxial tests. Liquefaction is a phenomenon that occurs during rapid undrained loading and is typified by increase in pore pressure and decrease in effective stress. Cyclic simple shear and cyclic triaxial tests have been used to study liquefaction in sands. Both testing procedures exhibit similar behavior: the sample liquefied when the pore pressure equaled the confining pressure, increasing the cyclic shear stress caused liquefaction in a fewer number of cycles, and increasing the confining pressure caused liquefaction in a greater number of cycles. The cyclic shear stress required to cause liquefaction in the cyclic shear test was considerably lower than in the cyclic triaxial test. However, the direct shear test is a better approximation of the shearing caused by a seismic wave experienced in situ.

All laboratory test data and results should be scrutinized for quality of test procedures, and soil samples. In selection of strength parameters, the engineer should realize that test results are indicative of a very small percentage of the soil mass, and the natural variability of these materials at

the site should be considered.

In addition, the entire stress path from start to finish can be followed. Prior to assigning laboratory tests, all soil samples submitted to a laboratory should be subjected to visual examination and identification. It is advisable for the engineer to be present during the opening of samples for visual inspection. He should remain in contact with the laboratory, as he can offer valuable assistance in assessing soil properties.



## References

1. Arion1 C., Neagu C. 2 Laboratory investigation for estimation of seismic response of the ground. *International Symposium on Strong Vrancea Earthquakes and Risk Mitigation Bucharest, Romania. Oct. 4-6, 2007.*
2. ASTM D3999-91, *Standard test methods for the determination of the modulus and damping properties of soils using the cyclic triaxial apparatus*
3. ASTM D5311-92, *Standard test method for load controlled cyclic triaxial strength of soil.*
4. Atkinson, J.H. (2000) Non-linear soil stiffness in routine design. *Geotechnique* 50, No5, 487 - 508 p.
5. Bolton M. D. & J. M.R.Wilson. Soil stiffness and damping. *Cambridge University UK Structural Dynamics, Kretzigetal. (eds), Balkema, Rotterdam. 1990 210-216p.*
6. Bile Serra, J. Patrick Hooker. A New Computer Controlled Hollow Cylinder Torsional Shear Apparatus GDS Instruments Ltd, United Kingdom. Instituto Superior Tecnico, Universidade Tecnica de Lisboa (in Portuguese). biles@lnec.pt
7. Dynamic properties and liquefaction potential of soils. Engineering and design. Laboratory soils testing. Department of the army . U. S. Army Corps of Engineers .Washington, D. C. 1986.
8. James N. Dismuke. Cyclic Loading, Cyclic Laboratory Tests, and Liquefaction Studies in Cyclic Simple Shear and Cyclic Triaxial Tests. University of California at Davis. ECI 281A, 2001.
9. Karg C. Cone Penetrometer Equipped with Piezoelectric Sensors for Measurement of Advanced Cyclic Triaxial and Bender Element Testing Supervisor: Wim Haegeman
10. Karg C. & W. Haegeman, *Advanced Cyclic Triaxial Testing and Bender Element Testing*, Proceedings of ICSV12, J.L. Bento Coelho (ed.), Lisbon, Portugal, July 11-14, 2005.
11. Luan, M. T., Jin, D., Xu, C., Zhang, Q., and Zhang, Z. (2008). "Liquefaction of sand under bidirectional cyclic loading." *Chinese Journal of Geotechnical Engineering*, 30(6): 747-749 (in Chinese).
12. Manual on subsurface investigations. Paul W. Mayne, Barry R. Christopher, and Jason DeJong. National Highway Institute, Federal Highway Administration Washington, DC. 2001.
13. Minh, N.A. The anisotropic stress-strain-strength characteristics of London Clay in Hollow Cylinder Apparatus *Internal report*. Imperial College, London. 2003.
14. O'Reilly, M. P., and Brown, S.F., *Cyclic Loading of Soils*, Blackie and Son, Inc., New York, NY, 1991.
15. Prakash, Shamsher, *Soil Dynamics*, McGraw-Hill, Inc., 1981.
16. Puech A., France F., Rivoallan X., ChereL L, The use of surface waves in the characterisation of seabed sediments: development of a MASW system for offshore applications. Institut Francais du Petrole Seatechweek, Colloque " Characterisation in situ des fonds marins" Brest, France – 21, 22 Octobre 2004.

17. Sassa Kyoji, Jurko Jozef, and Hiroshi Fukuoka. Dynamic Behavior of Gentle Silty Slopes Based on Undrained Cyclic Shear Test. *Disaster Mitigation of Debris Flows, Slope Failures and Landslides* 411-420 p. Internet.
18. Schneider, J.A., Hoyos, L., Jr., Mayne, P.W., Macari, E.J., and Rix, G.J. (1999), Field and laboratory measurements of dynamic shear modulus of Piedmont residual soils, Behavioral Characteristics of Residual Soils, GSP 92, ASCE, Reston, VA, pp. 12-25.
19. Sitharam T. G., Govinda Raju L. and Sridharan A. Developing an enhanced triaxial testing system with cyclic pore-pressure capabilities. Jeffrey Wade Frank. University of Florida 2004. 170p.
20. Sitharam T. G., Govinda Raju L. and Sridharan A. Dynamic properties and liquefaction potential of soils. *Current Science*, VOL. 87, N 10, 2004. 1370-1378 p
21. Soil Mechanics – Laboratory Manual, B.M. DAS
22. Steven L. Kramer, Ahmed-W. Elgamal Modeling soil liquefaction hazards for performance-based earthquake engineering. Pacific Earthquake Engineering Research Center College of Engineering University of California, Berkeley. 2001. 186 p.
23. Soil Properties, Testing, Measurement, and Evaluation, C. Liu, J. Evett.
24. Soil Stiffness in Highway Pavement. Xiangwu (David) Zeng and Heather Hlasko. Department of Civil Engineering, Case Western Reserve University for the Ohio Department of Transportation. 2005.
25. Stokoe, K.H., Joh, S.H. and Woods, R.D. (2004) “The contribution of in situ geophysical measurements to solving geotechnical engineering problems”, Proceedings of the 2nd International Conference on Site Characterization, ISC’2, Porto, 19-22 September 2004.
26. Wagner, A. A. 1957. The use of the unified soil classification system by the bureau of reclamation. Proceedings. 4th International Conference SMFE, Butterworths, London, Vol. 1. pp. 125 - 134.
27. [www.geonor@geonor.com](http://www.geonor@geonor.com).
28. [www.Tecnotest.com](http://www.Tecnotest.com).
29. [www.ele.com](http://www.ele.com).
30. [www.gdsinstruments.com](http://www.gdsinstruments.com).
31. [www.geo-observations.com](http://www.geo-observations.com).
32. [www.uic.edu/classes/cemm/cemmlab/Experiment](http://www.uic.edu/classes/cemm/cemmlab/Experiment).
33. Yoshida N. Susumu IAI. Nonlinear site response and its evaluation and prediction. Proc. 2nd International Symposium on the Effect of Surface. Geology on Seismic Motion, Yokosuka, Japan, pp. 71-90, 1998.

## TABLE OF CONTENTS

6. DYNAMIC PROPERTIES OF SOILS .....	3
6.1. Dynamic deformation characteristics of soil .....	3
6.2. Application of dynamic parameters in engineering practice .....	6
6.2. Methods of measurement of dynamic characteristics of soil .....	14
6.3. Laboratory tests of soil .....	21
6.3.1. A brief introduction to experimental laboratory devices .....	21
6.3.2. Resonant Column Test .....	24
6.3.3. Cyclic Triaxial Test .....	29
6.3.4. Cyclic direct simple shear test .....	37
6.3.5. Hollow cylinder torsional shear test .....	45
6.3.6. Ultrasonic test, shaking tables and centrifuge devices .....	53
6.4. Measurement of dynamic soil stiffness by piezoelectric sensors .....	55
6.4.1. The structure of piezoelectric ceramics .....	55
6.4.2. Application of piezoelectric sensors in soil property determination ..	62
6.3.3. Problems connected with the Bender Element application .....	69
CONCLUSION .....	71
References .....	75

Учебное издание

СОСТАВИТЕЛЬ  
КРАМАРЕНКО Виолетта Валентиновна

**LABORATORY TESTING OF SOILS**  
Part III. Dynamical properties of soils

Методические указания к выполнению лабораторных работ  
по курсу «Грунтоведение» для студентов обучающихся  
по направлению 130100 «Геология и разведка полезных  
ископаемых».

Научный редактор  
к.г.-м.н., доцент

Т.Я. Емельянова


**Отпечатано в Издательстве ТПУ в полном соответствии  
с качеством предоставленного оригинал-макета**

Подписано к печати 05.11.2010. Формат 60х84/16. Бумага «Снегурочка».  
Печать XEROX. Усл.печ.л. 9,01. Уч.-изд.л. 8,16.  
Заказ . Тираж 30 экз.



Национальный исследовательский Томский политехнический университет  
Система менеджмента качества  
Томского политехнического университета сертифицирована  
NATIONAL QUALITY ASSURANCE по стандарту ISO 9001:2008



**ИЗДАТЕЛЬСТВО**  ТПУ. 634050, г. Томск, пр. Ленина, 30  
Тел./факс: 8(3822)56-35-35, [www.tpu.ru](http://www.tpu.ru)